

Oil & Natural Gas Technology

DOE Award No.: DE-FE0024297

Quarterly Research Performance

Progress Report (Period Ending 09/30/2020)

Marcellus Shale Energy and Environment Laboratory (MSEEL)

Project Period (October 1, 2014 – March 31, 2021)

Submitted by:
Samuel Taylor



Signature

West Virginia University Research Corporation
DUN's Number: 191510239
886 Chestnut Ridge Road,
PO Box 6845, Morgantown WV, 26505
Tim.Carr@mail.wvu.edu
304-293-9660

Prepared for:
United States Department of Energy
National Energy Technology Laboratory

09/30/2020



U.S. DEPARTMENT OF
ENERGY
Office of Fossil Energy



NATIONAL
ENERGY
TECHNOLOGY
LABORATORY



U.S. DEPARTMENT OF
ENERGY

NATIONAL ENERGY
TECHNOLOGY LABORATORY

Executive Summary

Quarterly Progress Report

June 1 – September 30, 2020

The objective of the Marcellus Shale Energy and Environment Laboratory (MSEEL) is to provide a long-term field site to develop and validate new knowledge and technology to improve recovery efficiency and minimize environmental implications of unconventional resource development.

Impacts from COVID-19 have started to diminish, as laboratories reopened in many cases. Still impacted is the work of Dr. Sharma (Task 3 in this report), which has lab chemical safety requirements for multiple persons in the lab when testing is underway. This is reflected in updated dates for milestones/deliverables. Other work has progressed relatively on-schedule, and analysis from the samples and data collected from the Boggess Pad has continued as planned.

This quarter's work focused on monitoring initial production from the MSEEL Phase 3 wells at the Boggess Pad. As of this report total production ranges from 2.2 to 3.0 Bcf. Two wells were geometrically completed, a private consultant engineered two wells, and two wells were engineered using software developed by the MSEEL team. While it is early, it appears based on rate transit analysis (RTA) and production that the wells engineered using software developed by the MSEEL team may be some of the better wells on the pad. Numerous papers were presented at various professional conferences including URTeC AAPG-ACE, SPE-ATCE and SEG (See Appendix B). In addition, papers that use publically available MSEEL data are being published (e.g., Li, W. et al. 2020 and Tran et al., preprint).

Research on machine learning for improved production efficiency with LANL continues and we have provided data and consultation and have contributed to a paper on use of artificial intelligence for a better understanding of reservoir properties. We also presented papers involving machine learning at American Association of Petroleum Geologist Annual meeting (Li, L. et al 2020a) and the Society Petroleum Engineers (SPE) annual technical conference and exhibition (ACTE) (Li, L. et al. 2020b).

We are integrating the core data received from the Schlumberger/Terra Tek lab and using that data to revise the production analysis and to prepare for flow simulation.

We continue to sample and monitor produced fluids, and monitor air quality and performance at both MSEEL sites (MIP and Boggess).

We continue to process the 108 terabytes of data from the Boggess pad and are working to develop an improved workflow for delivering the data to the public. Papers for this quarter have been added to Appendix B and if available will be posted to OSTI. Several additional papers will be reported in the next quarterly report.

Project Performance

This report summarizes the activities of Cooperative Agreement DE-FE0024297 (Marcellus Shale Energy and Environment Laboratory – MSEEL) with the West Virginia University Research Corporation (WVURC) during the 3rd quarter of FY2020 (April 1 through June 30, 2020).

This report outlines the approach taken, including specific actions by subtopic. If there was no identified activity during the reporting period, the appropriate section is included but without additional information.

A summary of major lessons learned to this point of the project are provided as bullet points and will be added to as research progresses. New lessons listed below are:

- The engineered wells at the Boggess Pad (1H and 3H) show the importance of designed stages and cluster placement to improved well performance.

Phase 3 Plans

Phase 3 of MSEEL has completed the stimulation and started production from the Boggess Pad in this reporting quarter. Six 10,000+ foot horizontal Marcellus Shale wells off a single pad (Boggess) are near the initial MIP pad (Figure 0.1). The pad has one permanent fiber optic (FO) cable installed in the Boggess 5H lateral provided digital acoustic sensing (DAS) during stimulation, and was monitored during initial production. Distributed temperature sensing (DTS) was monitored during stimulation and continues during initial and long-term production. We acquired DAS data for the entire 5H well, but the FO failed around stage 30 and we do not have long-term DTS data below that stage to the toe. We have data from the upper stages through the heel and continue to download the data. Deployable FO systems were proposed (Boggess 1H and 17H), but due to the fiber failure in the 5H the fiber was not placed in the 17H. However, we acquired significant DAS and DTS and microseismic data from the 5H and 1H that provided insight of stimulation effectiveness in near real-time and the 100's of terabytes of data to evaluate and model the reservoir across each individual stage, and at individual clusters within stages for the 5H, which will be used for all Boggess wells. This data formed the basis of several papers presented at professional conferences (Appendix B).

Based on production and rate transient analysis (RTA), the new methodology appears to improve completion efficiency. As the wells have come on production, the 1H and 3H wells still have a higher gross production efficiency than either the geometrically completed wells (9H and 17H with identical 200 foot stages with identical number of clusters in each stage) or the commercial design provided which only used the geomechanical logs and ignored the imaged fractures (5H and 13H) (Figure 0.2). On a net production efficiency controlling for variable lateral length (Mcf/1000') outside wells (1H and 17H) are better than interior wells, but engineered wells had a slower ramp-up but are gaining on their counterparts (Figure 0.3).

We have finally received the core analysis, and initiated a detailed analysis of the cored and logged vertical pilot well to develop a high-resolution geomechanical model (stratigraphy) to type each 6 inches of the Marcellus. Logging while drilling (LWD) logs in each of the six laterals provided similar geomechanical logs and image logs to geomechanically type each foot of the laterals as the horizontal laterals move stratigraphically up and down through the Marcellus. This approach will permit direct coupling and evaluation of cost-effective LWD technologies to the relatively high-cost permanent FO data and the basis for engineering stages in all wells. It was applied to two of the Boggess wells.

We continue to gather fiber optic and production data from the Boggess wells to compare across each of the six wells, and with the two wells at the MIP pad (MSEEL 1) and use these data to form the basis for robust big data modeling.

We are working on a new workflow for simplified access to MSEEL data especially the large multi-terabyte data from the Boggess pad.

We have worked with NETL and other labs on various projects of the Marcellus at the MIP and Boggess site.



Figure 0.1: Boggess Pad with new generation permanent fiber in the central well (Boggess 5H, red star) and deployable fiber in adjoining wells skipping one (orange stars). We will be able to monitor in near-real time fracture stimulation in the central 3 wells (3H, 5H and 9H). A vertical pilot will be drilled, cored and logged.

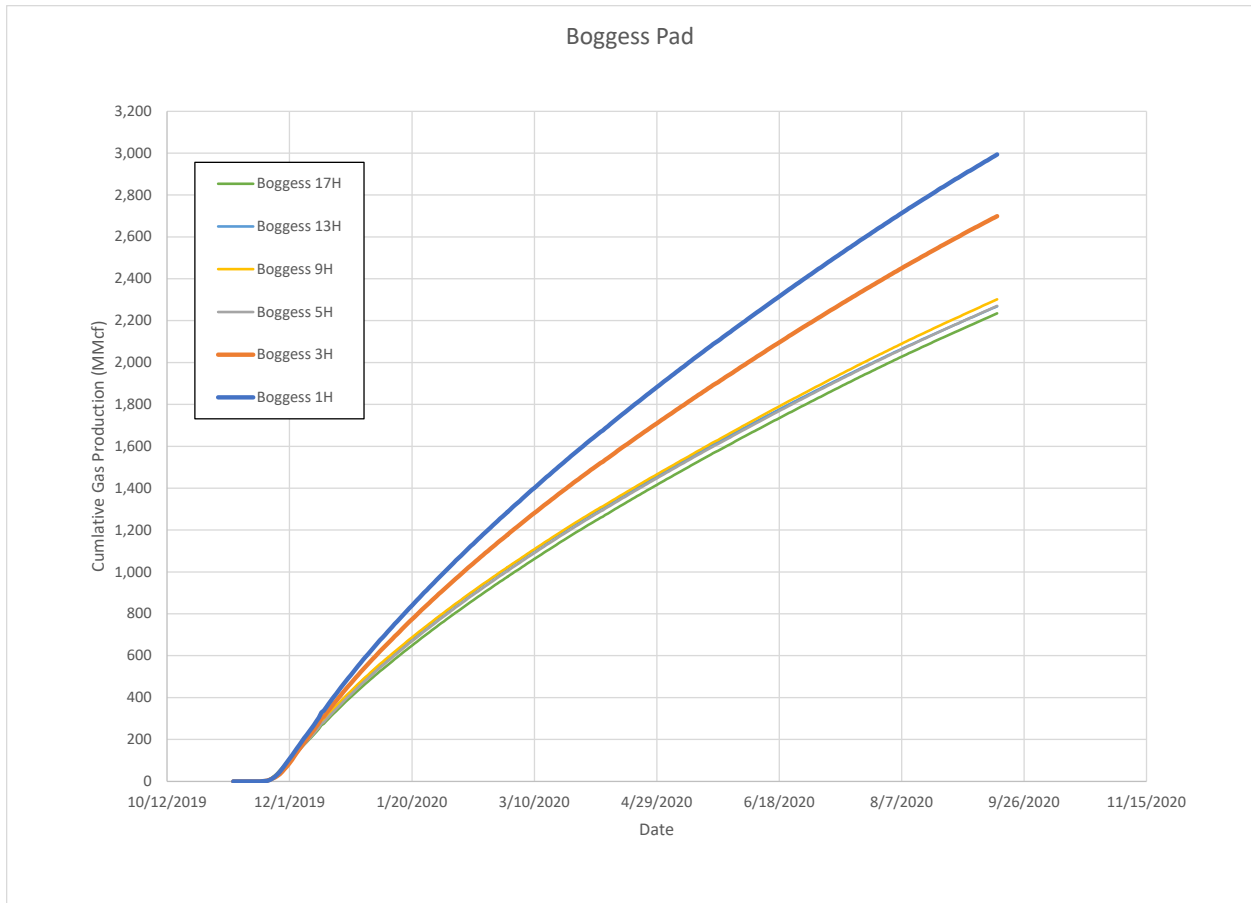


Figure 0.2: Initial daily gross production from the Bogges Pad. The wells engineered using the MSEEL software are highlighted with thicker lines (1H and 3H). Wells have different lateral lengths that need to be evaluated to derive a better evaluation of production efficiency. Also outside wells typically perform better than interior wells due to reduced competition. The production is very early and the picture could very easily change.

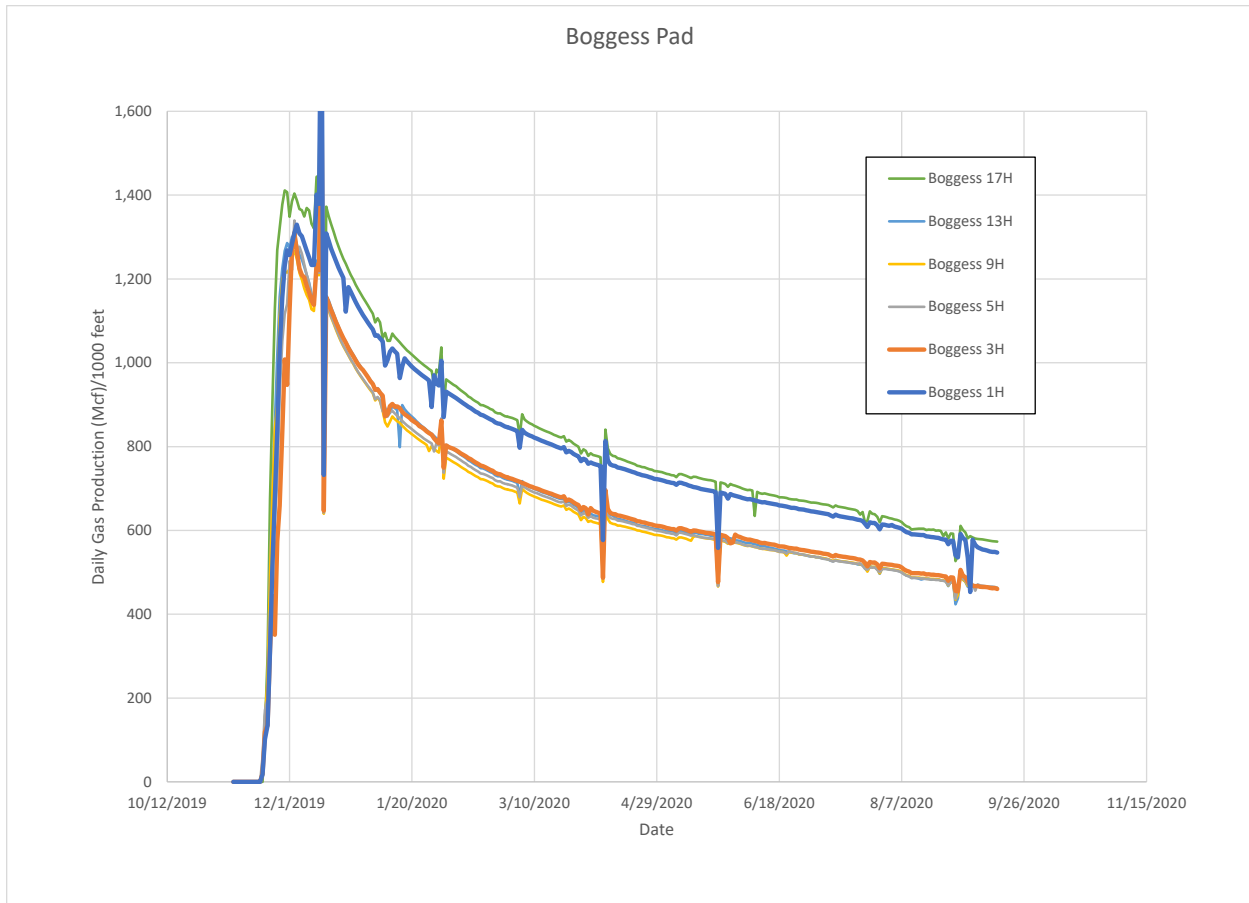


Figure 0.3: Initial daily net production from the Bogges Pad adjusted for Mcf per 1000’ of completed lateral. The wells engineered using the MSEEL software are highlighted with thicker lines (1H and 3H). As you can see outside wells (1H and 17H) perform better than interior wells due to reduced competition. Also wells engineered using the MSEEL approach got off to a slower start but have narrowed the gap in daily production and in the case of the 3H, it is producing more than any other interior well. In the case of the 17H more sand was used per stage and we need to adjust for sand per foot. The production is very early and the picture could very easily change.

Project Management Update

Approach

The project management team will work to generate timely and accurate reporting, and to maintain project operations, including contracting, reporting, meeting organization, and general oversight.

Results and Discussion

The project team is tracking ten (10) milestones in this budget period.

	Task	Milestone	Status	Due Date
1.	3.2.1	Sample collection and analysis of flowback/produced	Complete	20-Mar

		water; data analysis		
2.	3.2.1	Comparison of OTM33A vs. Methane Audits vs. Eddy Covariance System Measurements Complete	Complete.	20-Mar
3.	3.1.2	Characterization of organic matter - kerogen extraction and characterization complete	Delayed due to lab closures from COVID-19. Expect results by December 2020.	20-Dec
4.	3.1.2	Isotopic characterization of produced water and gases - comparison between MIP and Boggess wells and other wells in Marcellus and interpretation.	Complete.	20-Jun
5.	3.1.2	High-pressure and temperature fracture fluid/shale interaction experiments complete.	Delayed due to lab closures from COVID-19. Expect results by March 2021.	21-March
6.	3.1.4	Complete final reservoir characterization using Boggess 17H pilot well. Compare 17H to MIP 3H	Delayed due to lab closures from COVID-19. Expect results by March 2021.	21-March
7.	3.2.1	Methane Audit 14 Completed	Complete	20-Jun
8.	3.4.2	Synthetic data developed for model use	Delayed due to lab closures from COVID-19. Expect results by March 2021.	21-March

9.	3.2.1	Energy Audit Model Completed	Initial data analysis completed, model development continues.	20-Sep
10.	3.1.4	Extend reservoir characterization using logs, completion data and production data to identify good producing stages in Boggess wells.		20-Dec

Topic 1 – Geologic Engineering

Approach

This quarter the core data help to improve the production analysis of the Boggess wells (Ebrahim Fathi). The engineered Boggess wells appear to remain the best wells on the pad. Forecasting the production rates and expected ultimate recovery (EUR) of the well is of special interest in the oil and gas industry. It is emphasized that the Boggess wells are in transient flow regimes, so these are only minimum estimates of OGIP and EUR.

Results and Discussion

Production Analysis (Fathi).- In our previous report different type curves, diagnostic plots and unconventional models in IHS harmony commercial software have been used for well performance analysis of both MIPH (1H, 3H, 4H, and 6H) and Boggess (1H, 3H, 5H, 9H, 13H, and 17H) wells. The results obtained from both pads are then compared to gain more insight regarding completion design optimization and operation strategies.

The well performance analysis of the Boggess wells have been updated from last report including the following updates:

- 1- 3 months of new production data has been added to the database used for Boggess wells performance analysis.
- 2- The adsorption measurements obtained from the core samples are used in new well performance analysis.
- 3- The geomechanical properties of the crushed samples have been collected and compared against core sample measurements on Marcellus shale sample obtained from Burlington WV and measured at WVU lab to come up with a more realistic geomechanical model.
- 4- The vertical depth and lateral length of the Boggess wells have been adjusted based on the new adjustment to the reports.
- 5- The early time tubing pressures have been updated based on NNE recordings.

Flow Regime Identification (FRI):

It is extremely important to identify the flow regime of each well to make sure data obtained from a well in transient flow regime are not mixed with that of boundary dominated flow regime.

Transient flow regime can be observed during the early time of production and in extremely low permeability formations. In transient flow regime, flow occurs while a pressure response is moving out in an infinite acting reservoir. At late time and depending on the matrix permeability, flow experiences a boundary dominated flow regime where a reservoir is in a state of pseudo-equilibrium. In a boundary dominated flow regime accurate OGIP and EUR can be obtained.

The flow regime of Boggess wells in Marcellus shale has been revisited as more production data became available using different type curves, diagnostic plots and unconventional models. Based on these studies, all the wells in Boggess still showed transient flow (TF) regime.

Original gas in place (OGIP) and expected ultimate recovery

Various diagnostic plots were performed on Boggess wells including new pressure, production and adsorption data to determine the OGIP and EUR’s. Figure 1.1 compares the Minimum OGIP per 1000 ft of lateral obtained for different Boggess wells. Boggess wells 1H and 17H have the highest minimum OGIP/1000 ft of lateral. Next, Boggess 3H and 5H wells show higher minimum OGIP. Figure 1.2 also shows the comparison of EUR/1000 ft of lateral calculated for Boggess wells. In Boggess pad 17H and 1H show the highest EUR/1000 ft of lateral. One major reason could be the fact that these two wells are semi-bounded. This observation is in agreement with other observations in Marcellus shale stating the stand-alone wells and semi- bounded wells outperform the fully bounded wells. Among the fully bounded wells Boggess 3H shows the highest Minimum OGIP and EUR/ 1000 ft of lateral. Both EOR and OGIP calculations show improvement as new data became available.

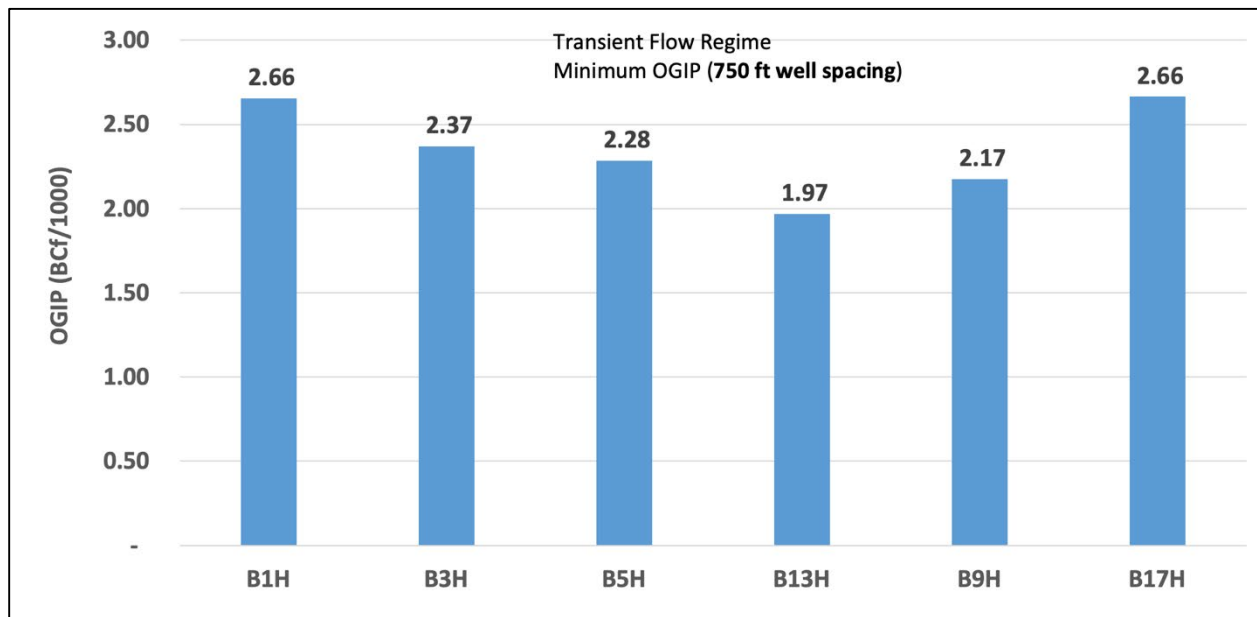


Figure 1.1 Comparison of Minimum OGIP (BCF/1000 ft) of Boggess wells.

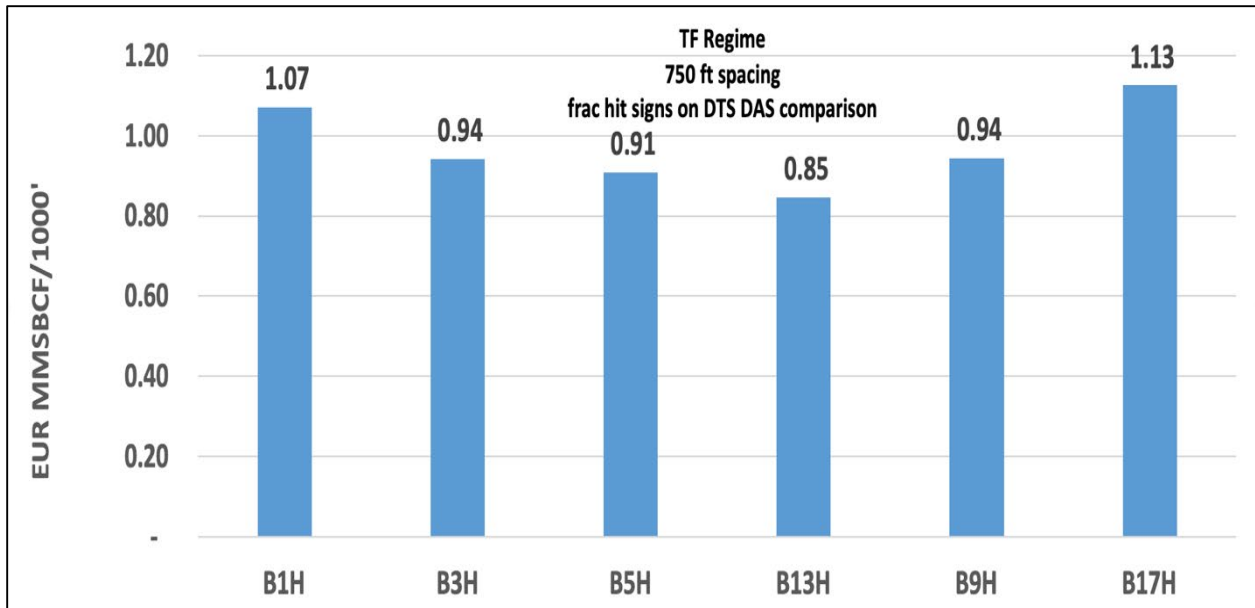


Figure 1.2 Comparison of EUR (BCF/1000 ft) of Boggess wells.

We have also updated the flow capacity measurements of Boggess wells as new data became available. The flow capacity of a well can be determined by plotting pseudo $\Delta P/q$ on the y-axis vs. material balance square root of time (CUM/q) on the x-axis (superposition plot) and determining the slope of the linear portion of the plot (i.e., inversely proportional to $A\sqrt{k}$). In $A\sqrt{k}$, A is the contacted surface area and k is the effective permeability of the contacted rock. The $A\sqrt{k}$ of each well then should be normalized by lateral length of the well. The $A\sqrt{k}$ reflects the flow capacity of the well and will not change as long as well is in the transient flow regime. Figure 1.3 depicts the flow capacity of the Boggess well. 1H, 17 H and 3H are having the highest flow capacity, these wells also showed higher OGIP and EUR/1000 ft of lateral. 1H and 17 H with the highest flow capacity are the semi-bounded wells. The completion design of the wells also shows great impact on flow capacity of the wells. Boggess1H and 3H have geomechanical spacing designed by MSEEL group based on DAS and DTS data obtained from fiber optics. The 9H well is comparable with 3H in terms of boundedness (i.e., they are both fully bounded), however the 9H shows lower flow capacity in comparison to 3H that could be due to having geometrical design versus engineering design. This required further investigation as more production data becomes available.

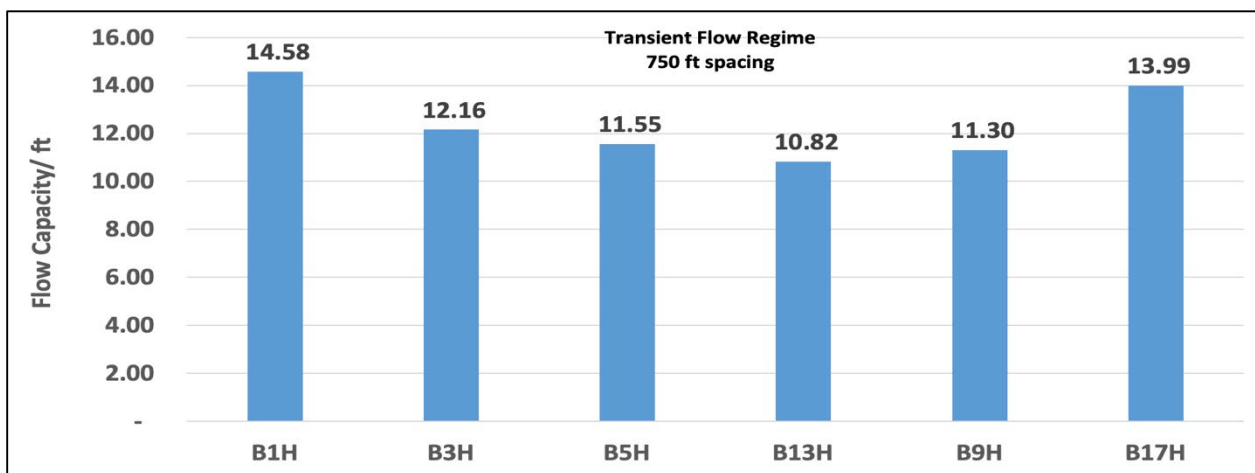


Figure 1.3 Flow capacity/ft of Boggess wells

Figure 1.4 shows great correlation exists between $A\sqrt{k}/ft$ (flow capacity) and EUR/ft (expected ultimate recovery) of the Boggess wells that can be used for well ranking and indexing. Boggess Wells 1H and 17H are showing the best performance and 13H is the weakest well among all the 6 wells drilled in Boggess pad.

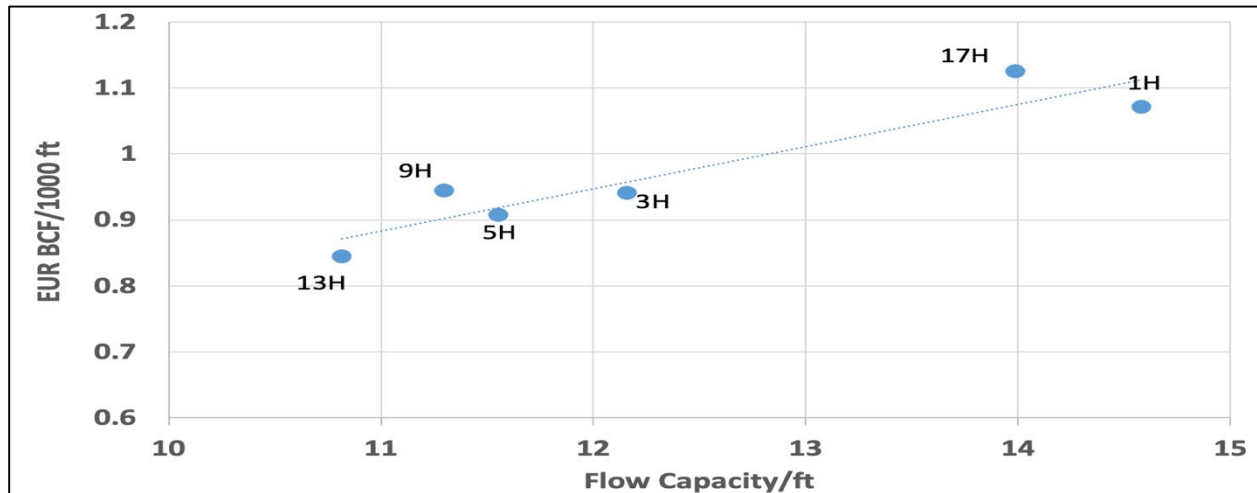


Figure 1.4 EUR/1000 ft of lateral vs flow capacity of Boggess wells

Products

Harmoney enterprise 2019 commercial software is used for this analysis and “.hldb” file were generated for further analysis. The results of the Boggess well analysis are summarized in Table 1.1. The results will be refined and integrated into the compositional reservoir simulation model and fracture models.

pad	Boggess					
Well	B1H	B3H	B5H	B13H	B9H	B17H
Flow Regime	Transient Flow Regime					
Completion design	Geomechanical Spacing			Geometrical Spacing		
TVD	8,030	8,030	8,035	8,020	8,030	8,020
MD	20,872	21,075	20,226	20,298	19,835	19,026
LL	12,544	13,117	11,128	10,801	11,201	8,823
Stages	63	66	56	55	57	45
Pi	5,139.20	5,139.20	5,142.40	5,132.80	5,139.20	5,132.80
Stage Length (ft)	199	199	199	196	197	196
Boundedness	semi-bounded	bounded	bounded	bounded	bounded	semi-bounded
TIL (days)	216	216	216	216	216	215
Xf (fracture half length)	273.00	229.00	208	214	195	231
Min OGIP (MMScf)	33306	31090	25411	21273	24357	23510
OGIP BCF/1000 ft	2.66	2.37	2.28	1.97	2.17	2.66
A*Sqr(k)	182900	159454	128551	116818	126526	123413
A*Sqr(k)/ft Flow capacity	14.58	12.16	11.55	10.82	11.30	13.99
EUR (MMscf)	13,436.00	12,344.00	10,100.00	9,127.00	10,575.00	9,926.00
EUR BCF/1000ft	1.07	0.94	0.91	0.85	0.94	1.13

Table 1.1 Boggess wells analysis summary.

Plans for Next Quarter

Continued monitoring of all the Boggess wells while still in transient flow regime as the analysis provides only the minimum of OGIP and EUR to come up with more robust and accurate estimation.

Initiate compositional reservoir simulation model will be built for Boggess pad and production and pressure of the wells will be history matched using commercial software CMG-GEM. Use the hydraulic fracturing software Fracpro to obtain the hydraulic fracture dimensions using hydraulic fracturing sand schedules and rock geomechanical properties obtained from core samples. The hydraulic fracture dimensions will be used in history matched CMG models to generate probabilistic production forecasting models.

Topic 2 – Geophysical & Geomechanical

Approach

This quarter we have undertaken to integrate the core analysis (Brian Panetta) with the log analysis and improving the rate transit analysis of the Boggess wells (Ebrahim Fathi).

Results & Discussion

Core and Log Analysis (Panetta and Fathi) - We received the reprocessed Shale Analysis log from Schlumberger for the Boggess 17H pilot well. The original lithoscanner log was processed using regional data. The new interpretation was calibrated to core analyses results from the Boggess pilot well.

Core sample points were selected on the Boggess core for mechanical property analyses. Three points were selected for triaxial compression testing (TXC) and one sample was selected for multiple stress path compression testing (MSC). The TXC testing produces values for Young's Modulus (YM) and Poisson's Ratio (PR) normal to bedding. The MSC test produces values for both YM and PR, not only normal to bedding, but also at 45 degrees to and parallel to bedding. Data is summarized in Table 2.1.

Test	Sample	CORE DEPTH	AVERAGE AS-RECEIVED BULK DENSITY	EFFECTIVE CONFINING PRESSURE	YOUNG'S MODULUS NORMAL TO BEDDING	YOUNG'S MODULUS PARALLEL TO BEDDING	POISSON'S RATIO NORMAL TO BEDDING	POISSON'S RATIO PARALLEL TO BEDDING	SHEAR MODULUS NORMAL TO BEDDING
unitless	unitless	FT	g/cc	psi	psi	psi	unitless	unitless	psi
txc; ultrasonic	Bog-05-1	7893.25	2.553	2150	2.051E+06	#N/A	0.18	#N/A	#N/A
msc; ultrasonic	Bog-14-1:4	7940.38	2.467	2150	2.451E+06	5.108E+06	0.15	0.19	1.395E+06
txc; ultrasonic	Bog-15-2	7944.20	2.471	2150	3.003E+06	#N/A	0.16	#N/A	#N/A
txc; ultrasonic	Bog-24-2	7971.20	2.409	2150	2.320E+06	#N/A	0.21	#N/A	#N/A
Test	Sample	SHEAR MODULUS PARALLEL TO BEDDING	ANISOTROPY INDEX *	C11	C13	C33	C44	C66	BULK MODULUS
unitless	unitless	psi	unitless	psi	psi	psi	psi	psi	psi
txc; ultrasonic	Bog-05-1	#N/A	#N/A	#N/A	#N/A	#N/A	#N/A	#N/A	#N/A
msc; ultrasonic	Bog-14-1:4	2.146E+06	0.5306	5.712E+06	1.070E+06	2.771E+06	1.395E+06	2.146E+06	2.082E+06
txc; ultrasonic	Bog-15-2	#N/A	#N/A	#N/A	#N/A	#N/A	#N/A	#N/A	#N/A
txc; ultrasonic	Bog-24-2	#N/A	#N/A	#N/A	#N/A	#N/A	#N/A	#N/A	#N/A
TXC:	Triaxial Compression Test								
MSC:	Multiple Stress-path Compression Test								

Table 2.1 Summary of Geomechanical Properties Obtained for 6 samples generated by Schlumberger Reservoir Laboratory 9/2/2020

Schlumberger (SLB) provided their updated lithoscanner petrophysical interpretation calibrated to the Boggess core data. Overall, their total gas in place calculations increased in the Boggess

well in the core calibrated results as compared to the previous interpretation using regional data. Table 2.2 shows a comparison of GIP values for several zones as calculated by Schlumberger before and after core calibration as well as initial values calculated by West Virginia University's petrophysical model. Work on the petrophysical model is not complete, therefore OGIP values may change and will be reconciled to other approaches.

Zone	SLB Non-Core Calibrated GIP (Bcf/mi ²)	SLB Core Calibrated GIP (Bcf/mi ²)	WVU GIP (Bcf/mi ²)
Middlesex to Tully	53	75	91
Tully to Onondaga	84	112	134
Total	137	187	225

Table 2.2 Comparison of gas in place calculations of the Boggess 17 pilot well.

We continue to work on a geo-mechanical model now that the geo-mechanical core results have been received. Core data for Young's Modulus and Poisson's Ratio were plotted against values computed by Schlumberger in order to core-calibrate the logs (Figures 2.1 and 2.2).

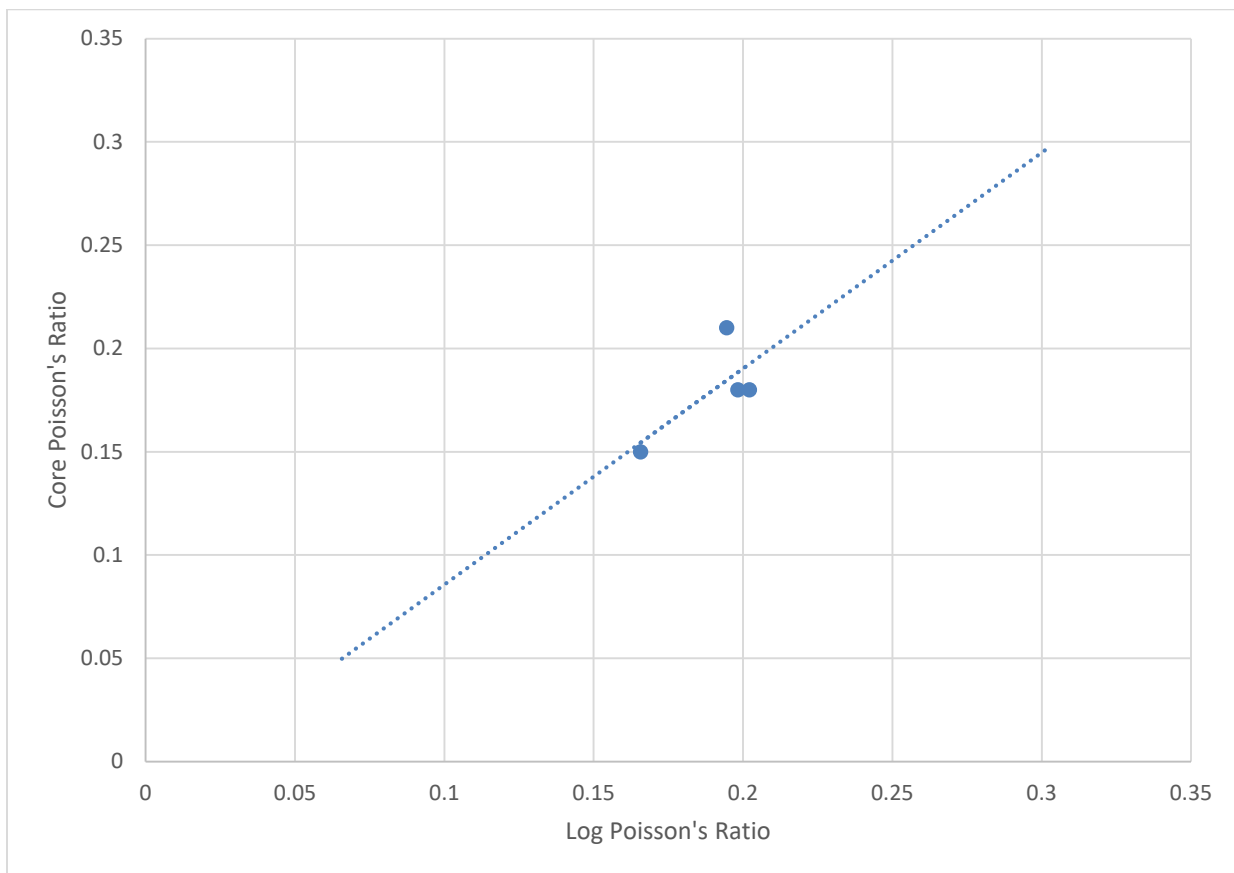


Figure 2.1 Plot of Poisson's Ratio derived from the Sonic Log (x) vs Poisson's Ratio derived from core analysis (y).

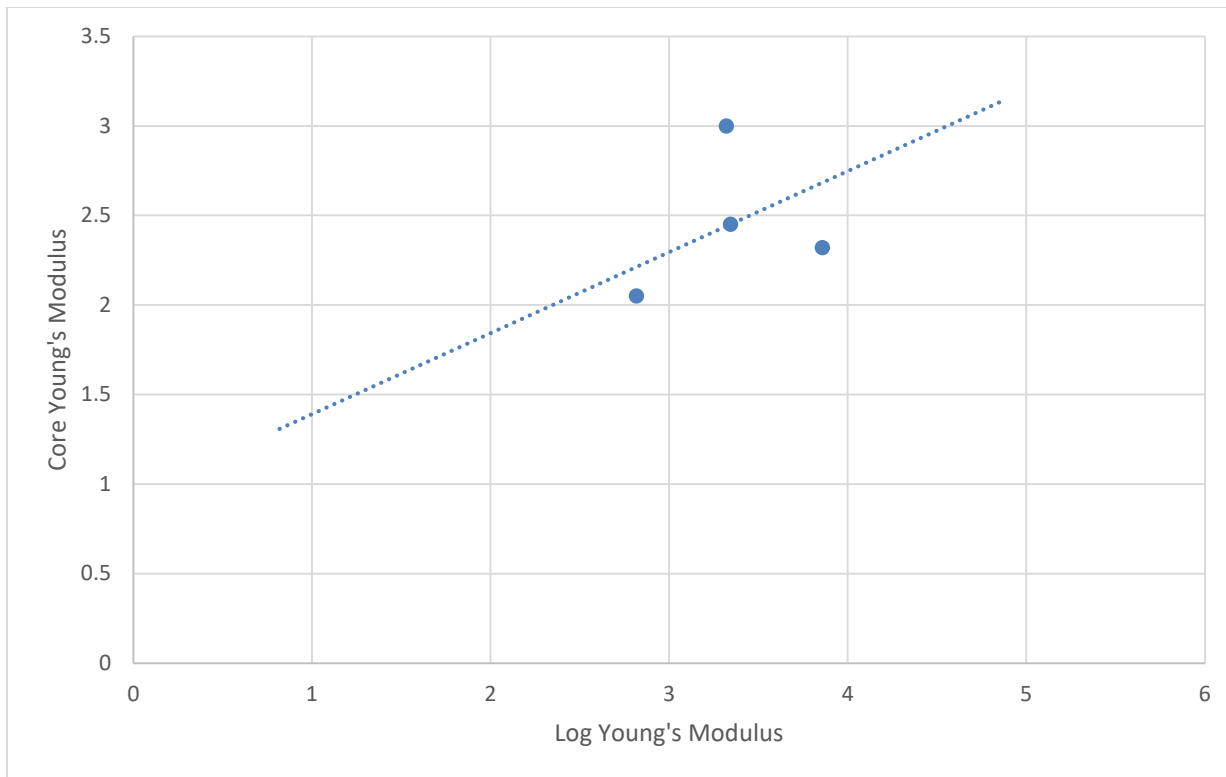


Figure 2.2. Plot of Young's Modulus derived from the Sonic Log (x) vs Young's Modulus derived from core analysis (y).

The core-calibrated Young's Modulus and Poisson's Ratio logs were then used to recompute the SH_{min} log for the vertical pilot. Figure 2.3, shows the comparison of the original SH_{min} log to the core-calibrated one. Overall, the core-calibrated log has higher values for SH_{min} throughout the more organic-rich portions of the log.

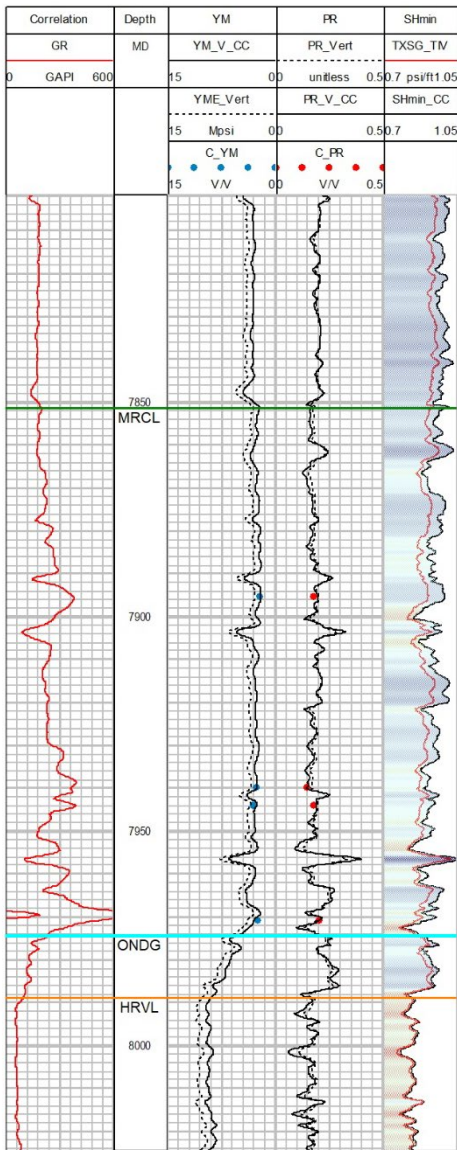


Figure 2.3. Boggess 17 pilot log showing the comparison of the original Young's Modulus, Poisson's Ratio and SH_{min} logs to the core calibrated logs. Core data points for YM and PR are shown in blue and red respectively. The fourth track shows the original SH_{min} log in red compared to the newly core calibrated SH_{min} shown color filled.

Marcellus

Onondaga

Huntersvill

The new core analysis included adsorption measurement of two samples (i.e., raw and dry basis) both taken from Boggess well 17-H. Figure 2.4 shows the Langmuir adsorption measurements of two samples and Table 1.2 summarizes the Langmuir adsorption results. The adsorption measurements are done on crushed samples with particle size of 60 mesh. The adsorption results for both dry and raw bases are found to be very similar. Followings are the properties of the samples used for adsorption measurement.

- Depth: 7971 ft
- TOC: 12.4
- Temp: 148 F
- As Received Moisture: 0.75%

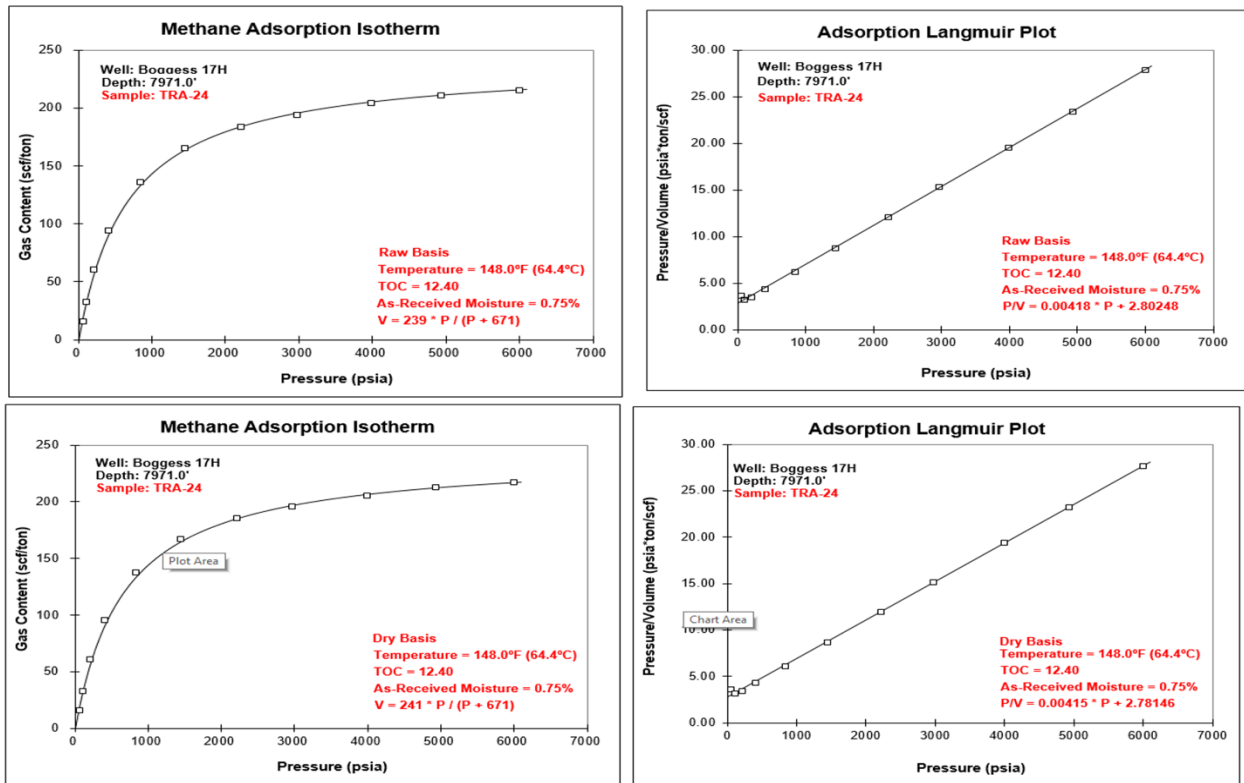


Figure 2.4 Langmuir adsorption measurements (top Raw basis and bottom Dry basis) courtesy of Schlumberger Reservoir Laboratory 20/Jul/2020

Sample	PL (Langmuir Pressure)		VL (Langmuir Volume)	
	Psia	MPa	scf/ton	scc/gm
Raw basis	670.7	4.62	239.3	7.5
Dry basis	670.7	4.62	241.1	7.5

Table 2.3 Summary of Langmuir adsorption parameters generated by Schlumberger Reservoir Laboratory 20/Jul/2020

Products

Results of the core analysis will be integrated into the various efforts including the production analysis in section 2.

Plans for Next Quarter

Work using the newly acquired core analyses was initiated on calibrating Young's Modulus, Poisson's Ratio and SH_{min} derived from Fracture-ID logs that were run in the vertical Boggess pilot well and extend the analysis to the laterals. Fracture ID derived these geomechanical property values not from traditional sonic logs, but rather from vibrational data that has been recorded while drilling. Initial calibration attempts have yielded poor results and we are looking at our approach as discussed by Liwei Li at AAPG-ACE and SPE-ATCE (2002a and 2002b). Once a good calibration fit has been achieved, the results will be used to calibrate the Fracture ID logs that were run in the Boggess horizontal wells. Horizontal mechanical property logs will then be used in the 3-D geologic model.

Once data is available we will compare the geo-mechanical properties to lithological properties derived from XRD and XRF analyses. The XRD analysis has been completed; however, the XRF analysis has not. This work will be performed at the NETL lab in Morgantown once all testing has been completed in Schlumberger's lab in Houston and the core has been shipped back to West Virginia University.

Topic 3 – Deep Subsurface Rock, Fluids, & Gas

Cole Group – Ohio State

Approach

Flowback/Produced fluid samples from several wells were collected from five wells at two Utica/Point Pleasant (UPP) sites (UPPW and UPPS) in Ohio, and two wells at the Marcellus (Marcellus Shale Energy and Environment Laboratory (MSEEL)) site in West Virginia over a period of approximately two years. These samples were analyzed for major, minor and trace elements plus several anions (chloride, carbonate, sulfate). In addition, O, H, C and Sr isotopes were measured in select waters.

Results and Discussion

Although these formations have different ages, depositional environments, diagenetic histories, and geochemical and mineralogical compositions (i.e. the UPP is significantly more carbonate rich than the Marcellus which is more siliceous), analysis of trends in fluid species over time shows that, overall, the TDS and major solubilized elements (Na, Ca, Cl) in the UPP and Marcellus brines are remarkably similar. Total dissolved solutes (TDS) in these brines ranged from approximately 40 to 250 g/L salt, and in general, concentrations increased with time elapsed since natural gas well completion and stimulation. The behavior of Na, Br, and Cl suggests that the produced water signatures from these formations are derived from the native formational brines which display evidence of originating from evaporated seawater. There is a strong correlation between Cl and Br, indicating that as anticipated both species behave conservatively, and the similarity among each of these brines suggests no appreciable contribution of salt from halite dissolution because Br is excluded from the halite structure. Other elements, such as K, which readily reacts between fluids and ion exchange sites on clays, generally exhibit conservative behavior for an individual site, but show significant variations among each of the different well pads.

The concentrations of Sr and Ba vary dramatically among well sites, and increase with respect to Cl⁻ over time, suggesting increasing solubilization presumably from desorption from clay minerals or dissolution of carbonates or sulfates from the source formation(s). The UPPW well site has very low Ba due to high-sulfate input fluid, which apparently resulted in precipitation of barite/celestite in the brines. In contrast the UPPS well site had elevated Sr (~ 3500 mg/L), presumably due to the use of Sr-rich recycled brine used in hydraulic fracturing. The Marcellus site displayed the highest Ba concentrations (up to 10 g/l) and highest Ba/Sr ratios in the fluids, due to the high concentration of barium in the Marcellus target (~ 1000 ppm, as compared to ~200 ppm in the UPP). These observations suggest that solutes in the FP fluids are derived from native brines, water-rock interactions that have occurred over geologic time scales, as well as some contribution from contemporaneous reactions in the subsurface. The results also show that input fluid volume and chemistry can influence flowback fluid chemistry and possibly production efficiency.

Products

Manuscript submitted to *Chemical Geology* now under review.

Comparative Geochemistry of Flowback Chemistry from the Utica/Point Pleasant and Marcellus Formations- Implications for the Source of Salts

Susan A. Welch¹, Julia M. Sheets¹, Rebecca A. Daly², Andrea Hanson³, Shikha Sharma⁴, Thomas Darrach^{1,5}, John Olesik¹, Anthony Lutton¹, Paula J. Mouser⁶, Kelly C. Wrighton², Michael J. Wilkins², Tim Carr⁴, and David R. Cole¹

Plan for Next Quarter

A manuscript on the mineralogy and its relationship to pore features in MSEEL core is being finalized.

Mineralogical, geochemical and petrophysical observations of core from the MSEEL: observations of lower Marcellus hydraulic fracturing target and associated formations.

Authors: Julia M. Sheets, Susan A. Welch, Alexander M. Swift, Tingting Liu, Rebecca A. Daly, Andrea J. Hanson, Tim Kneafsey, Stefano Cabrini, Paula Mouser, Shikha Sharma, Tim Carr and David R. Cole

Sharma Group MSEEL Report

- 1. Characterization of organic matter - kerogen extraction and characterization.** Core sample from the producing zone of Boggess 17H is crushed and the kerogen is being extracted. Extracted kerogen will be analyzed using ¹³C solid state analysis to determine its structural parameters. Using the NMR structural parameters, an average unit molecular model will be built. Similar analysis will be performed on 6 other kerogen samples isolated from Hue shale and Haynesville Shale and kerogen unit structure will be compared with the Boggess 17H kerogen and MSEEL sample. The NMR analysis and building kerogen unit structure of the samples are delayed due to COVID-19 but they are planned to be completed by December 2020.

Deliverables: 1) Complete NMR analysis and kerogen unit structural model building by Dec 2020 2) Present key findings in a conference in Spring 2021.

- 2. High-pressure and temperature fracture fluid/shale interaction experiments.** Shale-hydraulic fracturing fluid experiments (HFF) were conducted using the MSEEL sample from the producing zone. The experiment was conducted to understand the impact of a novel oxidative breaker sodium bromate on shale porosity/permeability of shales and contaminant release. The preliminary experiment is completed and the FI-ICP, ICP-MS, and GC-MS analysis was performed on the reacted fluids to determine the concentration of major elements, trace elements and organic compounds (VOCs and PAHs) respectively (Table. 1). The analysis show clear evidence of clay dissolution (High Al and Si), carbonate dissolution (high Ca), pyrite dissolution (high S), organic matter degradation (high U), and trace metal release (higher Sr, Zn, Cu, Se, Co, As, Li). The

organic analysis did not detect any BTEX compounds. However, they were not detected primarily because of non-targeted organic compounds concentration was too high. Interestingly, it was found one of the non-targeted compounds that was hindering BTEX analysis was high concentration bromoform which is toxic and probable carcinogenic. Among PAHs, acenaphthylene was also detected. In future experiments, we plan to perform non-targeted organic analysis to get a whole suite of organic compounds released by shale-HFF reactions. We also plan to perform ¹³C solid state NMR and porosity analysis on the reacted shale to determine the change in kerogen molecular structure and changes in pore structure.

Deliverable: 1) Conduct shale-HFF interaction experiments on more core samples with different HFF compositions by spring 2021. 2) Present key findings in a conference in Summer-Fall 2021.

Publications Submitted:

1. Sharma S, Agrawal V, Akondi R., Wang Y, Hakala A. 2020 Understanding controls on the geochemistry of hydrocarbon produced waters from different basins across the US. *Env. Sci. Processes and Impacts (in review)*
2. Sharma S, Agrawal V, Steven M, Hakala A, Lopano C. and Goodman A. 2020 Geochemical controls on CO₂ interactions with deep subsurface shales. *Int. Journal of Greenhouse Control* (submitted to NETL for review)
3. Brennan F, Agrawal V, Sharma S, Hakala A, Stuckman M. 2020. Effects of carbonate minerals on shale hydraulic fracturing fluid interactions in the Marcellus Shale. *Env. Sci. Processes and Impacts* (submitted to NETL for review)
4. V. Agrawal, S. Sharma 2020. Impact of Kerogen Heterogeneities on Hydrocarbon Production in Unconventional Shale Reservoirs. *AAPG Annual Convention*

	Detection limit	Unit	Conc. detected
Al	0.025	mg/L	3.754
As	0.018	mg/L	0.181
B	0.155	mg/L	8.999
Ba	0.016	mg/L	0.031
Be	0.001	mg/L	0.011
Ca	0.055	mg/L	1,756.57
Cd	0.001	mg/L	0.98
Co	0.003	mg/L	0.926
Cr	0.004	mg/L	0.045
Cu	0.004	mg/L	1.609
Fe	0.028	mg/L	0.277
K	0.161	mg/L	365.107
Li	0.048	mg/L	0.483
Mg	0.038	mg/L	364.676
Mn	0.023	mg/L	0.097
Mo	0.004	mg/L	0.039
Na	0.197	mg/L	12,837.36
Ni	0.007	mg/L	10.949
Pb	0.006	mg/L	0.049
S	-	mg/L	1,187.49
Sb	0.03	mg/L	0.031
Se	0.019	mg/L	1.369
Si	0.029	mg/L	40.872
Sr	0.002	mg/L	59.835
Tl	0.008	mg/L	0.008
V	0.002	mg/L	0.032
Zn	0.003	mg/L	57.337
TH	0.007	ug/L	0.055
U	0.002	ug/L	6.527
Acenaphthylene	0.5	ug/L	0.88
BTEX	500	ug/L	N.D.

Table 3.1. Major elements, trace elements and organic compounds (VOCs and PAHs) determined using FI-ICP, ICP-MS, and GC-MS analysis on fluid sample after shale-HFF reaction.

Topic 4 – Produced Water and Solid Waste Monitoring

Approach

MIP Site

Over three years into the post completion part of the program, the produced water and solid waste component of MSEEL has continued to systematically monitor changes in produced water quality and quantity. During year one of the study, hydraulic fracturing fluid, flowback, produced water, drilling muds and drill cuttings were characterized according to their inorganic, organic and radiochemistries. In addition, surface water in the nearby Monongahela River was monitored upstream and downstream of the MSEEL drill pad. Toxicity testing per EPA method 1311 (TCLP) was conducted on drill cuttings in both the vertical and horizontal (Marcellus) sections to evaluate their toxicity potential. Sampling frequency has been slowly scaled back following well development. Table 1 shows an “X” for sample collection dates. Wells 4H and 6H were brought back online in late 2016. Other blank sample dates in Table 1 indicate that samples were not collected, due to lack of availability of produced water from the well(s).

Year	2015						2016									
Day/Month	10-Dec	17-Dec	22-Dec	6-Jan	20-Jan	3-Feb	2-Mar	23-Mar	20-Apr	18-May	2-Jul	17-Aug	21-Jun	19-Oct	16-Nov	14-Dec
3H	X		X	X	X	X		X	X	X	X	X	X	X		X
4H															X	X
5H	X	X	X	X	X	X	X	X	X	X	X	X	X	X	X	
6H															X	X

Year	2017							2018						
Day/Month	13-Jan	14-Feb	13-Mar	7-Apr	5-May	12-Jul	3-Nov	20-Dec	22-Jan	23-Feb	16-May	2-Aug	16-Oct	15-Dec
3H	X	X	X	X	X	X	X	X	X	X	X	X		X
4H	X	X	X	X	X				X	X	X	X	X	X
5H		X			X			X	X		X		X	X
6H	X	X	X	X	X						X	X		

Year	2019							2020						
Day/Month	24-Jan	5-Mar	6-May	13-Jun	18-Sep	21-Oct	21-Nov	30-Dec	29-Jan	27-Feb	25-Mar	28-Apr	27-May	30-Jul
3H	X	X	X	X	X	X	X	X	X	X	X	X	X	X
4H	X	X					X	X	X	X	X	X	X	
5H	X	X	X	X	X	X	X	X	X	X	X	X	X	X
6H		X					X	X	X	X	X	X		

Table 4.1. MIP sampling events are indicated with an "X".

Bogges Site

Two control wells; 9H and 17H were selected for solids and aqueous studies at the newly developed Bogges well site.

Tophole was completed in Feb 2019 for 9H and Jan 2019 for 17H. Samples of vertical drilling were not obtained due to completion prior to the start of the Bogges project.

Horizontals were initiated on 19 June 2019 for 17H and 20 May 2019 for 9H (Table 2). A drilling mud sample along with depth samples at 8,500ft; 10,000ft; 11,000ft; 13,000ft; and 15,000ft were collected and analyzed for parameters shown in Table 3.

Table 4.2. Sample depth and dates for collection of horizontal drilling mud and cutting samples.

Depth/Well	Mud 9H	8500 9H	10000 9H	11000 9H	13000 9H	15000 9H
Date	5/27/2019	5/27/2019	5/28/2019	5/29/2019	5/29/2019	5/30/2019
Depth/Well	Mud 17H	8500 17H	10000 17H	11000 17H	13000 17H	15000H
Date	7/1/2019	7/1/2019	7/1/2019	7/1/2019	7/1/2019	7/1/2019

Table 4.3 Solids analysis list.

Analysis	Method	Units	Parameter	
Diesel Range Organics by GC-FID	SW8015M	mg/kg-dry	DRO (C10-C28)	
			ORO (C28-C40)	
			% Rec Surr: 4-terphenyl-d14	
Gasoline Range Organics by GC-FID	SW8015D	ug/Kg	GRO C6-C10)	
			% Rec Surr: Toluene-d8	
Volatile Organic Compounds	SW8260B	ug/kg-dry	Ethylbenzene	
			m,p- Xylene	
			o- Xylene	
			Styrene	
		% Rec	Toluene	
			Xylenes total	
			Surr: 1,2- Dichloroethane-d4	
			Surr: 4-Bromofluorobenzene	
Radionuclides	EPA 901.1	pCi/g	Surr: Dibromofluoromethane	
			Surr: Tolouene-d8	
	9310		Potassium-40	
			Radium-226	
			Radium-228	
Inorganics	SW9056A	mg/kg-dry	Gross Alpha	
			Gross Beta	
	SW9034		Br	
			Cl	
		SO4		
	E353.2	sulfide		
	E354.1	nitrate		
	A2510M	nitrite		
	SW9045D	μS/cm	EC	
		units	pH	
	SW6020A	A4500-CO2 D	mg/kg-dry	alk bicarb
				alk carb
				alk t
				TP
		E365.1 R2.0	Ag	
			Al	
			As	
			Ba	
			Ca	
			Cr	
			Fe	
			K	
Li				
Mg				
Mn				
Na				
Ni				
Pb				
Se				
Sr				
Zn				
Moisture	E160.3M	%	Moisture	
Chemical Oxygen Demand	E4104 R2.0	mg/kg-dry	COD	
Organic Carbon - Walkley-Black	TITRAMETRIC	% by wt-dry	OC-WB	
Oil & Grease	SW9071B - OG	mg/kg-dry	O&G	

Flowback sampling was initiated on 18 Nov 2019 with weekly collection at 9H and 17H for the first four weeks (Table 4). Monthly sampling began following the initial weekly sampling effort. Samples were not collected in June and August.

Table 4.4. Boggess sampling events are indicated with an "X".

Year	2019						2020					
Day/Month	18-Nov	25-Nov	2-Dec	10-Dec	16-Dec	27-Dec	29-Jan	27-Feb	25-Mar	28-Apr	27-May	30-Jul
9H	X	X	X	X	X	X	X	X	X	X	X	X
17H	X	X	X	X	X	X	X	X	X	X	X	X

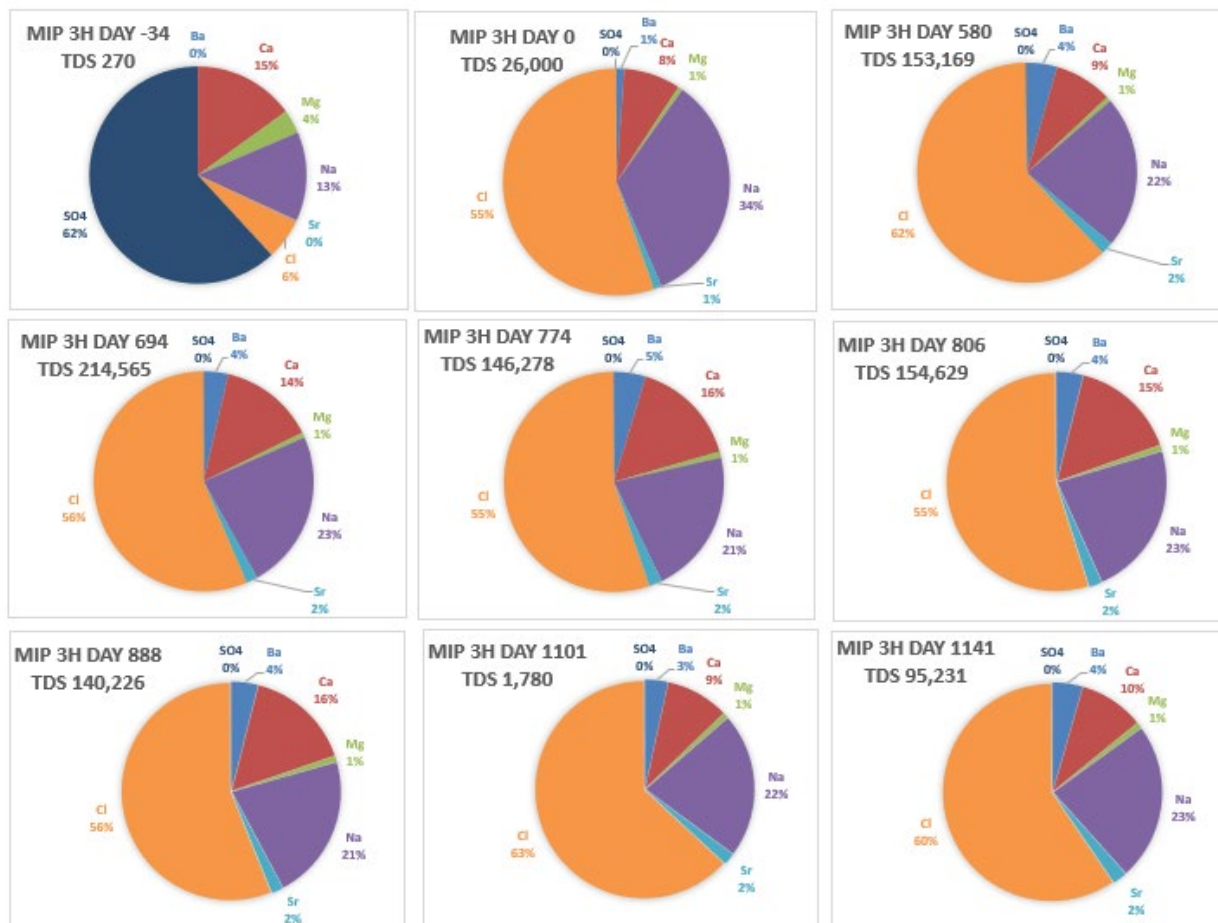
Results & Discussion

MIP Site

Major ions analysis results are pending for samples collected on 30-Jul-2020 from MIP 3H and 5H. Results will be included in the FY21 Q1 report.

Major ions – trends in produced water chemistry

While makeup water was characterized by low TDS (total dissolved solids) and a dominance of calcium and sulfate ions, produced water from initial flowback is essentially a sodium/calcium chloride water (**Figure 4.1**).



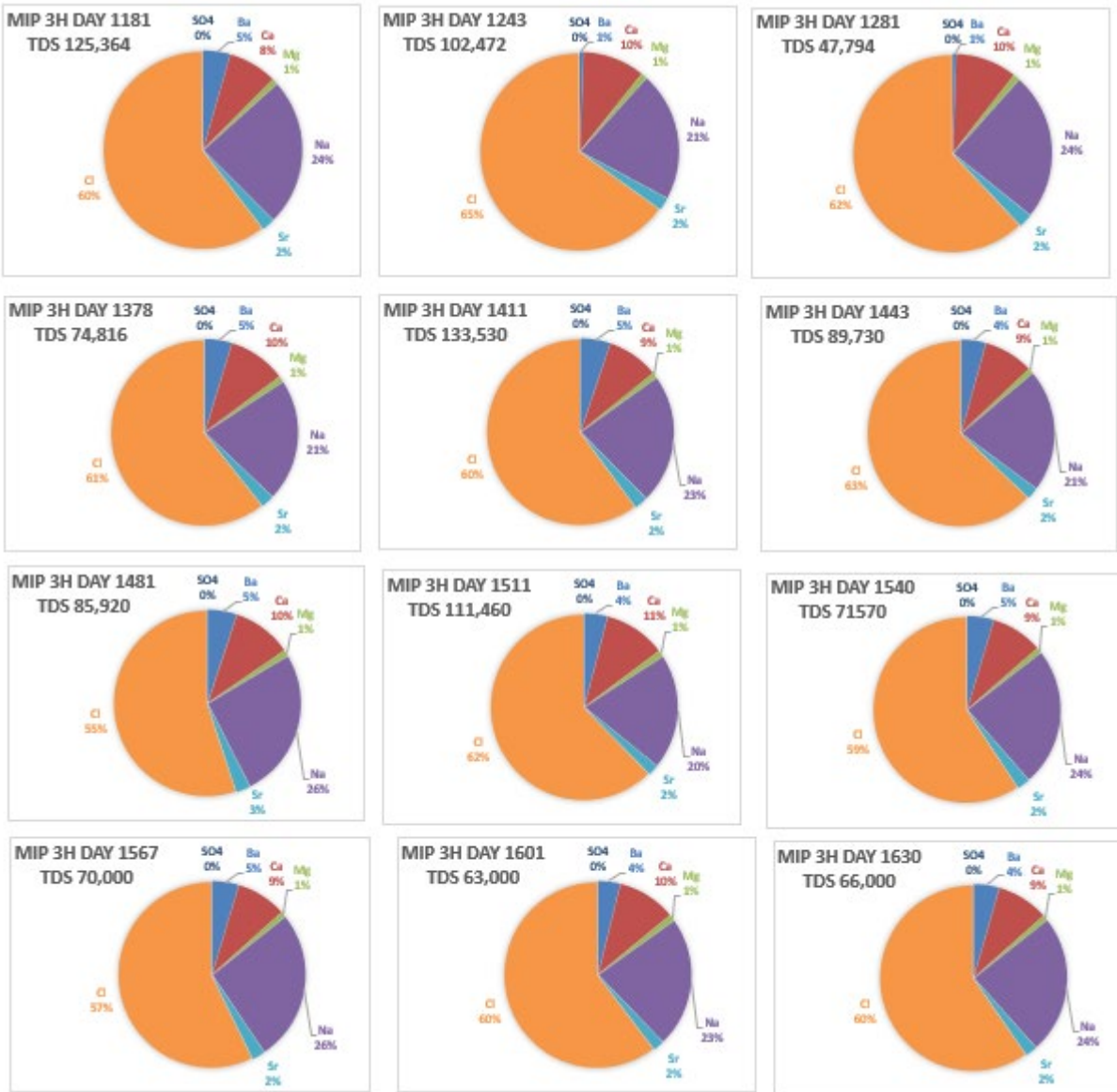


Figure 4.1. Changes in major ion concentrations in produced water from well MIP 3H. Top left Day -34 represents makeup water from the Monongahela River, top center is produced water on the first day (Day 0) and the remainder of pie charts show flowback and produced water on sampling dates through the 1630th day post completion.

In wells 3H and 5H, TDS increased rapidly over the initial 90 days post completion while TDS stabilized between 100,000 and 200,000 mg/L through day 1181(3H) (Figure 2). Note that 3H and 5H were both shut-in near day 966 and brought back online prior to sampling on day 1101. 3H and 5H are showing an upward trend following day through day 1243 (e.g. May 2019). Results from day 1281 (e.g. June 2019), TDS declined in both wells. It's uncertain if the wells were shut down between day 1243 and day 1281, which might explain the decrease in TDS.

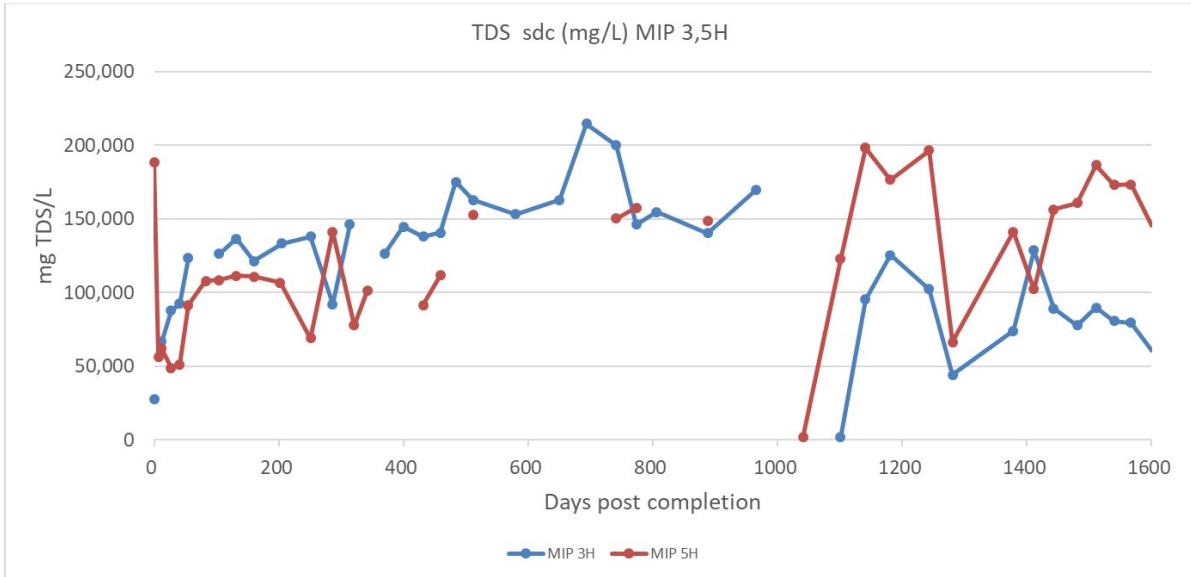


Figure 4.2. Changes in produced water TDS sdc (sum of dissolved constituents) through the first 1630 days post completion (3,5H).

The older 4H and 6H wells offer insight into the longer-term TDS trend. Those wells only came back on line during this quarter after a shut-in period of 315 days and those results vary but they are much lower than the current values for wells MIP 3H and 5H. Both 4H and 6H were shut down during late 2017. TDS was very low at MIP 4H during the first sampling event of early 2018. Calculated TDS was 2,455 mg/L and lab reported TDS was 2,300 mg/L. A similarly low TDS trend was noted when well 4H went back online around 1793 days post-completion (after being shut-in for 315 days) and again when 6H went online around day 2339, a rise in TDS subsequently follows the initial return to online status with TDS on an upward trend, reaching 160,000 mg/L for 6H. MIP 6H was shut down between August 2018 and March 2019 and again after March 2019 through November 2019. TDS was 30,970 mg/L on day 2632 (March 2019) and is downward trending following day 2893 (November 2019) through day 2991 at 10,683 mg/L at day 2991. 6H noted an increase from 21,708 to 91,211 mg/L TDS between day 3018 and 3052. (Figure 4.3).

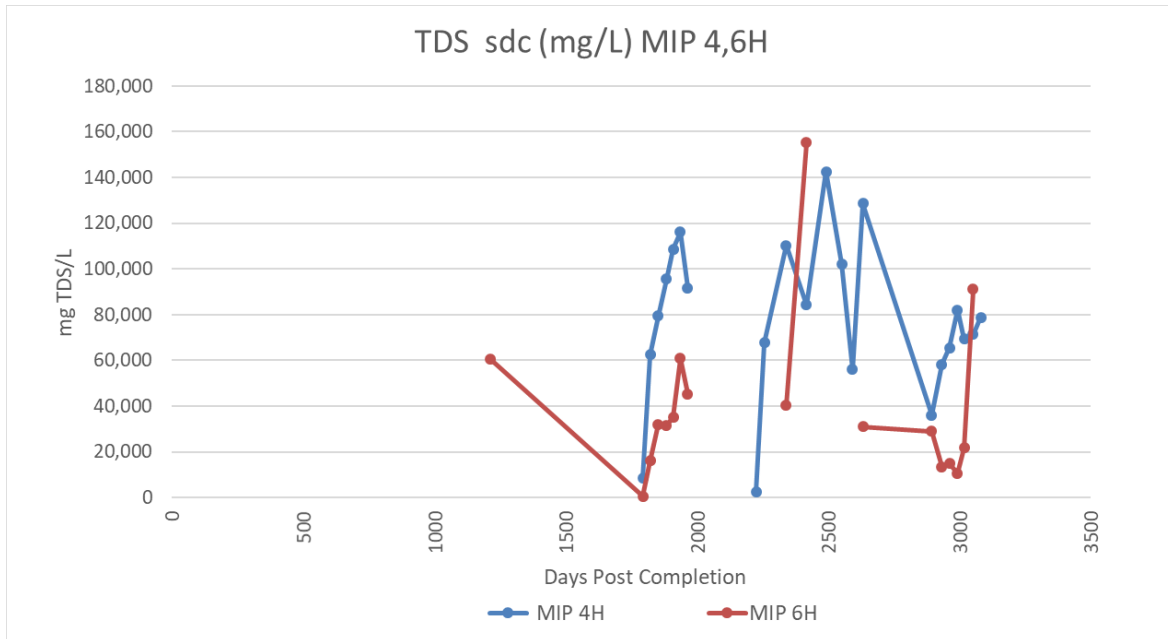


Figure 4.3. Changes in produced water TDS sdc (sum of dissolved constituents) through the first 1793 through 3081 days post completion (4,6H).

Water soluble organics

The water-soluble aromatic compounds in produced water: benzene, toluene, ethylbenzene and xylene were never high. With two exceptions at post completion day 314 and 694, benzene has remained below 30 µg/L (Figure 4.4). This seems to be a characteristic of dry gas geologic units. After five years, benzene has mostly declined below the drinking water standard of 5 µg/L.

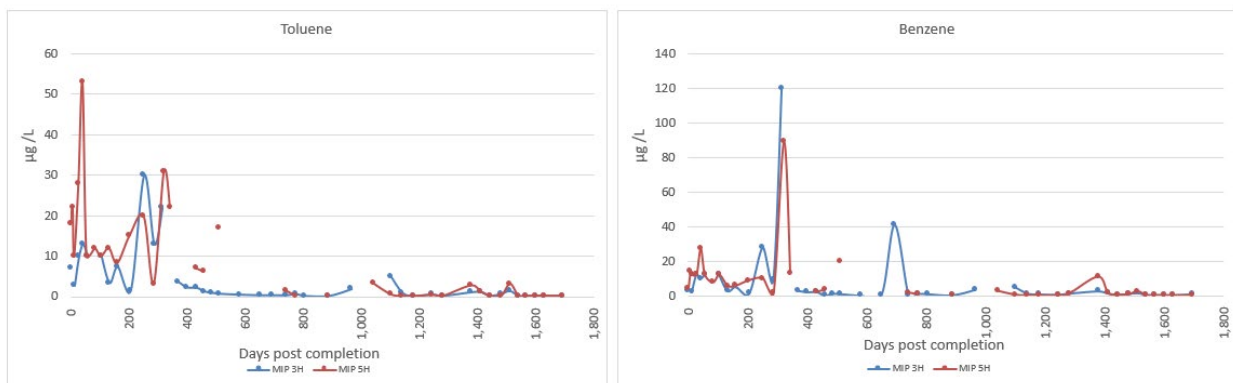


Figure 4.4. Changes in benzene and toluene concentrations. The figure shows data from well both 3H and 5H.

Radium isotopes

The radiochemical concentrations were determined by Pace Analytical in Greensburg PA, a state certified analytical lab. Radium concentrations generally increased through 800 days post completion at wells MIP 3H and 5H. Maximum levels of the radium isotopes reached about 21,800 pCi/L at the unchoked 3H well and around 17,800 pCi/L 5H. After returning online prior to day 966, both wells have remained below 15,000 pCi/L through day 1694 (Figure 5).

Radioactivity in produced water

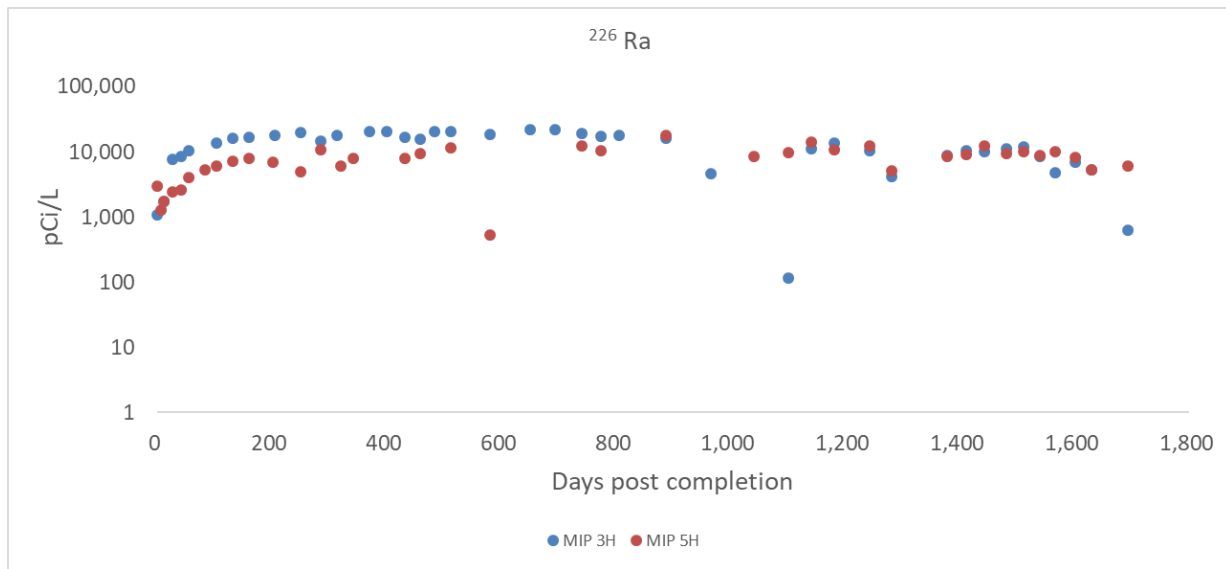


Figure 4.5. The radium isotopes are plotted against days post well completion. Well 5H was choked more frequently than the 3H well.

Radium concentrations at wells 4H and 6H were below 9,000 pCi/L during all sampling periods. Both wells were choked after day 1963. Well 4H was reopened at day 2225, radium was 58 pCi/L on the first sampling after the reopening and 3719 pCi/L at day 2257, a month later (Figure 6) peaked at 5,127 pCi/L then returned to 3,892 pCi/L. The same trend is noted at day 2339 when 4H returned online with 57 pCi/L then peaked at day 2632 with 8,197 pCi/L. Both wells were shut down during summer months, between days 2632 and 2893. 6H is on a downward trend from 1901 pCi/L to 739 pCi/L from day 2893 through the most recent collection on day 2991. Additional data is needed to capture long-term trends.

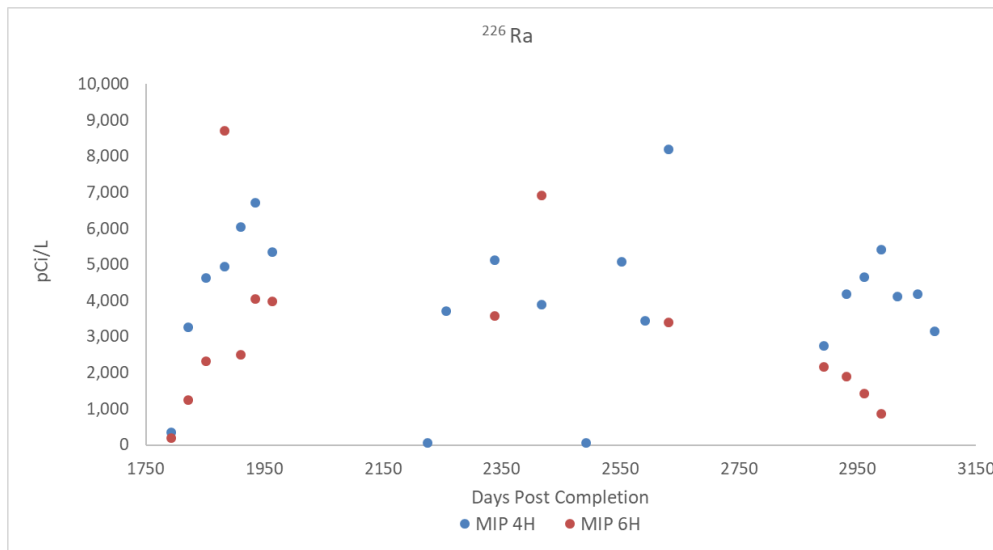


Figure 4.6. The radium isotopes are plotted against days post well completion. Well 4H and 6H were choked at day 1963 and again at day 2632. At day 2225, 4H was reopened showing a value of 58 pCi/L and reopened again at day 2192 showing a value of 57 pCi/L.

Figure 4.7 and Figure 8 show the relationship between gross alpha and ^{226}Ra at 3H and 5H. Analysis for alpha was not conducted after day 1181.

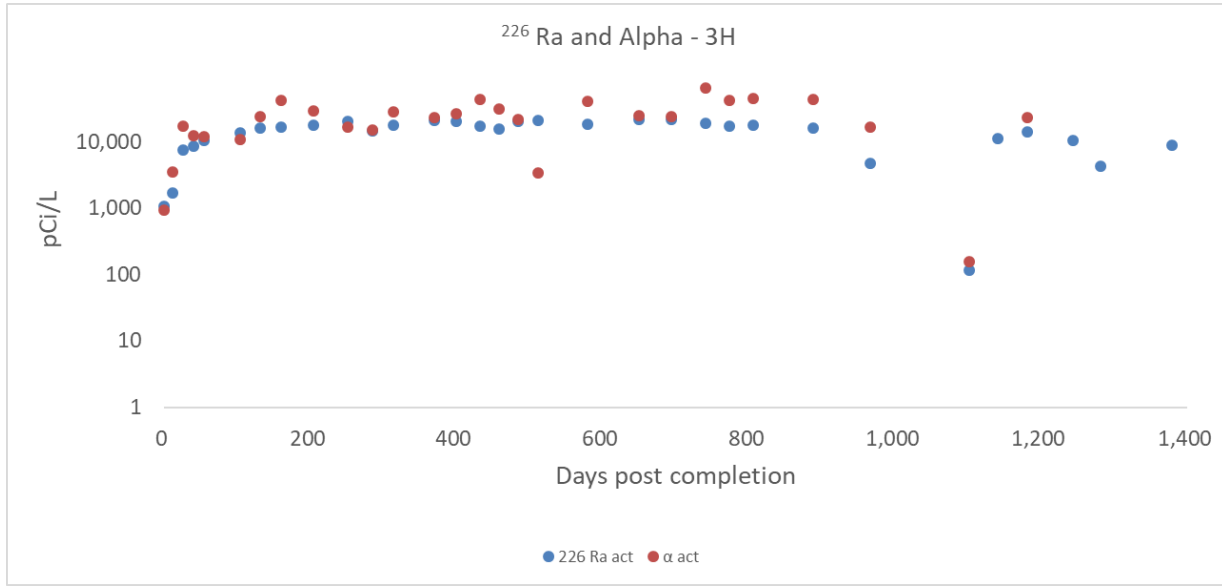


Figure 4.7. The relationship between gross alpha and ^{226}Ra as a function of time post completion at 3H. Note: analysis for alpha was not conducted after day 1181.

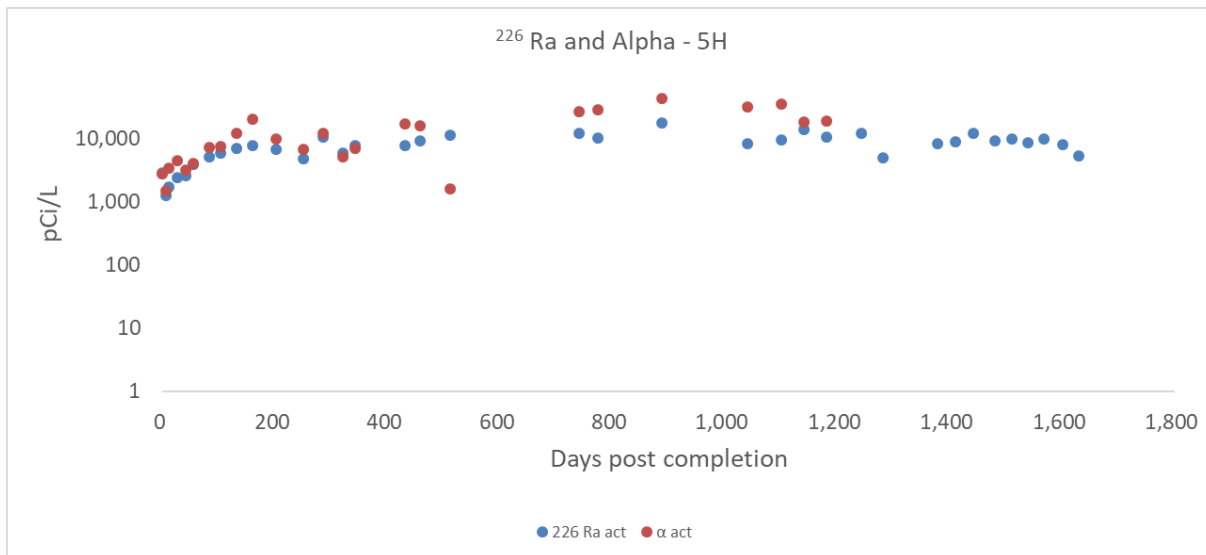


Figure 4.8. The relationship between gross alpha and ^{226}Ra as a function of time post completion at 5H. Note: analysis for alpha was not conducted after day 1181.

The highest values reported in the older wells at 4H and 6H were 17,550 pCi/L gross alpha and 8,197 pCi/L ^{226}Ra . The relationship between gross alpha and ^{226}Ra for wells 4H and 6H are shown in figures 9 and 10. Alpha was not determined after day 2632.

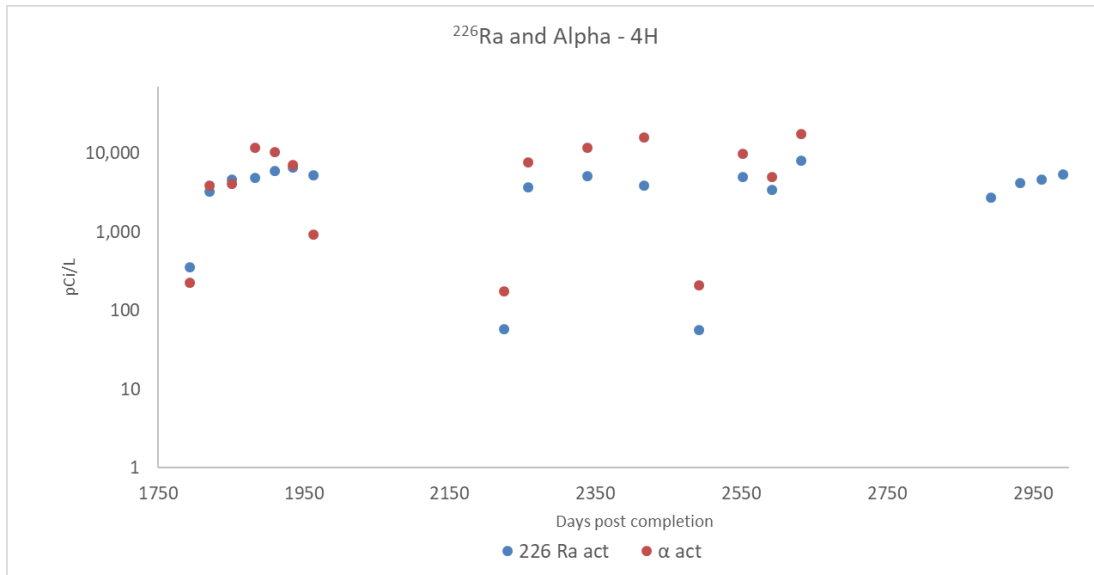


Figure 4.9. The relationship between gross alpha and ²²⁶Ra as a function of time post completion at 4H. Note: analysis for alpha was not conducted after day 2632.

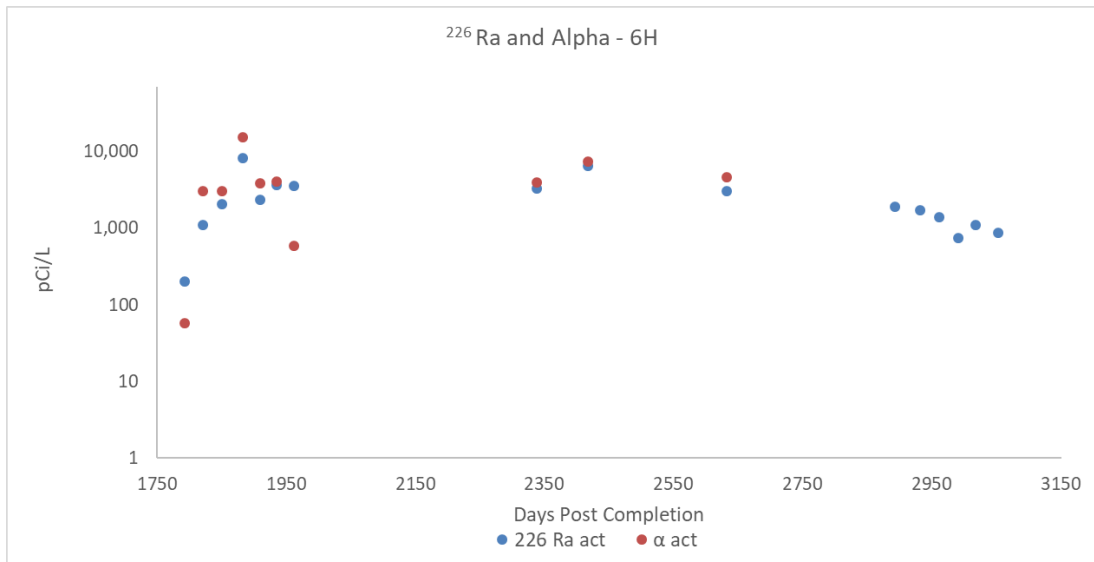


Figure 4.10. The relationship between gross alpha and ²²⁶Ra as a function of time post completion at 6H. Note: analysis for alpha was not conducted after day 2632.

Bogges Well

Solids

Analytical results have been received for drilling muds and cuttings collected at 9H at depth intervals of 8,500ft; 10,000ft; 11,000ft; 13,000ft; and 15,000ft. Anions (e.g. Br, Cl, and SO₄) and Cations (e.g. Ba, Ca, Mg, Mn, Na, and Sr) are shown in Figure 11. Drill cuttings from 9H are predominately Calcium. The full list of solids parameters and methods are shown in Figure 3.

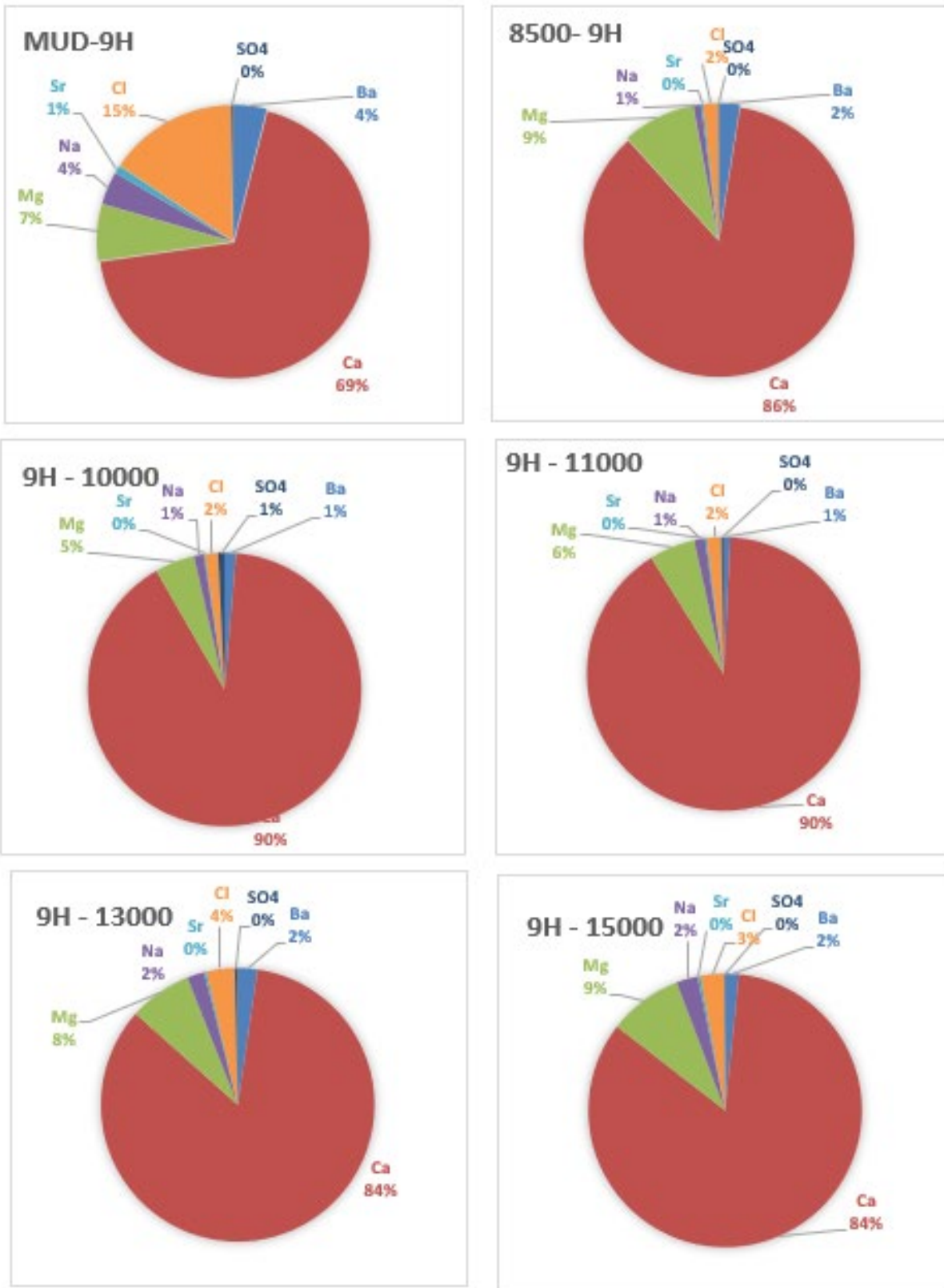


Figure 4.11. Anions/cations of drilling mud and cutting solids from 9H.

Figure 4.12 depicts anions/cations of drilling mud and cuttings from 17H. Magnesium was more prevalent in the 8,500ft and 10,000ft depths for 17H in comparison to the same depths for 9H.

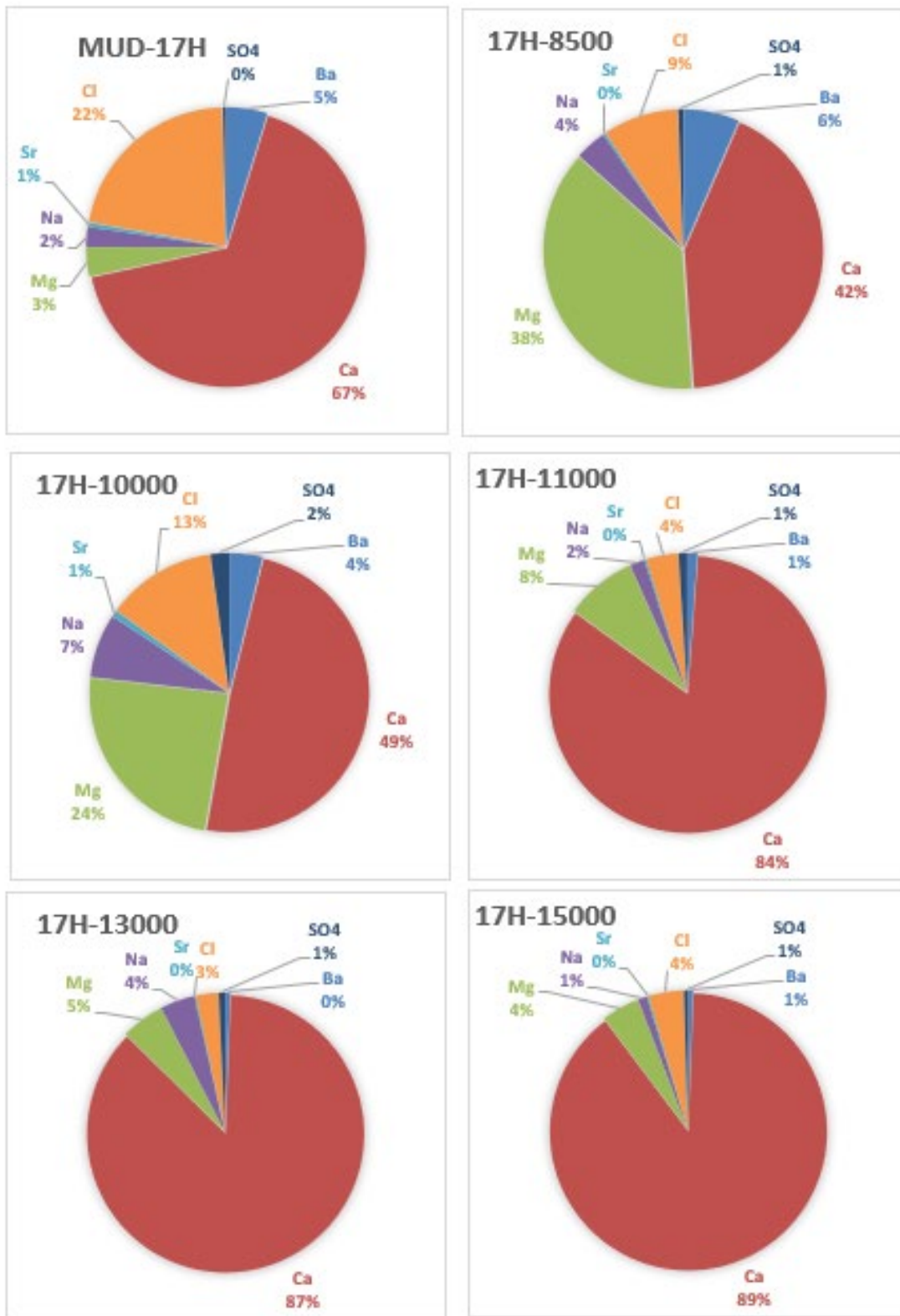


Figure 4.12. Anions/cations of drilling mud and cuttings solids from 17H.

Figure 4.13 and 4.14 depict combined radium 226 and 228 of solids in drilling mud and cuttings solids from 9H and 17H.

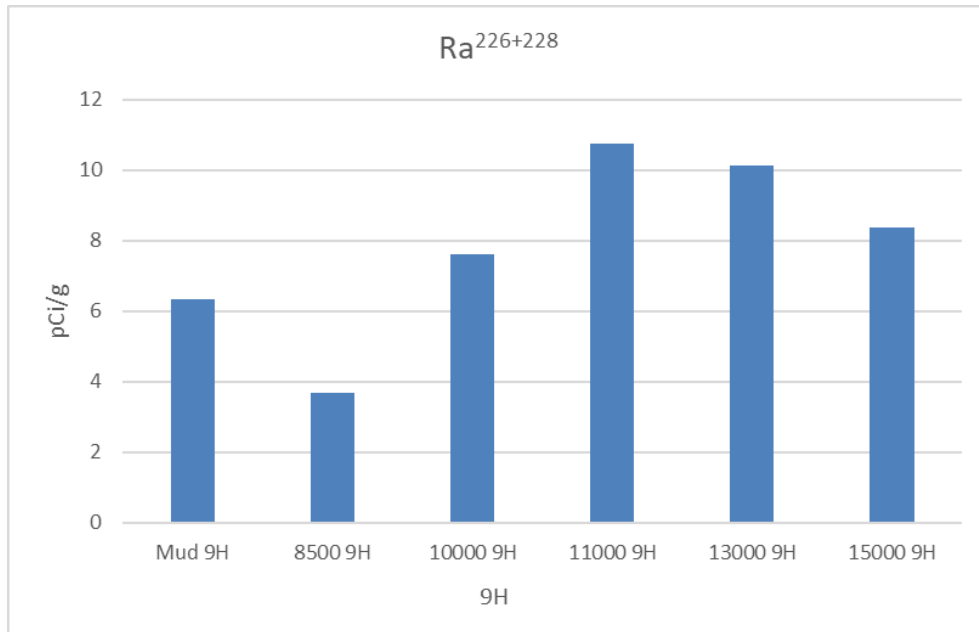


Figure 4.13. 9H Combined radium 226 and 228 for drilling mud and cuttings solids.

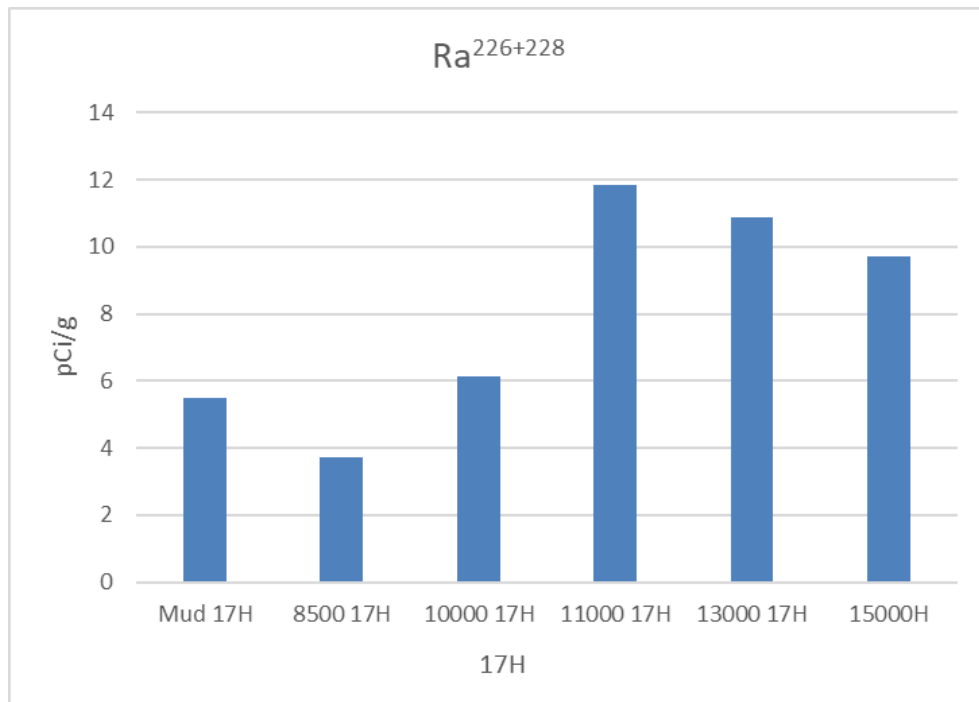


Figure 4.14. 17H Combined radium 226 and 228 for drilling mud and cuttings solids.

For comparison purposes, solids radium analysis from MIP 5H and 3H are shown in Figure 15 and Figure 16. In all wells analyzed, 3H and 5H from MIP along with 9H and 17H at Bogges, combined radium 226 and 228 remained below 12 pCi/g.

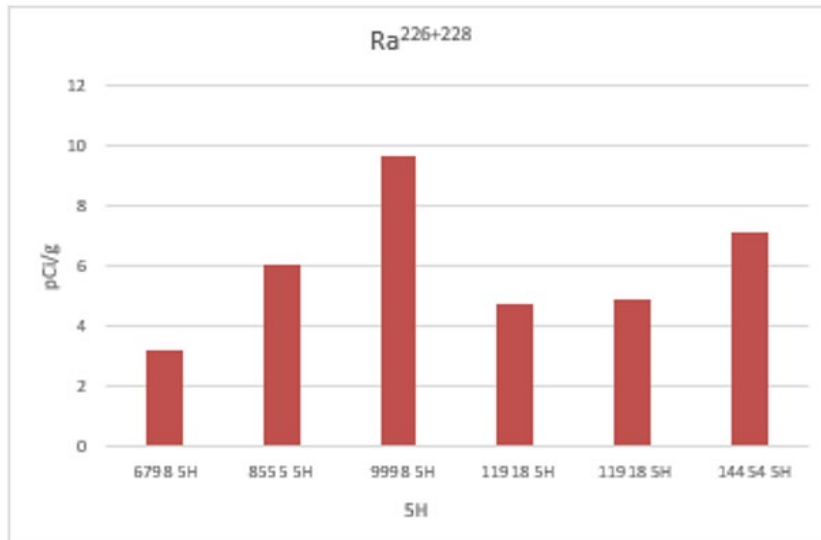


Figure 4.15. Combined Ra 226 + 228 for 5H MIP sites.

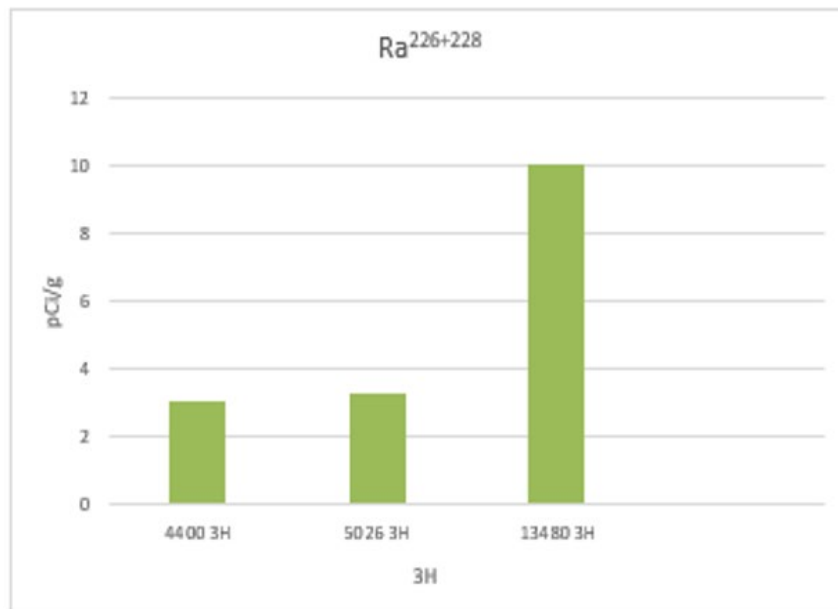
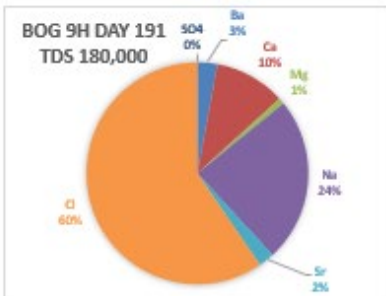
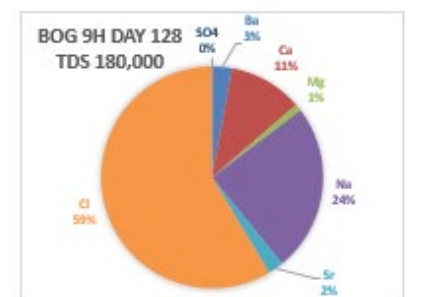
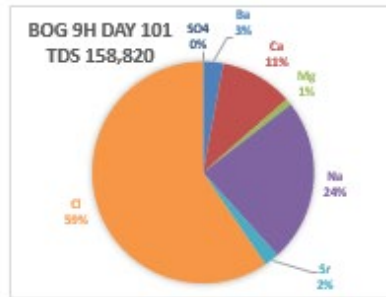
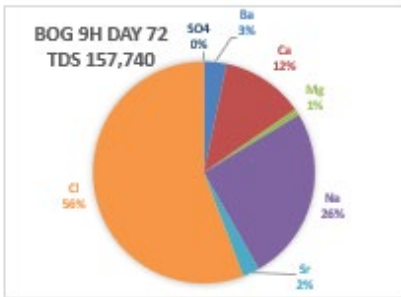
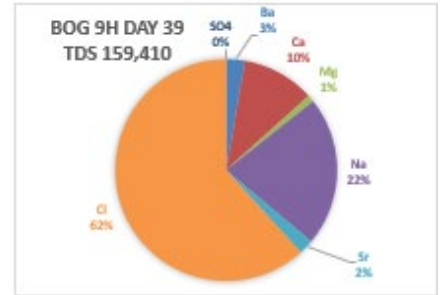
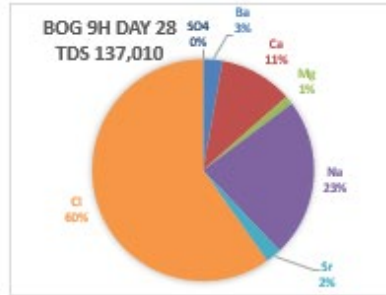
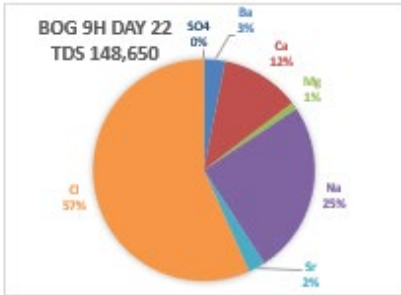
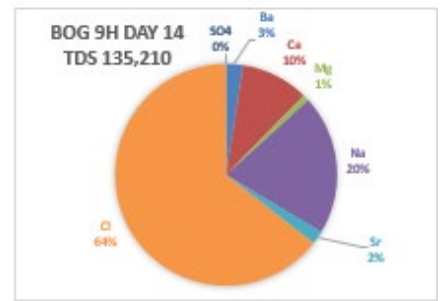
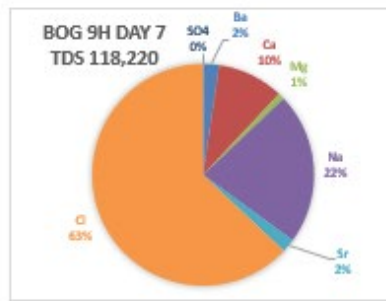
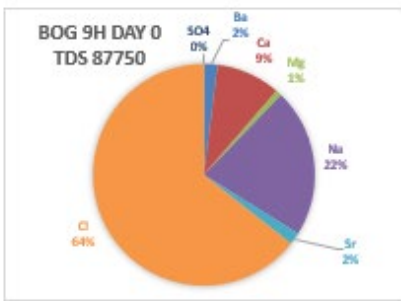


Figure 4.16. Combined Ra 226 + 228 for 3H MIP sites.

Major ions – trends in produced water chemistry

While makeup water was characterized by low TDS and a dominance of calcium and sulfate ions, produced water from initial flowback is essentially a sodium/calcium chloride water as noted in the earlier discussion regarding results from MIP. Preliminary results from days 0-191 at Bogges 9H and 17H are consistent with earlier results from MIP (Figure 17).

Major ions analysis results are pending for samples collected on 30-Jul-2020 from Bogges 9H and 17H. Results will be included in the FY21 Q1 report.



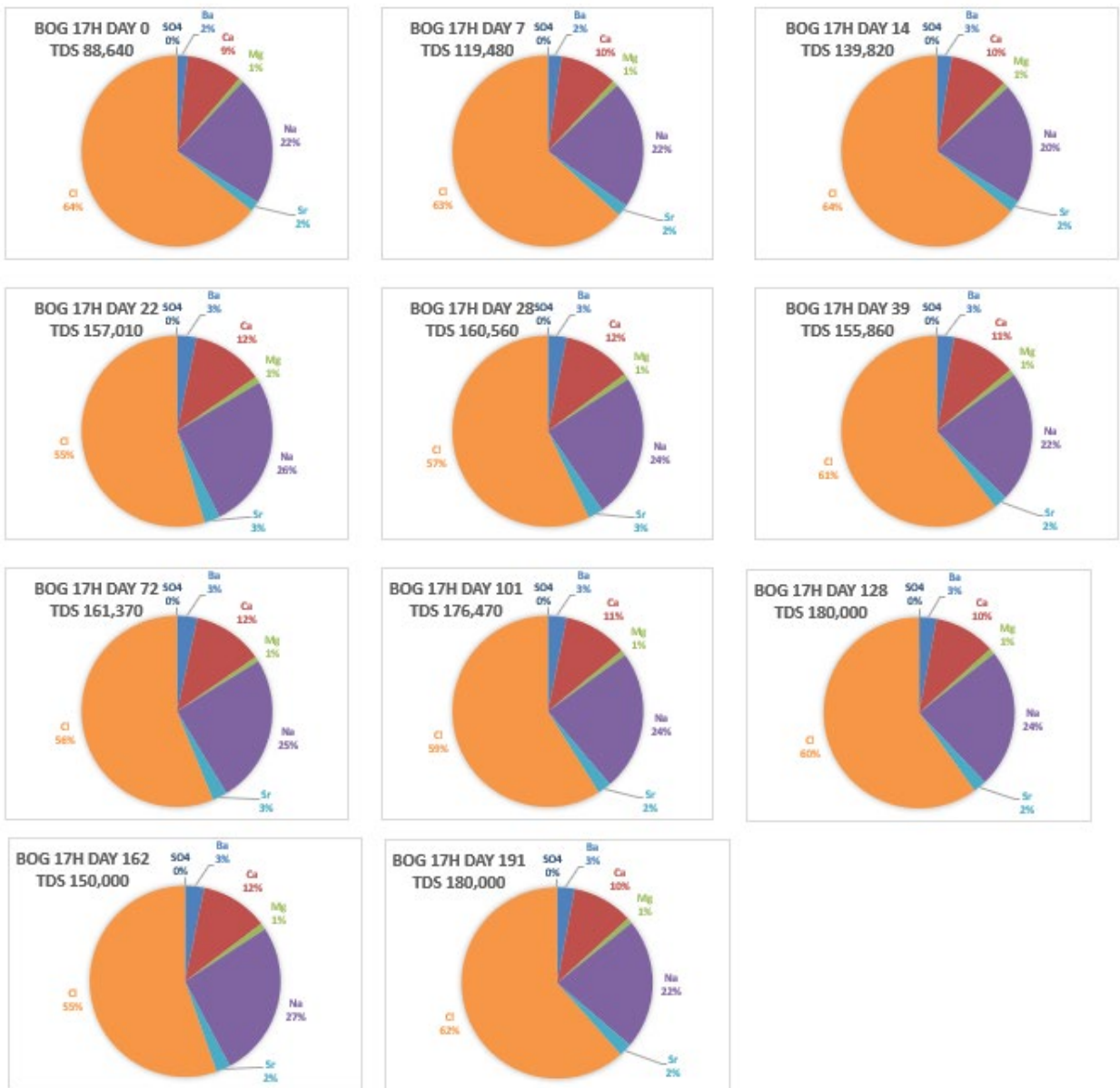


Figure 4.17. Major ion concentrations in produced water from wells BOGGESS 9H and 17H.

Preliminary TDS (scd) at Boggess 9H and 17H show a slight upward trend between days 0 and 191 (Figure 18).

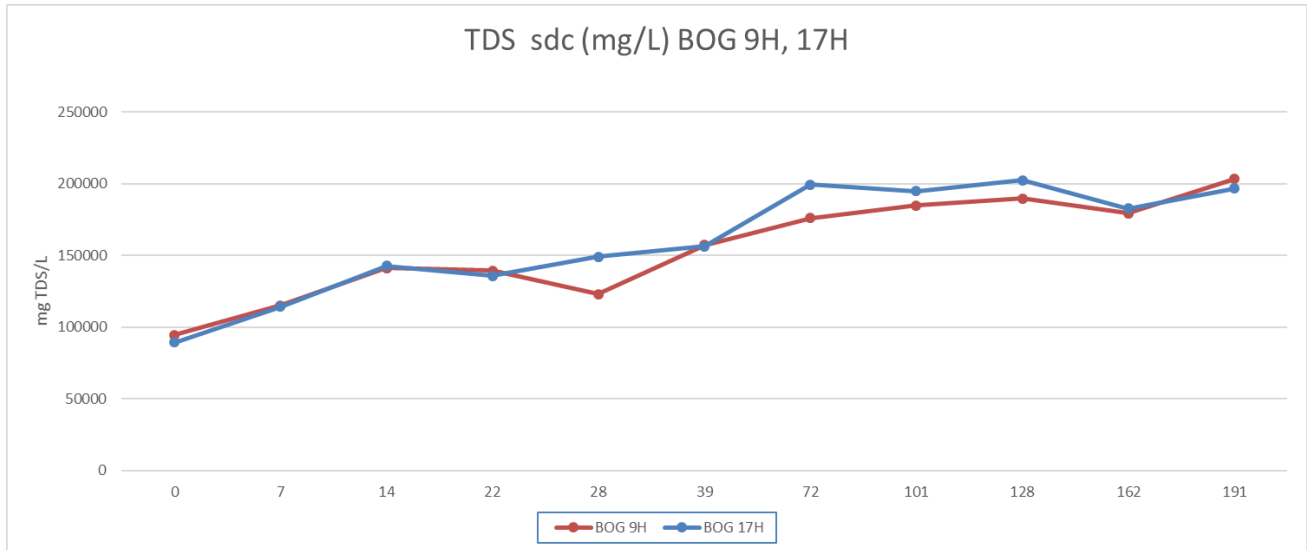


Figure 4.18. TDS (sdc) at Boggess 9H and 17H; days 0-191.

Radium concentrations were below 15,000 pCi/L at both 9H and 17H at 255 days post completion (Figure 19).

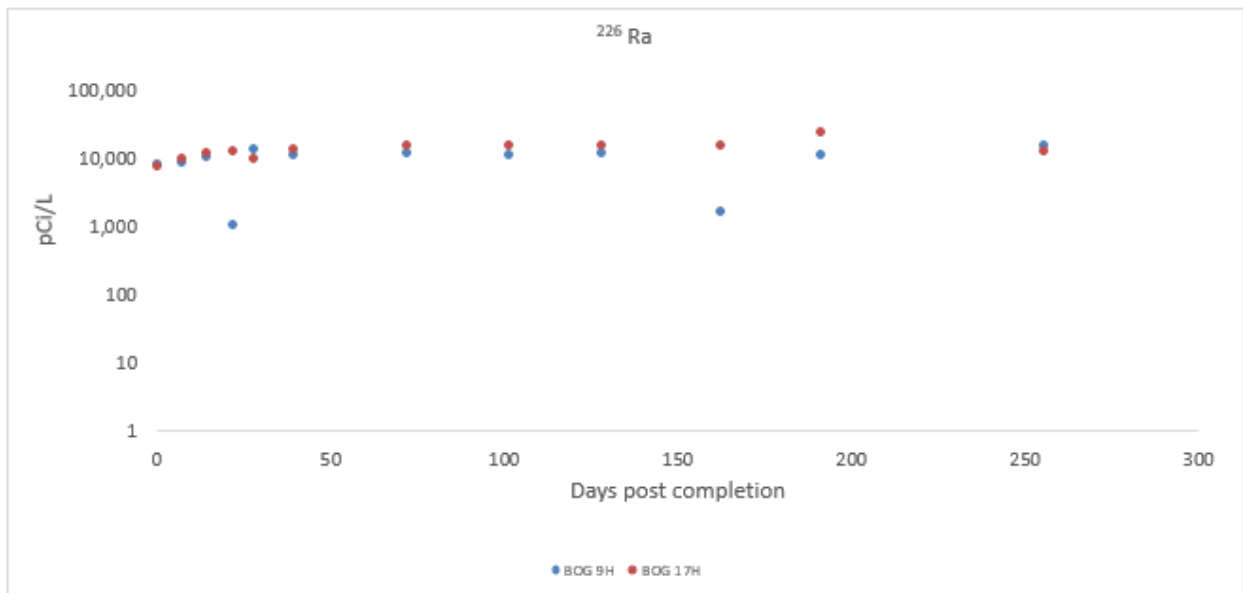


Figure 4.19. The radium isotopes are plotted against days post well completion at Boggess 9H and 17H; days 0-255.

Products

None for this quarter.

Plan for Next Quarter

We will continue monthly sampling at MIP and analyze flowback/produced water (FPW) from MIP 3H, 4H, 5H and 6H if they are online.

We will continue sampling produced water at Boggess Pad control wells 9H and 17H on a monthly basis. Following the same protocols used at MIP wells, we will continue to characterize their inorganic, organic and radio chemistries.

Topic 5 – Environmental Monitoring: Air & Vehicular

Approach

During the past quarter, the team completed its 16th methane audit at MSEEL 1.0 (MIP). Based on our confidence in the fast methane ethane analyzer (FMEA) it was deployed as the primary analyzer for this audit. The 16th audit was completed on September 23rd with approval from NNE. This required approval by the research office and the team used social distancing at all times and when social distancing was not feasible, face coverings were deployed in addition to standard PPE. Regarding the unmanned tower operation, the tower continues to operate and is collecting data for OTM 33A and Eddy Covariance analysis. We are in discussions to continue additional audits and tower operation until March 2021. While active data collection continues using the controlled release data and the MSEEL data on methods to improve indirect quantification techniques with multiple joint (NSF/DOE funded) publications under development. Regarding the energy audit analysis, we previously reported on baseline comparisons between boiler diesel fuel demand compared with available exhaust energy from an alternative well pad. The results showed potential to completely offset boiler operation. However, additional model was required to examine realistic heat exchanger effectiveness. ChemCAD software has been obtained from the Chemical Engineering Department. As such, the program has enabled software design of an ASME compliant gas liquid exchanger operating on boundary conditions obtained from the field. Additional modeling in both ChemCAD and now in Simulink are ongoing. Summary results from these key areas are presented below.

Results and Discussion

Audits

Figure 5.1 shows the updated audit results including the 16th audit conducted on September 23rd. The methane emissions rate was 0.29 kg/hr, which decreased the average of all audits downward to 4.48 kg/hr while the geometric mean was 0.85 kg/hr. The ethane emissions of Audits 13-16 are presented in Figure 5.2. Ethane emissions for Audit 16 were only 1.24 g/hr. This brought the average of all audits to 4.24 g/hr and the geometric mean to 2.3 g/hr. Now that the 16th audit has been completed, we are downloading historical production data to examine if there are trends in production or site activity that correlate with methane trends. We recently held discussion with the site operator to discuss the audit results and they may be able to offer some insight on “atypical” operations associated with elevated tank emissions earlier in the program.

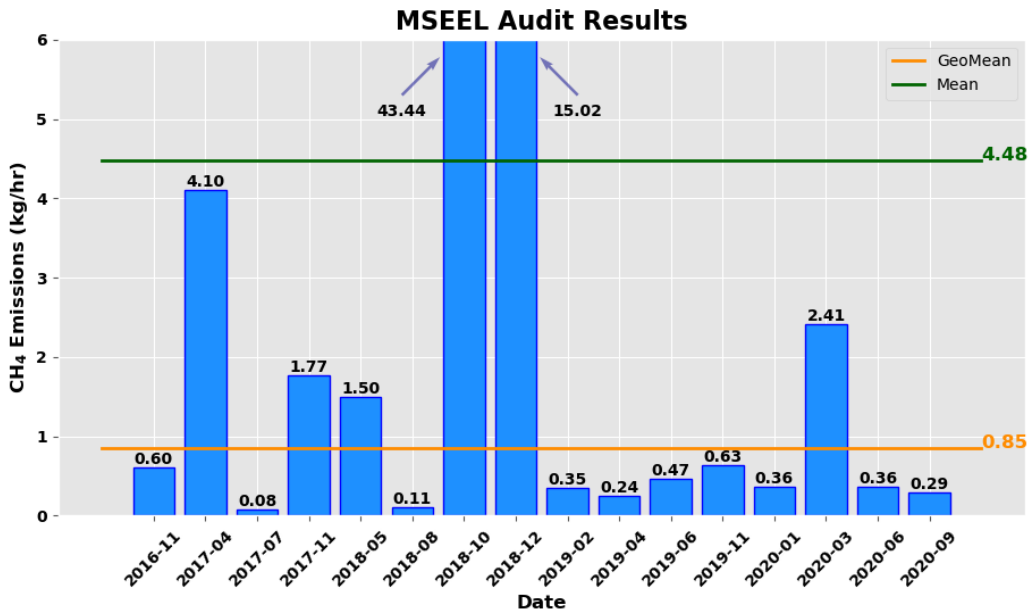


Figure 5.1: MSEEL CH₄ Audit Results.

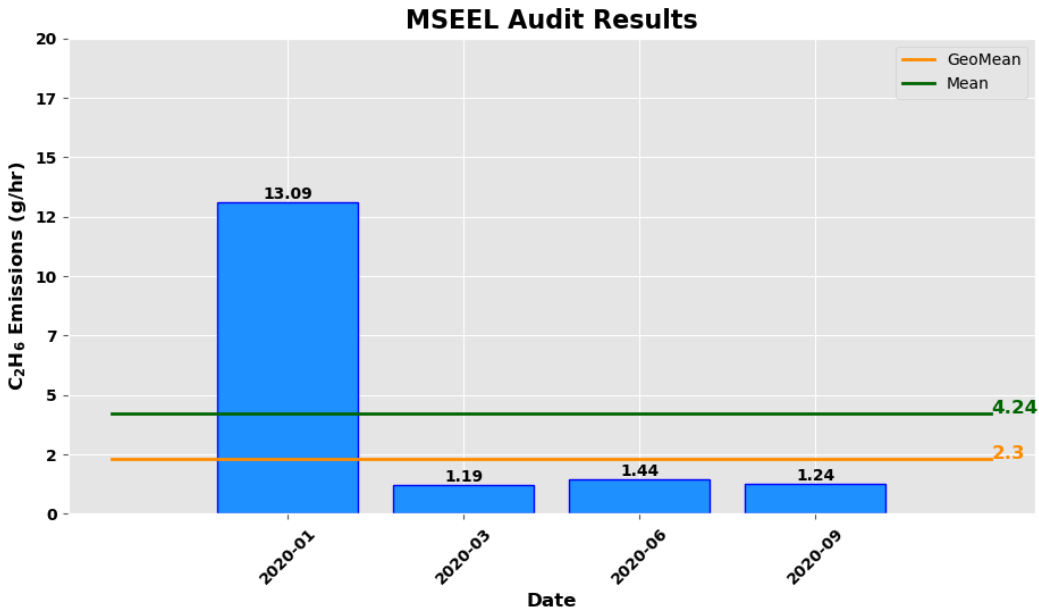


Figure 5.2: MSEEL C₂H₆ Audit Results.

Indirect Quantification System Comparison

An indirect quantification measurement system was placed on site in November of 2019 and is currently measuring atmospheric methane, CO₂, and other variables at the site. The goal of this application is to develop a method of methane quantification that does not require site access for direct measurements (those from audits).

Indirect quantification measurements were compared to site methane emission for the 16th audit from September 23rd, 2020. The indirect quantification techniques evaluated included OTM 33A and Eddy Covariance (EC). These measurements were used from a period of ± 1 day of the audit. Both methods used an average period of 30 minutes, producing an average emissions rate for each half hour analyzed. The OTM 33A results provide true comparisons as this method provides mass emissions rates that can be compared to site level emissions from audits. These estimations require a distance to determine an estimate. The average distance from the four component groupings on site was used as the input distance for the calculations. The distances used to determine the average distance of 122 m from an average distance of 167° east of north are presented on the map of Figure 5.3. The EC method produces a flux estimation in ($\mu\text{mol}/\text{m}^2\text{s}$) and were converted to a mass emission rate using a simple cumulative normal contribution to flux (CNF) estimation presented by Shuepp et al. (1990) which is based on an analytical solution to the diffusion equation. The area used for the estimation of the flux was based on the distance of 80% of the flux contribution and was assumed to a circle for simplicity. This area estimation combined with conversion factors for methane allowed for a mass rate estimation.



Figure 5.3: Directions to Component Groups.

To determine the indirect emissions estimates data were filtered based on several criteria. OTM 33A and eddy covariance estimates were filtered by different criteria. We developed a rating

system for the OTM 33A estimates based on the wind direction, curve fitting of the method, and differences between the maximum methane concentration, wind direction, and direction of components. The rating scales from 0 to 1 with 0 representing more reliable data periods. OTM 33A data were eliminated if the total rating was greater than 0.5. OTM 33A estimates were also removed if the difference between the average wind direction and the average component direction greater than was $\pm 45^\circ$. The number of OTM 33A estimates after these filters was 35. Eddy covariance data were also filtered by criteria typically employed by users of the method. A quality control value was used based on Mauder and Foken (2004) which utilizes a 0-2 rating system with 0 being the best. Data were eliminated from consideration if the rating was 2. A u-star filtering method is typically used for eddy covariance estimations; however, not enough data were evaluated to find a valid cut-off value. The resultant number of valid eddy covariance periods was 37. The eddy covariance data were also filtered using the same wind direction difference as the OTM 33A data. An example of the wind filter is presented in Figure 5.4.

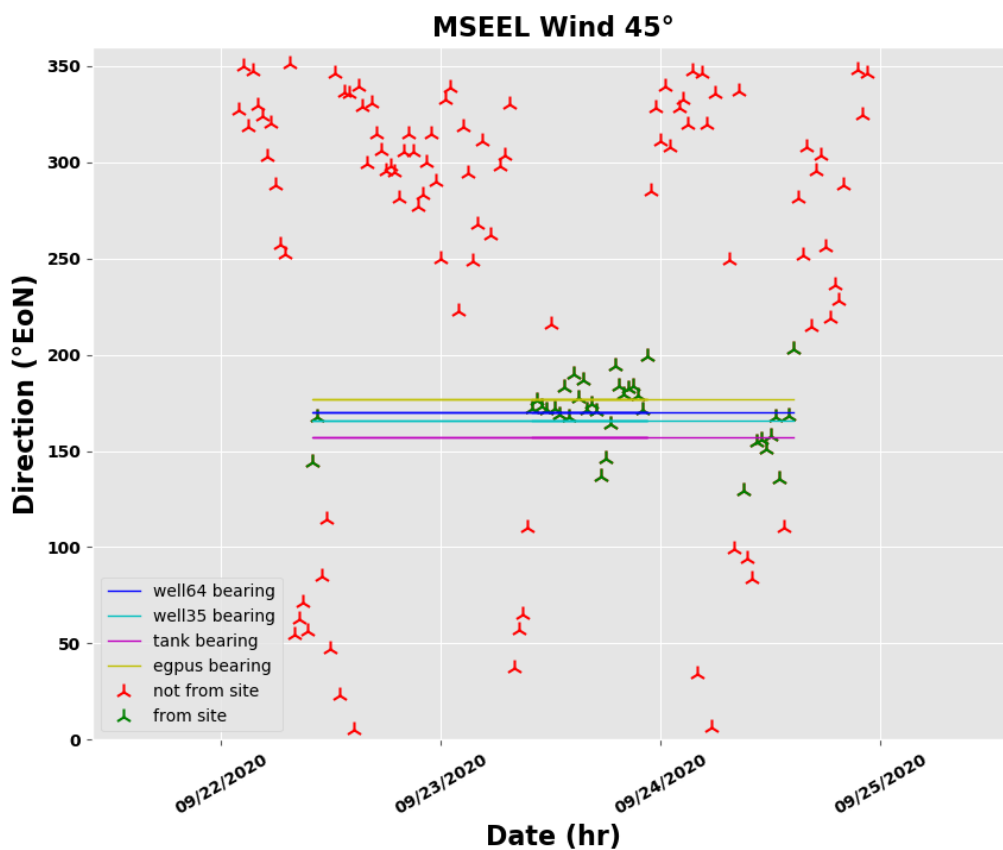


Figure 5.4: Wind Filter Example from the September 23rd Audit.

Statistics of the datasets are presented in Table 5.1. Estimates from both methods are presented in Figure 5.5 along with the actual methane emissions rate estimate from the September 23rd audit. The OTM 33A estimates tended to overestimate emissions significantly, with the average estimate being 1514 g/hr compared to the site rate of 290 g/hr. Clearly the distance estimate had a large impact on this and because of the nature of the calculations, wind speed during the audit may not have been significant enough to yield good results as the mean wind speed was only 1.65 m/s or 3.7 mph. Flux estimates were much more encouraging but these involved a large number of

assumptions, including the area from which the emissions were emanating. Typically, these values are difficult to approximate for short-term EC estimates and simply using short-term averages do not yield reliable results. However, the mass emissions estimates from the EC method were only 359 g/hr and the geometric mean estimate was 139 g/hr which is encouraging for future research given that the actual estimated emission rate was 239 g/hr.

Table 5.1: Statistics of Estimates from September 23rd Audit.

<i>Variable</i>	<i>OTM 33A Estimate (g/hr)</i>	<i>Eddy Covariance Flux (g/hr)**</i>
Count (#)	35	37
Positive Count	35	33
Negative Count	0	4
Mean	1514	359
Geometric Mean	1418	139
Median	1477	144
Standard Deviation	523	589
Maximum	2847	2912
Minimum	596	6

**only positive fluxes were used to estimate mass emissions rates

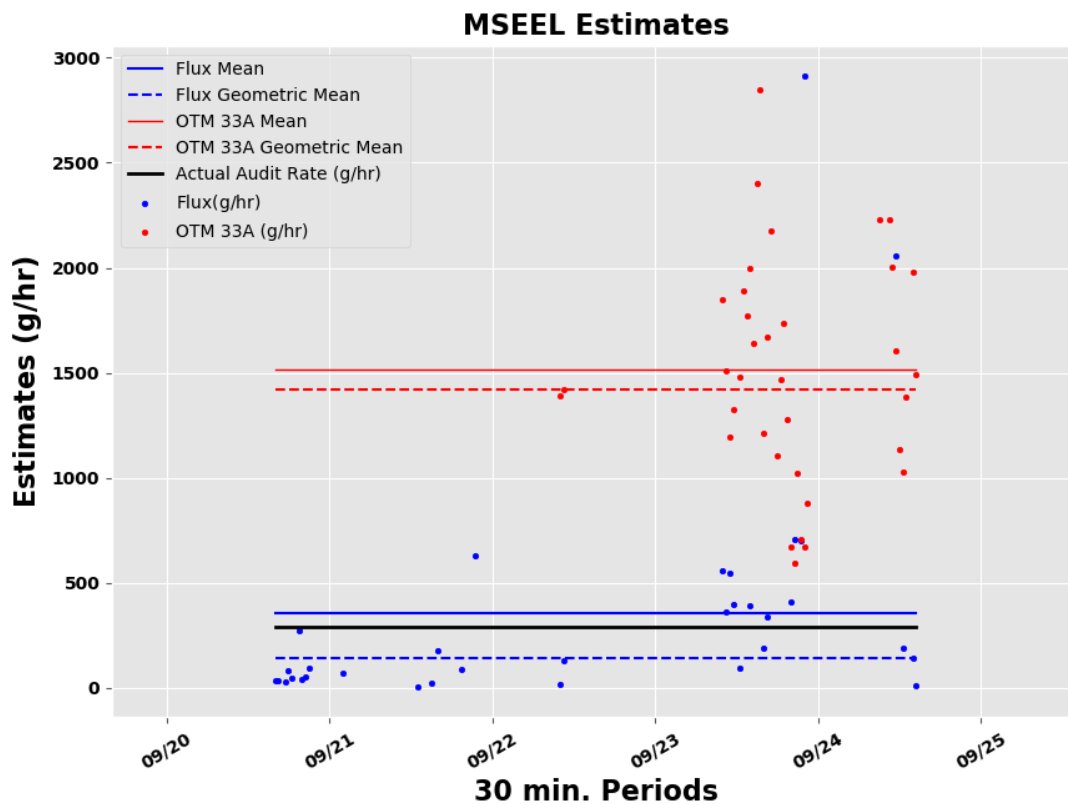


Figure 5.5: OTM 33A and Eddy Covariance Estimates from September 23rd Audit (±1 day).

Energy Audit Analysis

We used previously collected emissions data to estimate the volume flow rate of the exhaust for the energy analysis. We modified the method utilizing manufacturer's laboratory data for 50, 75, and 100% loads to create a linear volumetric exhaust flow relationship as a function load.

$$y = 1.842x + 34.317$$

Though this provided an updated tool, we still utilized water concentration measurements from an FTIR analyzer during previous research to determine an average exhaust water content of 4.96%, since this water is a superheated vapor it was important to be cognizant of its heat capacity. The remaining was assumed as air. With these relationships the volume of dry air and water vapor were calculated in 5% increments for engine operation from 5-100% load. Manufacturer data were also collected on exhaust heat rejection for 50, 75, and 100% load. With the new volumetric flows of dry air and water vapor, the heat rejection relationship was verified to match at 100% load. The error at 75% load was 1.5% and at 50% load was 3.4%. Though the relative error increased with decreasing load, the engines often experienced greater than 50% load and we feel this new method to account for exhaust thermal energy is sufficient.

With this new method, we were able to model a realistic heat exchanger. A shell and tube heat exchanger was designed and sized using the CC-THERM tool contained within ChemCAD software package. This software bases a design on the Logarithmic Mean Temperature Difference Method (LMTD) which consists of an iterative method that converges to the best design for the required heat transfer coefficient (U) and the area (A).

$$Q = U \times A \times LMTD$$

Where LMTD is the logarithmic man temperature defined as:

$$LMTD = \frac{\Delta T_A - \Delta T_B}{\ln \frac{\Delta T_A}{\Delta T_B}}$$

The parameters chosen to design and size the shell and tube heat exchanger assisted by ChemCAD were maximum mass exhaust flow rate modeled (6797 kg/hr), maximum exhaust flow temperature modeled (402 °C), and water outlet temperature was set to be the saturation temperature of saturated vapor at 110 psi. The water outlet condition was selected so it matched the water outlet conditions of currently deployed diesel fueled boilers. The heat exchanger was designed for each individual engine due to size and modularity when applied on the field. The TEMA heat exchanger specification sheet is found at the end of this section. Mechanical design of the heat exchanger was outside the scope of this project. After the heat exchanger was designed, a two-dimension matrix was built with various exhaust mass flow rates and temperatures where the SIMULINK model extracts the values. The heat exchanger water inlet temperature was set at 70 °C which was the day tank set point temperature that was verified during data collection. Figure 5.6 shows an illustration of the heat exchanger simulation. Figure 5.7 shows the engine and heat exchanger model in SIMULINK while Figure 5.8 shows the boiler model in SIMULINK.

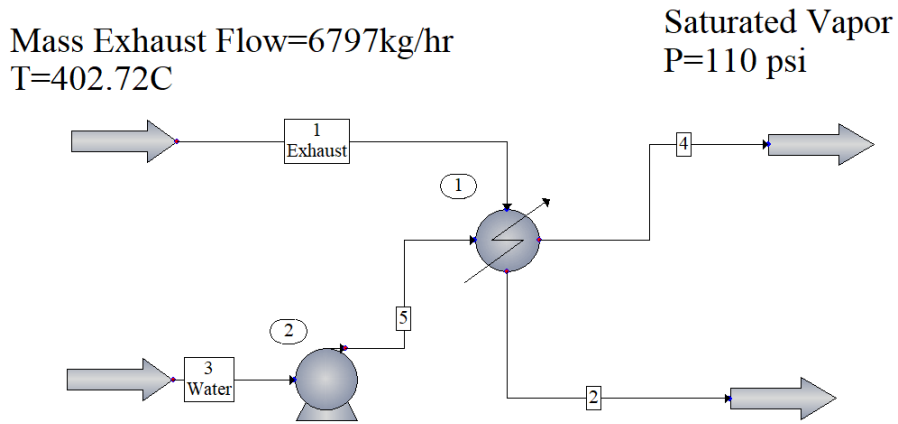


Figure 5.6: Basic ChemCAD model to design/evaluate a realistic shell and tube liquid air heat exchanger.

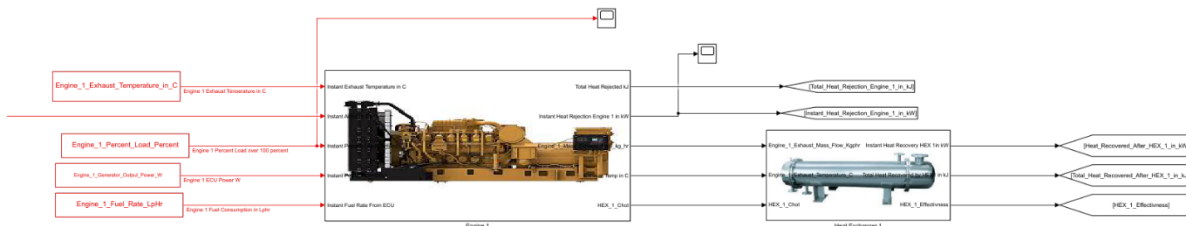


Figure 5.7: Overview of models for engines and heat exchangers.

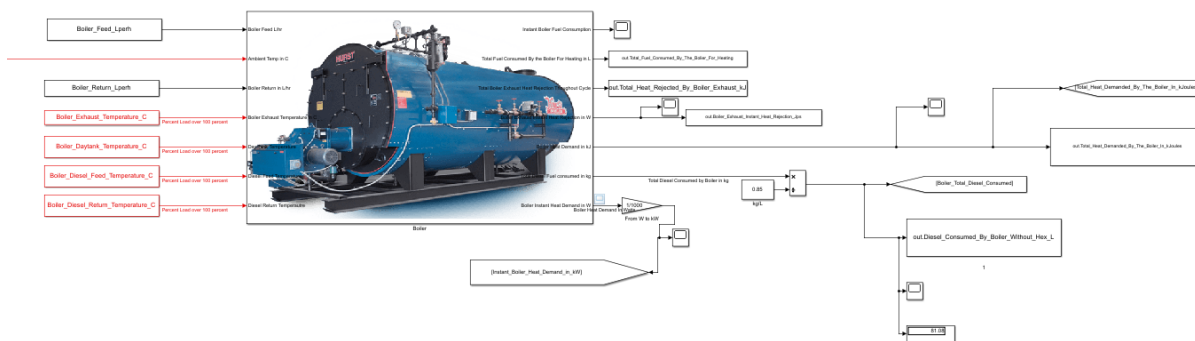


Figure 5.8: Overview of model conventional diesel fueled boiler.

The SIMULINK model was ran for the four cycles extracted from the data recorded on the McClelland well pad, the results are shown in Table 5.2. Results are still encouraging even though modeling is now more realistic and includes the estimated effectiveness of the heat exchanger.

Table 5.2: Example energy (heat) recovery analysis for four sample cycle cases. Note the savings are per total cycle time.

Cycle	Heat Balance for Each Cycle					
	Total Heat Rejected by Engines (kJ)	Total Heat Produced by Boiler (kJ)	Total Heat Recovered by Heat Exchangers (kJ)	Diesel Fuel Saved (L)	Diesel Fuel Consumed by Boiler (L)	%of Heat Demand Recovered
3 Engines on, 1hr	5.43E+06	2.49E+06	3.35E+06	79	0	134
2 Engines on, 1hr	5.00E+06	2.79E+06	3.35E+06	88	0	120
Drilling, 24 hr	6.45E+08	6.47E+07	6.21E+07	1979	83.03	96
Low Transient, 1hr	2.94E+06	2.54E+06	1.43E+06	45	35.53	56

This analysis shows that for heavy drilling cycles, the boiler heat demand could be met by the exhaust heat captured by the heat exchanger. However, under lower load, transient cycles the heat captured by the heat exchanger only covers 56% of the heat demand. Figure 4 shows the detailed instant engine heat rejection, heat exchanger heat recovery, and boiler heat demand in kW throughout the length of the 24 hour drilling cycle.

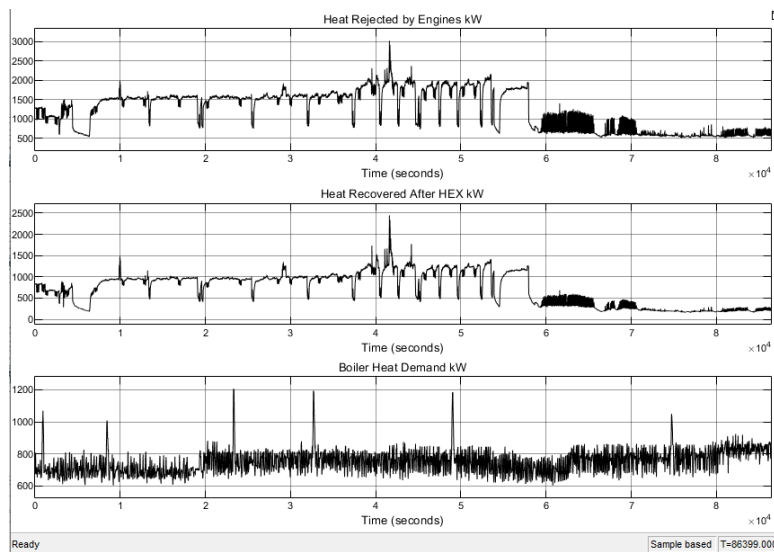


Figure 5.9: Continuous exhaust heat rejected, recovered in the HEX, and demanded by boiler for a 24-hour period (kW).

Products

Nothing to report.

Plan for Next Quarter

- Finish audit results with production data analysis.
- Continue periodic audits (at least until March)
- Maintain tower (at least until March)
- Continue OTM 33A and EC analysis and optimization
- Increase energy/heat model fidelity
- Examine weather conditions (only limited data – needs extrapolated)
- Include CO₂ reduction potentials
- Examine heat recovery for dedicated natural gas engines
- Additional low quality heat recovery (pre-heat day tank with engine coolant – delta T=20 °C).

Topic 6 – Water Treatment

This task is complete and will not be updated in future reports.

Topic 7 – Database Development

Approach

All MSEEL data is online and available to researchers (Figure 7.1 and 7.2). The website has been updated with the latest production beyond the end of the quarter (Figure 7.3). Work continues and we are adding data from MSEEL 3 Boggess Pad. MSEEL 3 data will be publically available by the end of the next quarter (One year after initial production at the Boggess Pad. The amount of data is a challenge and we are also working to stream line data updating and public access.

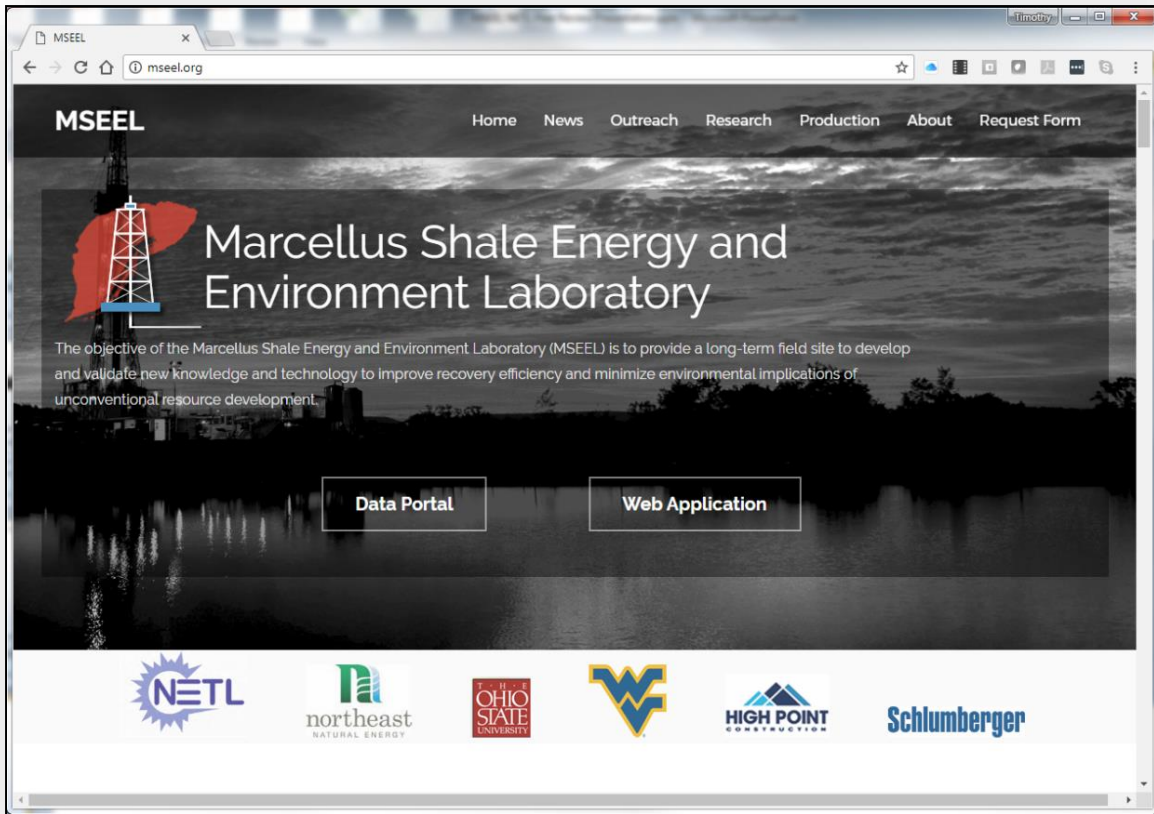


Figure 7.1: MSEEL website at <http://mseel.org/>.

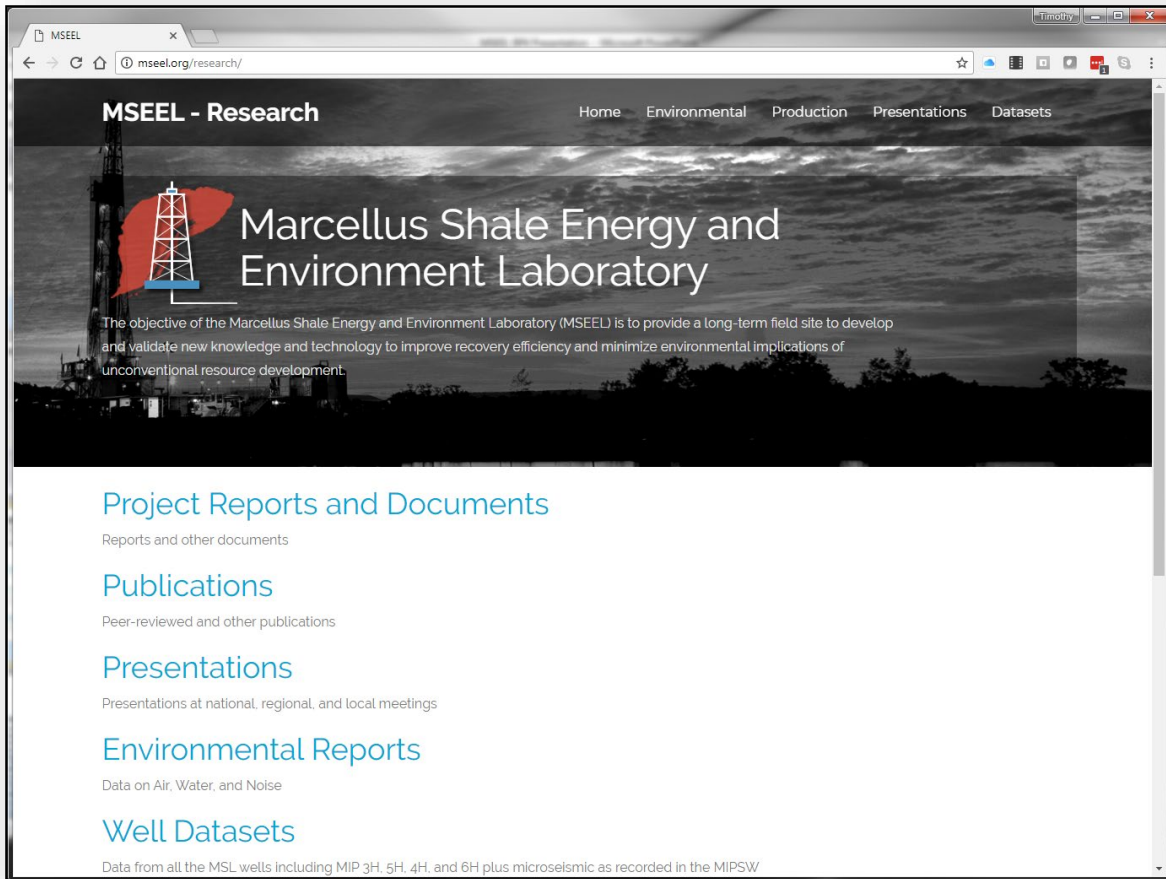
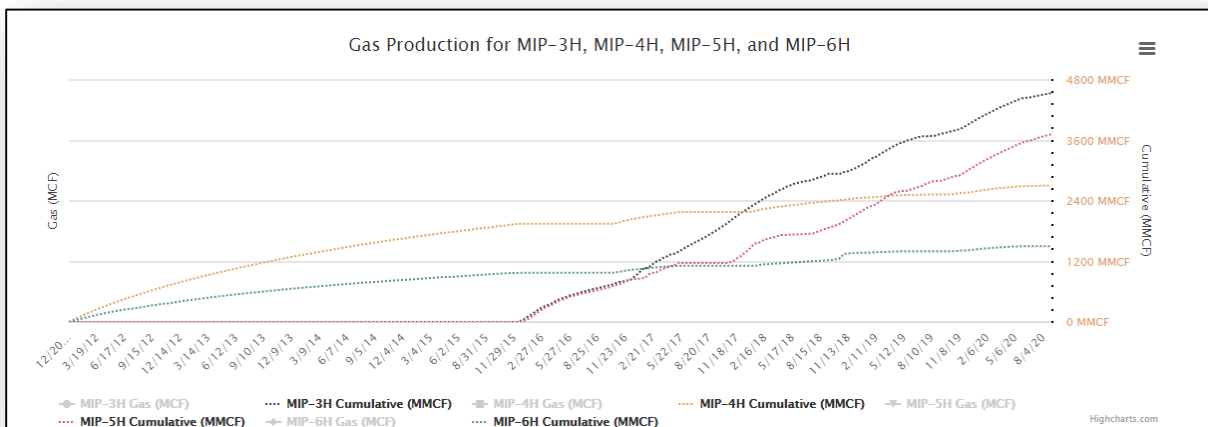


Figure 7.2: All data generated by the MSEEL project is available for download at <http://mseel.org/>.



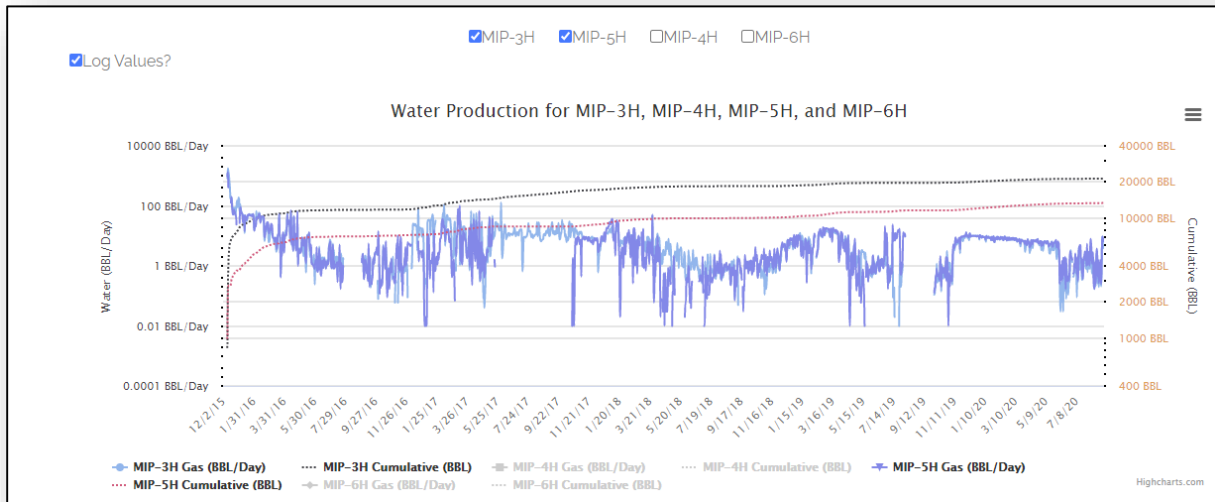


Figure 7.3: Gas and water production have been updated through the end of the quarter and are available at <http://mseel.org/>.

Results & Discussion

Data and publications have been updated at <http://mseel.org/>.

Products

Web site enhanced and updated.

Plan for Next Quarter (Liwei Li)

We are working on an improved system of upstream digital data management and analytics, which could be helpful for public access, the building reservoir models, and other applications of modeling and analytics that require large quantities of diverse data. Therefore, our objectives are to deliver tailored digital data management and analytics solutions.

For MSEEL data, we aim to move through a digital progression using the MSEEL 3 Boggess wells and then move to the MSEEL 2 MIP wells. First, the transformation should begin with integrating diverse data for all six wells. From drilling to production segments, we will standardize the report formats to improve the efficient access to the data. Figure 7.4 shows our evaluation of the main data formats and maturity. We also show our anticipated path to improved digital maturity.

These are the three planned short-term steps using the Boggess MSEEL 3 wells:

1. **Exploration/Coring.** We will annotate and augment the information given in bottom-hole assembly PDF files provided by Schlumberger, as well as experiments performed on cores.
2. **Logging/Well completion.** We will develop Python modules for rapid access to large volumes of DAS files. These datasets are currently stored in server. We will also add data visualization capabilities to help with understanding these datasets.

3. **Well production/monitoring.** We will build MySQL database to manage the well production history time series datasets. The SCADA system can be accessed in daily basis. This real-time data acquisition and analysis could be helpful in anomaly detection.

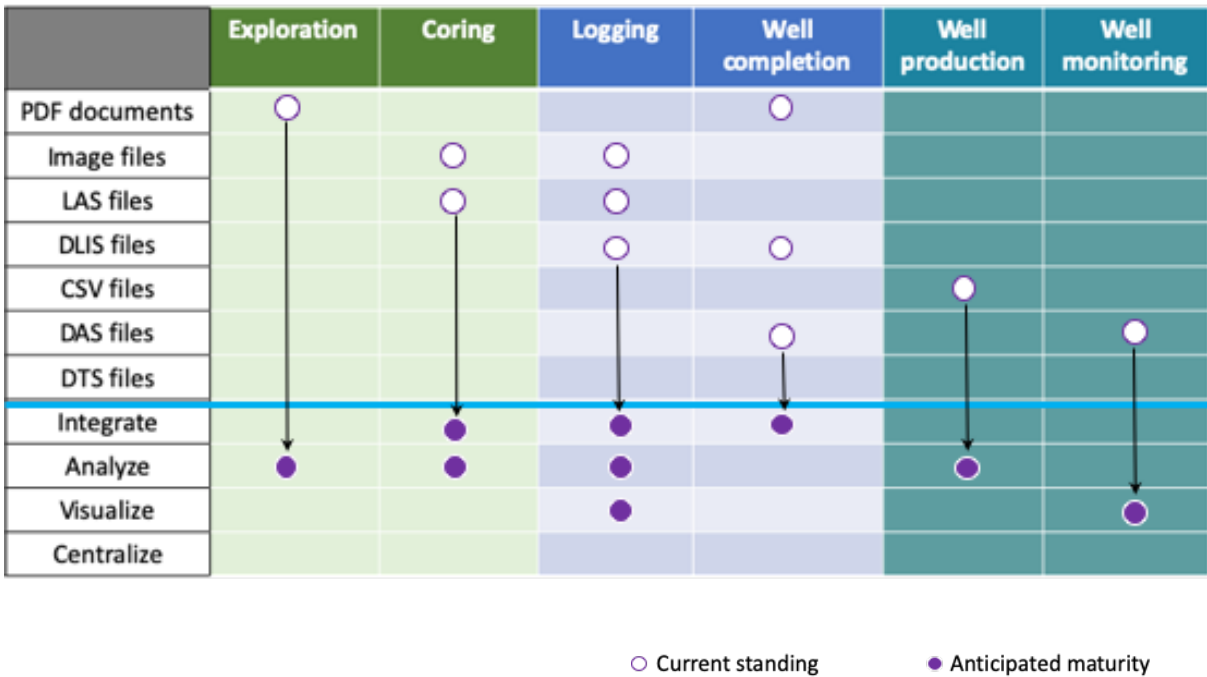


Figure 7.4: Current digital files for MSEEL 3 Boggess wells and digital goal mapping.

Topic 8 – Economic and Societal

This task is complete and will not be updated in future reports.

Cost Status

Year 1

Start: 10/01/2014 End:
03/31/2021

Baseline Reporting Quarter

	Q1 (12/31/14)	Q2 (3/31/15)	Q3 (6/30/15)	Q4 (9/30/15)
<u>Baseline Cost Plan</u>	(From 424A, Sec. D)			
<u>(from SF-424A)</u>				
Federal Share	\$549,000		\$3,549,000	
Non-Federal Share	\$0.00		\$0.00	
Total Planned (Federal and Non-Federal)	\$549,000		\$3,549,000	
Cumulative Baseline Costs				
<u>Actual Incurred Costs</u>				
Federal Share	\$0.00	\$14,760.39	\$237,451.36	\$300,925.66
Non-Federal Share	\$0.00	\$0.00	\$0.00	\$0.00
Total Incurred Costs - Quarterly (Federal and Non-Federal)	\$0.00	\$14,760.39	\$237,451.36	\$300,925.66
Cumulative Incurred Costs	\$0.00	\$14,760.39	\$252,211.75	\$553,137.41
<u>Uncosted</u>				
Federal Share	\$549,000	\$534,239.61	\$3,296,788.25	\$2,995,862.59
Non-Federal Share	\$0.00	\$0.00	\$2,814,930.00	\$2,814,930.00
Total Uncosted - Quarterly (Federal and Non-Federal)	\$549,000	\$534,239.61	\$6,111,718.25	\$5,810,792.59

Start: 10/01/2014 End:
03/31/2021

Baseline Reporting Quarter

	Q5 (12/31/15)	Q6 (3/31/16)	Q7 (6/30/16)	Q8 (9/30/16)
<u>Baseline Cost Plan</u>	(From 424A, Sec. D)			
<u>(from SF-424A)</u>				
Federal Share	\$6,247,367		\$7,297,926	
Non-Federal Share	2,814,930		\$4,342,480	
Total Planned (Federal and Non-Federal)	\$9,062,297	\$9,062,297.00	\$11,640,406	
Cumulative Baseline Costs				
<u>Actual Incurred Costs</u>				
Federal Share	\$577,065.91	\$4,480,939.42	\$845,967.23	\$556,511.68
Non-Federal Share	\$0.00	\$2,189,863.30	\$2,154,120.23	\$0.00
Total Incurred Costs - Quarterly (Federal and Non-Federal)	\$577,065.91	\$6,670,802.72	\$3,000,087.46	\$556,551.68
Cumulative Incurred Costs	\$1,130,203.32	\$7,801,006.04	\$10,637,732.23	\$11,194,243.91
<u>Uncosted</u>				
Federal Share	\$5,117,163.68	\$636,224.26	\$1,004,177.30	\$447,665.62
Non-Federal Share	\$2,814,930.00	\$625,066.70	(\$1,503.53)	(\$1,503.53)
Total Uncosted - Quarterly (Federal and Non-Federal)	\$2,418,796.68	\$1,261,290.96	\$1,002,673.77	\$446,162.09

Start: 10/01/2014

End: 03/31/2021

Baseline Reporting

Quarter

Q9
(12/31/16)

Q10
(3/31/17)

Q11
(6/30/17)

Q12
(9/30/17)

<u>Baseline Cost Plan</u>	(From 424A, Sec. D)			
<u>(from SF-424A)</u>				
Federal Share				\$9,128,731
Non-Federal Share				\$4,520,922
Total Planned (Federal and Non-Federal)				\$13,649,653
Cumulative Baseline Costs				
<u>Actual Incurred Costs</u>				
Federal Share	\$113,223.71	\$196,266.36	\$120,801.19	\$1,147,988.73
Non-Federal Share	\$0.00	\$0.00	\$0.00	\$0.00
Total Incurred Costs - Quarterly (Federal and Non-Federal)	\$113,223.71	\$196,266.36	\$120,801.19	\$1,147,988.73
Cumulative Incurred Costs	\$11,307,467.62	\$11,503,733.98	\$11,624,535.17	\$12,772,523.90
<u>Uncosted</u>				
Federal Share	\$334,441.91	\$138,175.55	\$17,374.36	\$700,190.63
Non-Federal Share	(\$1,503.53)	(\$1,503.53)	(\$1,503.53)	\$176,938.47
Total Uncosted - Quarterly (Federal and Non-Federal)	\$332,938.38	\$136,672.02	\$15,870.83	\$877,129.10

Start: 10/01/2014 End:
03/31/2021

Baseline Reporting
Quarter

	Q13 (12/31/17)	Q14 (3/31/18)	Q15 (6/30/18)	Q16 (9/30/18)
<u>Baseline Cost Plan</u>	(From 424A, Sec. D)			
<u>(from SF-424A)</u>				
Federal Share				\$11,794,054
Non-Federal Share				\$5,222,242
Total Planned (Federal and Non-Federal)				\$17,016,296.00
Cumulative Baseline Costs				
<u>Actual Incurred Costs</u>				
Federal Share	\$112,075.89	\$349,908.08	\$182,207.84	\$120,550.20
Non-Federal Share	\$0.00	\$31,500.23	\$10,262.40	\$4,338.00
Total Incurred Costs - Quarterly (Federal and Non-Federal)	\$112,075.89	\$381,408.31	\$192,470.24	\$124,888.20
Cumulative Incurred Costs	\$12,884,599.79	\$13,266,008.10	\$13,458,478.34	\$13,583,366.54
<u>Uncosted</u>				
Federal Share	\$588,114.74	\$238,206.66	\$55,998.82	\$2,600,771.62
Non-Federal Share	\$176,938.47	\$145,438.24	\$135,175.84	\$832,157.84
Total Uncosted - Quarterly (Federal and Non-Federal)	\$765,053.21	\$383,644.90	\$191,174.66	\$3,432,929.46

Start: 10/01/2014 End:
03/31/2021

Baseline Reporting
Quarter

	Q17 (12/31/18)	Q18 (3/31/19)	Q19 (6/30/19)	Q20 (9/30/19)
<u>Baseline Cost Plan</u>	(From 424A, Sec. D)			
<u>(from SF-424A)</u>				
Federal Share			\$15,686,642.00	
Non-Federal Share			\$9,180,952.00	
Total Planned (Federal and Non-Federal)			\$24,867,594.00	
Cumulative Baseline Costs				
<u>Actual Incurred Costs</u>				
Federal Share	\$80,800.03	\$133,776.98	\$714,427.48	\$1,136,823.21
Non-Federal Share	\$4,805.05	\$130,449.21	\$4,099,491.20	\$334,919.08
Total Incurred Costs - Quarterly (Federal and Non-Federal)	\$85,605.08	\$264,226.19	\$4,813,918.68	\$1,471,742.29
Cumulative Incurred Costs	\$13,668,971.62	\$13,933,197.81	\$18,747,116.49	\$20,218,858.78
<u>Uncosted</u>				
Federal Share	\$2,519,971.59	\$2,386,194.61	\$5,564,355.13	\$4,427,531.92
Non-Federal Share	\$827,352.79	\$696,903.58	\$412,612.38	\$221,203.30
Total Uncosted - Quarterly (Federal and Non-Federal)	\$3,347,324.38	\$3,083,098.19	\$5,976,967.51	\$4,948,735.22

Start: 10/01/2014

End: 03/31/2021

Baseline Reporting

Quarter

Q21
(12/31/19)

Q22
(3/31/20)

Q23
(6/30/20)

Q24
(9/30/20)

<u>Baseline Cost Plan</u>	(From 424A, Sec. D)			
(from SF-424A)				
Federal Share				\$16,608,355.00
Non-Federal Share				\$9,180,952.00
Total Planned (Federal and Non-Federal)				\$25,789,307.00
Cumulative Baseline Costs				
<u>Actual Incurred Costs</u>				
Federal Share	\$3,098,337.44	\$735,358.08	\$159,437.40	\$276,916.50
Non-Federal Share	\$3,163,776.74	\$750,301.90	\$0.00	\$163,643.13
Total Incurred Costs - Quarterly (Federal and Non-Federal)	\$6,262,114.18	\$1,485,659.98	\$159,437.40	\$440,559.63
Cumulative Incurred Costs	\$26,480,972.96	\$27,966,632.94	\$28,126,070.34	\$28,566,629.97
<u>Uncosted</u>				
Federal Share	\$1,629,041.48	\$893,683.40	\$734,246.00	\$1,079,195.50
Non-Federal Share	-\$2,942,573.44	-\$3,692,875.34	-\$3,692,875.34	-\$3,856,518.47
Total Uncosted - Quarterly (Federal and Non-Federal)	-\$1,313,531.96	-\$2,799,191.94	-\$2,958,629.34	-\$2,777,322.97

APPENDIX A – Scientific Journal Submissions Supported By MSEEL

Scientific Journals and Associated Media
Evans MV, Sumner A, Daly RA, *Luek JL, Plata D, Wrighton KC, Mouser PJ. Hydraulically fractured natural-gas well microbial communities contain genomic (de)halogenation potential. (2019). <i>Environmental Science & Technology Letters</i> , 6, (10), 585-591.
The manuscript from Nixon et al. was published in mSphere. S.L. Nixon, R.A. Daly, M.A. Borton, L.M. Solden, S.A. Welch, D.R. Cole, P.J. Mouser, M.J. Wilkins, K.C. Wrighton. Genome-resolved metagenomics extends the environmental distribution of the Verrucomicrobia phylum to the deep terrestrial subsurface. mSphere. DOI: 10.1128/mSphere.00613-19
Sharma, S., Agrawal, V., & Akondi, R. N. 2020. Role of biogeochemistry in efficient shale oil and gas production. <i>Fuel</i> , 259, 116207.
We have worked with LANL to generate a conference paper for the spring meeting of the Association for the Advancement of Artificial Intelligence (March 23-25) at Stanford University. The paper is entitled Physics-informed Machine Learning for Real-time Unconventional Reservoir Management
Sharma, S. Agrawal, V., Akondi R. 2019. Role of Biogeochemistry in efficient shale oil and gas production. <i>Fuel</i> . https://doi.org/10.1016/j.fuel.2019.116207
Phan T., Hakala A., Sharma S. 2019. Application of geochemical signals in unconventional oil and gas reservoir produced waters towards characterizing in situ geochemical fluid-shale reactions. <i>International Journal of Coal Geology</i> (in review)
Akondi, R., Sharma S., Texler, R., Pfifner S. (2019). Effects of Sampling and Long-Term Storage on Microbial Lipid Biomarker Distribution in Deep Subsurface Marcellus Shale Cores. <i>Geomicrobiology</i> (in review)
Agrawal, V. and Sharma, S. 2019. Are we modelling properties of unconventional shales correctly? <i>Fuel</i> (in review)
Evans, Morgan, Andrew J. Sumner, Rebecca A. Daly, Jenna L. Luek, Desiree L. Plata, Kelly C. Wrighton, and Paula J. Mouser, 2019, Hydraulically Fractured Natural-Gas Well Microbial Communities Contain Genomic Halogenation and Dehalogenation Potential, <i>Environmental Science and Technology Letters</i> , online preprint, 7p., DOI: 10.1021/acs.estlett.9b00473.
Song, Liaosha, Keithan Martin, Timothy R. Carr, Payam Kavousi Ghahfarokhi, 2019, Porosity and storage capacity of Middle Devonian shale: A function of thermal maturity, total organic carbon, and clay content, <i>Fuel</i> 241, p. 1036-1044, https://doi.org/10.1016/j.fuel.2018.12.106 .
Akondi, R., Sharma S., Texler, R., Pfifner S. (2019). Effects of Sampling and Long Term Storage on Microbial Lipid Biomarker Distribution in Deep Subsurface Marcellus Shale Cores. <i>Frontiers in Microbiology</i> (in review).
Johnson, D., Heltzel, R., and Oliver, D., “Temporal Variations in Methane Emissions from an Unconventional Well Site,” <i>ACS Omega</i> , 2019. DOI: 10.1021/acsomega.8b03246.
Evans MV, Daly RA, *Luek JL, Wrighton KC, Mouser PJ . (Accepted with revisions). Hydraulically fractured natural-gas well microbial communities contain genomic (de)halogenation potential. <i>Environmental Science & Technology Letters</i> .
Plata DL, Jackson RB, Vengosh A, Mouser PJ . (2019). More than a decade of hydraulic fracturing and horizontal drilling research. <i>Environmental Sciences: Processes & Impacts</i> 21 (2), 193-194.

Pilewski, J., S. Sharma, V. Agrawal, J. A. Hakala, and M. Y. Stuckman, 2019, Effect of maturity and mineralogy on fluid-rock reactions in the Marcellus Shale: <i>Environmental Science: Processes & Impacts</i> , doi:10.1039/C8EM00452H.
Phan, T. T., J. A. Hakala, C. L. Lopano, and S. Sharma, 2019, Rare earth elements and radiogenic strontium isotopes in carbonate minerals reveal diagenetic influence in shales and limestones in the Appalachian Basin: <i>Chemical Geology</i> , v. 509, p. 194–212, doi: 10.1016/j.chemgeo.2019.01.018.
Booker AE, Hoyt DW, Meulia T, Eder E, Nicora CD, Purvine SO, Daly RA, Moore JD, Wunch K, Pfiffner SM, Lipton MS, Mouser PJ, Wrighton KC, and Wilkins MJ (2019) Deep Subsurface Pressure Stimulates Metabolic Plasticity in Shale-Colonizing <i>Halanaerobium</i> . <i>Applied and Environmental Microbiology</i> . doi:10.1128/AEM.00018-19
Kavousi Ghahfarokhi, P., Wilson, T.H., Carr, T.R., Kumar, A., Hammack, R. and Di, H., 2019. Integrating distributed acoustic sensing, borehole 3C geophone array, and surface seismic array data to identify long-period long-duration seismic events during stimulation of a Marcellus Shale gas reservoir. <i>Interpretation</i> , 7(1), pp. SA1-SA10. https://doi.org/10.1190/INT-2018-0078.1 .
Borton MA, Daly RA, O'Banion B, Hoyt DW, Marcus DN, Welch S, Hastings SS, Meulia T, Wolfe RA, Booker AE, Sharma S, Cole DR, Wunch K, Moore JD, Darrah TH, Wilkins MJ, and Wrighton KC (2018) Comparative genomics and physiology of the genus <i>Methanohalophilus</i> , a prevalent methanogen in hydraulically fractured shale. <i>Environmental Microbiology</i> . doi: 10.1111/1462-2920.14467
Booker AE, Hoyt DW, Meulia T, Eder E, Nicora CD, Purvine SO, Daly RA, Moore JD, Wunch K, Pfiffner S, Lipton MS, Mouser PJ, Wrighton KC, and Wilkins MJ. Deep subsurface pressure stimulates metabolic flexibility in shale-colonizing <i>Halanaerobium</i> . Submitted to <i>Applied and Environmental Microbiology</i> . In review.
Additionally since the last report, the team's shale virus paper has been published in <i>Nature Microbiology</i> . Citation provided below:
Daly RA, Roux S, Borton MA, Morgan DM, Johnston MD, Booker AE, Hoyt DW, Meulia T, Wolfe RA, Hanson AJ, Mouser PJ, Sullivan MB, Wrighton KC, and Wilkins MJ (2018) Viruses control dominant bacteria colonizing the terrestrial deep biosphere after hydraulic fracturing. <i>Nature Microbiology</i> . doi: 10.1038/s41564-018-0312-6
Johnson, D. , Heltzel, R.*, Nix, A., and Barrow, R.*, "Development of Engine Activity Cycles for the Prime Movers of Unconventional, Natural Gas Well Development," <i>Journal of the Air and Waste Management Association</i> , 2016. DOI: 10.1080/10962247.2016.1245220.
Johnson, D. , Heltzel, R.*, Nix, A., Clark, N., and Darzi, M.*, "Greenhouse Gas Emissions and Fuel Efficiency of In-Use High Horsepower Diesel, Dual Fuel, and Natural Gas Engines for Unconventional Well Development," <i>Applied Energy</i> , 2017. DOI: 10.1016/j.apenergy.2017.08.234.
3.) Johnson, D. , Heltzel, R.*, Nix, A., Clark, N., and Darzi, M.*, "Regulated Gaseous Emissions from In-Use High Horsepower Drilling and Hydraulic Fracturing Engines," <i>Journal of Pollution Effects and Control</i> , 2017. DOI: 10.4176/2375-4397.1000187.
Johnson, D. , Heltzel, R.*, Nix, A., Darzi, M.*, and Oliver, D.*, "Estimated Emissions from the Prime-Movers of Unconventional Natural Gas Well Development Using Recently Collected In-Use Data in the United States," <i>Environmental Science and Technology</i> , 2018. DOI: 10.1021/acs.est.7b06694.
Johnson, D. , Heltzel, R.*, Nix, A., Clark, N., and Darzi, M.*, "In-Use Efficiency of Oxidation and Threeway Catalysts Used In High-Horsepower Dual Fuel and Dedicated Natural Gas Engines," <i>SAE International Journal of Engines</i> , 2018. DOI: 10.4271/03-11-03-0026.

Luek JL, Hari M, Schmitt-Kopplin P, Mouser PJ , Gonsior M. (2018). Organic sulfur fingerprint indicates continued injection fluid signature 10 months after hydraulic fracturing. <i>Environmental Science: Processes & Impacts</i> . Available in advance at doi: 10.1039/C8EM00331A.
Evans MV, Panescu J, Hanson AJ, Sheets J, Welch SA, Nastasi N, Daly RA, Cole DR, Darrah TH Wilkins MJ, Wrighton KC, Mouser PJ . (in press, 2018), Influence of <i>Marinobacter</i> and <i>Arcobacter</i> taxa on system biogeochemistry during early production of hydraulically fractured shale gas wells in the Appalachian Basin. <i>Frontiers of Microbiology</i> .
“Economic Impacts of the Marcellus Shale Energy and Environment Laboratory” has been released by the WVU Regional Research Institute,
Panescu J, Daly R, Wrighton K, Mouser, PJ. (2018). Draft Genome Sequences of Two Chemosynthetic <i>Arcobacter</i> Strains Isolated from Hydraulically Fractured Wells in Marcellus and Utica Shales. <i>Genome Announcements</i> , 6 (20), e00159-18. doi:10.1128/genomeA.00159-18.
University of Vermont seminar, Department of Civil and Environmental Engineering. The Role of Microbial Communities in Hydraulically Fractured Shale Wells and Produced Wastewater, 4/2018.
Gordon Research Conference, Environmental Sciences: Water. The Outsiders: Microbial Survival and Sustenance in Fractured Shale, 6/2018.
Ziemkiewicz, P.F. and He, Y.T. 2015. Evolution of water chemistry during Marcellus shale gas development: A case study in West Virginia. <i>Chemosphere</i> 134:224-231.
“ <i>Candidatus Marcellius: a novel genus of Verrucomicrobia discovered in a fractured shale ecosystem.</i> ” To be submitted to <i>Microbiome</i> journal. This research is led by a visiting post-doc, Sophie Nixon, in the Wrighton laboratory.
“ <i>Genomic Comparisons of Methanohalophilus and Halanaerobium strains reveals adaptations to distinct environments.</i> ” This work is led by two graduate students: Mikayla Borton in the Wrighton lab and Anne Booker in the Wilkins lab.
Agrawal V and Sharma S, 2018. Molecular characterization of kerogen and its implications for determining hydrocarbon potential, organic matter sources and thermal maturity in Marcellus Shale. <i>Fuel</i> 228: 429–437.
Agrawal V and Sharma S, 2018. Testing utility of organogeochemical proxies to assess sources of organic matter, paleoredox conditions and thermal maturity in mature Marcellus Shale. <i>Frontiers in Energy Research</i> 6:42.
M.A. Borton, D.W. Hoyt, S. Roux, R.A. Daly, S.A. Welch, C.D. Nicora, S. Purvine, E.K. Eder, A.J. Hanson, J.M. Sheets, D.M. Morgan, S. Sharma, T.R. Carr, D.R. Cole, P.J. Mouser, M.S. Lipton, M.J. Wilkins, K.C. Wrighton. Coupled laboratory and field investigations resolve microbial interactions that underpin persistence in hydraulically fractured shales. <i>Proceedings of the National Academy of Sciences</i> . June 2018, 201800155; DOI: 10.1073/pnas.1800155115.
R.A. Daly, S. Roux, M.A. Borton, D.M. Morgan, M.D. Johnston, A.E. Booker, D.W. Hoyt, T. Meulia, R.A. Wolfe, A.J. Hanson, P.J. Mouser, M.B. Sullivan, K.C. Wrighton, M.J. Wilkins. Viruses control dominant bacteria colonizing the terrestrial deep biosphere after hydraulic fracturing. <i>Nature Microbiology</i> . (in revision)
R.A. Daly, K.C. Wrighton, M.J. Wilkins. Characterizing the deep terrestrial subsurface microbiome. In R. Beiko, W. Hsiao, J. Parkinson (Eds.), <i>Microbiome analysis: methods and protocols</i> , Methods in Molecular Biology. Clifton, NJ: Springer Protocols. (in press)
“ <i>In vitro interactions scaled to in situ conditions: microorganisms predict field scale biogeochemistry in hydraulically fractured shale.</i> ” Review comments have been

“Comparison of Methanohalophilus strains reveals adaptations to distinct environments.” Invited to submit to Frontiers in Microbiology special topic edition Geobiology in the Terrestrial Subsurface, to be submitted June 2018. An undergraduate researcher, Bridget O’Banion in the Wrighton lab, led this research.

Marcellus Shale model stimulation tests and microseismic response yield insights into mechanical properties and the reservoir DFN. Interpretation. 50p. published December 4, 2017, Interpretation, Society Exploration Geophysicists <https://doi.org/10.1190/int-2016-0199.1>

Thomas H. Wilson , Tim Carr , B. J. Carney , Malcolm Yates , Keith MacPhail , Adrian Morales , Ian Costello , Jay Hewitt , Emily Jordon , Natalie Uschner , Miranda Thomas , Si Akin , Oluwaseun Magbagbeola , Asbjorn Johansen , Leah Hogarth , Olatunbosun Anifowoshe , and Kashif Naseem,

Akondi R, Trexler R, Pfiffner SM, Mouser PJ, Sharma S 2017. Modified Lipid Extraction Method for Deep Subsurface Shale. Frontiers in Microbiology <https://doi.org/10.3389/fmicb.2017.01408>

the paper was submitted to the Journal Interpretation. The journal submission is titled Marcellus Shale model stimulation tests and microseismic response yield insights into mechanical properties and the reservoir DFN

Johnson, D., Heltzel, R., Nix, A., and Barrow, R., “Development of Engine Activity Cycles for the Prime Movers of Unconventional, Natural Gas Well Development,” Journal of the Air and Waste Management Association, 2016. DOI: 10.1080/10962247.2016.1245220

Preston County Journal: http://www.theet.com/news/local/wvu-project-setting-the-standard-for-researching-oil-and-gas/article_25e0c7d0-279d-59c1-9f13-4cbe055a1415.html

The statesman: <http://www.thestatesman.com/news/science/fracking-messiah-or-menace/81925.html>

Nova Next article: <http://www.pbs.org/wgbh/nova/next/earth/deep-life/>

NPR interview: <http://www.wksu.org/news/story/43880>

Midwest Energy News : <http://midwestenergynews.com/2015/11/17/researchers-study-microbes-living-in-shale-and-how-they-can-impact-drilling/>

McClatchyDC News: [“Could deep earth microbes help us frack for oil?”S. Cockerham](http://www.mcclatchydc.com/news/nation-world/national/article29115688.html)
<http://www.mcclatchydc.com/news/nation-world/national/article29115688.html>

APPENDIX B – Conference Papers/Presentations MSEEL

Conference Paper/Presentation
Li., L, Kavousi, P., Li, N., Carney, B.J. and Carr, T.R., 2020a, Data integration for engineered completion design in the Marcellus shale, AAPG Annual Convention & Exhibition Online and On Demand, 7 September – 1 October.
Li., L, Nasrabadi, N.M. and Carr, T.R., 2020b, Completion design improvement using a deep convolutional network, SPE Annual Technical Conference and Exhibition Virtual, doi:10.2118/201545-MS. 27-29 October.
Bohn, R., Hull, R., Trujillo, K., Wygal, B., Parsegov, S. G., Carr, T., & Carney, B. J. 2020a, Learnings from the Marcellus Shale Energy and Environmental Lab (MSEEL) Using Fiber Optic Tools and Geomechanical Modeling. Unconventional Resources Technology Conference. doi:10.15530/urtec-2020-2440. (2020, July 20)
Bohn, R., & Parsegov, S. 2020b, Diagnosing Fracture Stimulation Effectiveness: A Case Study of the Marcellus Shale Energy and Environmental Lab (MSEEL). Unconventional Resources Technology Conference. doi:10.15530/urtec-2020-3173. (2020, July 20)
Hull, Robert, Woerpel, C., Trujillo, K., Bohn, R., Wygal, B. Carney, B.J., Carr, T., 2020, Hydraulic fracture characterization using fiber optic DAS and DTT data, Society Exploration Geophysics Annual Technical Conference, Expanded Abstracts: 500-504, https://doi.org/10.1190/segam2020-3425789.1 , October 14, 2020.
Li, B., Carney, B. J., & Carr, T.. 2020, Characterizing Natural Fractures and Sub-seismic Faults for Well Completion of Marcellus Shale in the MSEEL Consortium Project, West Virginia, USA. Unconventional Resources Technology Conference. doi:10.15530/urtec-2020-2447. (2020, July 20)
Paronish, T. J., Toth, R., Carr, T. R., Agrawal, V., Crandall, D., & Moore, J. 2020, Multi-Scale Lithofacies and Chemostratigraphic Analysis of Two Middle Devonian Marcellus Shale Wells in Northern West Virginia, USA. Unconventional Resources Technology Conference. doi:10.15530/urtec-2020-2763. (2020, July 20)
Li, W. F., Frash, L. P., Welch, N. J., Carey, J. M., & Meng, M. (2020, September 18). A Simple Transient DFN Model with Stress-Dependent Fracture Permeability for Shale Gas Production. American Rock Mechanics Association.
Ding, J., Clark, A. C., Vanorio, T., Jew, A. D., & Bargar, J. R. 2020, Time-lapse Acoustic Monitoring of Fracture Alteration in Marcellus Shale. Unconventional Resources Technology Conference. doi:10.15530/urtec-2020-2956. (2020, July 20).
Li, W. F., Frash, L. P., Welch, N. J., Carey, J. M., & Meng, M. 2020, A Simple Transient DFN Model with Stress-Dependent Fracture Permeability for Shale Gas Production. American Rock Mechanics Association. (2020, September 18)
Tran, N. L., Gupta, I., Devegowda, D., Jayaram, V., Karami, H., Rai, C., & Sondergeld, C. H. Preprint, Application of Interpretable Machine-Learning Workflows To Identify Brittle, Fracturable, and Producing Rock in Horizontal Wells Using Surface Drilling Data. Society of Petroleum Engineers. doi:10.2118/202486-PA. (2020, August 1)
Agrawal, V., S. Sharma, N. Mahlstedt 2019, Determining the type, amount and kinetics of hydrocarbons generated in a Marcellus shale maturity series. Eastern Section AAPG 48th Annual Meeting in Columbus, OH.
Carney BJ, Carr TR, Hewitt J, Vagnetti R, Sharma S, Hakala A. 2019. Progress and Findings from “MSEEL 1” and the Transition to “MSEEL 2”: Creating Value from a Cooperative Project. Annual Eastern Section AAPG Meeting, Columbus, Ohio.

Phan TT, Hakala JA, Lopano C L, & Sharma S. 2019. Rare earth elements and radiogenic strontium isotopes in carbonate minerals reveal diagenetic influence in shales and limestones in the Appalachian Basin. GAC-MAC-IAH conference, Quebec City, Quebec, Canada.
Ferguson, B., Sharma, S., Agrawal, V., Hakala, A., 2019. Investigating controls on mineral precipitation in hydraulically fractured wells. Geological Society of America Annual Meeting, Phoenix, (GSA), Annual meeting, Phoenix, Arizona.
Akondi R, Sharma S. 2019. Microbial Signatures of Deep Subsurface Shale Biosphere. Geological Society of America (GSA), Annual meeting, Phoenix, Arizona.
Carr, Timothy R. MSEEL Seismic Attribute Application of Distributed Acoustic Sensing Data, presentation at 53rd US Rock Mechanics / Geomechanics Symposium, 2019 American Rock Mechanics Association (ARMA) Annual Meeting, New York City, NY.
Agrawal, V., S. Sharma, N. Mahlstedt 2019, Determining the type, amount and kinetics of hydrocarbons generated in a Marcellus shale maturity series. Eastern Section AAPG 48th Annual Meeting in Columbus, OH
Evans M, Luek J, Daly R, Wrighton KC, Mouser PJ. (2019). Microbial (de)halogenation in hydraulically fractured natural-gas wells in the Appalachian Basin. ACS annual conference, Orlando, FL, Mar 31-Apr 4, 2019.
Luek J, Murphy C, Wrighton KC, Mouser PJ. (2019). Detection of antibiotic and metal resistance genes in deep shale microbial community members. ACS annual conference, Orlando, FL, Mar 31-Apr 4, 2019.
Kumar, A., E. V. Zorn, R. Hammack, and W. Harbert, 2017a, Seismic monitoring of hydraulic fracturing activity at the Marcellus shale energy and environment laboratory (MSEEL) Site, West Virginia: Presented at the Unconventional Resources Technology Conference, Paper 2670481.
<i>Tufts University, Dept. of Civil and Environmental Engineering. Microbial Survival and Sustenance in Fractured Shale 10/2018.</i>
<i>University of New Hampshire, Dept. of Earth Science. Microbial Survival and Sustenance in Fractured Shale 09/2018.</i>
GSA conference in Indianapolis, Indiana. 2019
AAPG 2019, San Antonio, Texas.
Agrawal, V., Sharma, S., 2018. New models for determining thermal maturity and hydrocarbon potential in Marcellus Shale. Eastern Section AAPG 47th Annual Meeting in Pittsburgh, WV
Eastern Section SPE and AAPG by Yixuan Zhu and T. R, Carr entitled Estimation of "Fracability" of Marcellus Shale: A Case Study from the MIP3H in Monongalia County, WV, USA. The paper will be presented in Pittsburgh, PA during the meeting (October 9-11)
Kelly Wrighton -19th Annual Microbiology Student Symposium, University of California Berkeley, April 28, 2018
Kelly Wrighton - ASM Microbe, Atlanta, Georgia, June 9, 2018
Mouser PJ, Heyob KM, Blotevogel J, Lenhart JJ, Borch T (2018). Pathways and Mechanisms for Natural Attenuation of Nonionic Surfactants in Hydraulic Fracturing Fluids if Released to Agricultural Soil and Groundwater. ACS annual conference, New Orleans, LA, Mar 19-22, 2018.
Hanson AJ, Lipp JS, Hinrich K-U, Mouser PJ (2018). Microbial lipid biomarkers in a Marcellus Shale natural gas well: From remnant molecules to adapted communities. ACS annual conference, New Orleans, LA, Mar 19-22, 2018

<p><i>University of Maine, Department of Biology and Ecology. Biodegradation of Organic Compounds in the Hydraulically Fractured Shale Ecosystem, 2/2018.</i></p>
<p><i>“Top-down and bottom-up controls on Halanaerobium populations in the deep biosphere.”</i> Poster presentation at the Department of Energy’s Joint Genome Institute ‘Genomics of Energy and Environment Meeting’, San Francisco, CA, March 2018. A researcher, Rebecca Daly, in the Wrighton lab, led this work.</p>
<p>Sharma S, Wilson T, Wrighton, K, Borton M & O’Banion. 2017 Can introduction of hydraulic fracturing fluids induce biogenic methanogenesis in the shale reservoirs? Annual American Geophysical Union Conference, Dec 11-15, New Orleans, LA.</p>
<p>Booker AE, Borton MA, Daly R, C. Nicora, Welch S, Dusane D, Johnston M, Sharma S et. al., 2017. Potential Repercussions Associated with Halanaerobium Colonization of Hydraulically Fractured Shales. Annual American Geophysical Union Conference, Dec 11-15, New Orleans, LA.</p>
<p>Mouser P. <i>Colorado State University, Civil and Environmental Engineering and CSU Water Center, From the Land Down Under: Microbial Community Dynamics and Metabolic processes influencing organic additives in black shales, 11/2017.</i></p>
<p>Presentation at ISES (International Society for Exposure Science), Raleigh, NC Oct. 16th, 2017 on “Techniques for Estimating Community Exposure from Hydraulic Fracturing Operations</p>
<p>Kavousi, Payam, Timothy R. Carr, Robert J Mellors, Improved interpretation of Distributed Acoustic Sensing (DAS) fiber optic data in stimulated wells using seismic attributes, [S33B-0865] presented at December 2017 Fall Meeting, AGU, New Orleans, LA, 11-15, https://agu.confex.com/agu/fm17/meetingapp.cgi/Paper/282093</p>
<p>Mellors Robert J, Christopher Scott Sherman, Frederick J Ryerson, Joseph Morris, Graham S Allen, Michael J Messerly, Timothy Carr, Payam Kavousi, Modeling borehole microseismic and strain signals measured by a distributed fiber optic sensor, [S33B-0869] presented at 2017 Fall Meeting, AGU, New Orleans, LA, 11-15, https://agu.confex.com/agu/fm17/meetingapp.cgi/Paper/264800</p>
<p>Song, Liaosha and Timothy R. Carr, Microstructural Evolution of Organic Matter Pores in Middle Devonian Black Shale from West Virginia and Pennsylvania, USA, SEPM – AAPG Hedberg Research Conference, Mudstone Diagenesis, Santa Fe, New Mexico, October 16-19. http://www.searchanddiscovery.com/pdfz/abstracts/pdf/2017/90283hedberg/abstracts/ndx_song.pdf.html</p>
<p>Carr, Timothy R., The Importance of Field Demonstration Sites: The View from the Unconventional Resource Region of the Appalachian Basin (Invited), [H21K-06] presented at 2017 Fall Meeting, AGU, New Orleans, LA, 11-15 Dec. https://agu.confex.com/agu/fm17/meetingapp.cgi/Paper/242523</p>
<p>Ghahfarokhi, P. K., Carr, T., Song, L., Shukla, P., & Pankaj, P. (2018, January 23). Seismic Attributes Application for the Distributed Acoustic Sensing Data for the Marcellus Shale: New Insights to Cross-Stage Flow Communication. Society of Petroleum Engineers, doi:10.2118/189888-MS.</p>

Presentation of paper at 2017 Annual International SEG meeting: The paper titled *"Relationships of brittleness index, Young's modulus, Poisson's ratio and high TOC for the Marcellus Shale, Morgantown, West Virginia"* by Thomas H. Wilson*, Payam Kavousi, Tim Carr, West Virginia University; B. J. Carney, Northeast Natural Energy LLC; Natalie Uschner, Oluwaseun Magbagbeola and Lili Xu, Schlumberger, was presented at the annual SEG meeting, this past September in Houston, TX.

Thomas H. Wilson and Tim Carr, West Virginia University; B. J. Carney, Jay Hewitt, Ian Costello, Emily Jordon, Northeast Natural Energy LLC; Keith MacPhail, Oluwaseun Magbagbeola, Adrian Morales, Asbjorn Johansen, Leah Hogarth, Olatunbosun Anifowoshe, Kashif Naseem, Natalie Uschner, Mandy Thomas, Si Akin, Schlumberger, 2016, Microseismic and model stimulation of natural fracture networks in the Marcellus Shale, West Virginia: SEG International Exposition and 86th Annual Meeting, 3088-3092, <https://doi.org/10.1190/segam2016-13866107.1>.

Sharma S 2017. Shale Research at Marcellus Shale Energy and Environment laboratory. 23rd Annual CNSF Exhibition, May 16, Rayburn House, Washington DC.

Elsaig, M., Black, S., Aminian, K., and S. Ameri, S.: "Measurement of Marcellus Shale Properties," SPE-87523, SPE Eastern Regional Conf., Lexington, KY, October 2017.

El Sgher, M., Aminian, K., and S. Ameri: "The Impact of Stress on Propped Fracture Conductivity and Gas Recovery in Marcellus Shale," SPE-189899, SPE Hydraulic Fracturing Technology Conf., Woodlands, TX, January 2018.

Ebusurra, M.: "Using Artificial Neural Networks to Predict Formation Stresses for Marcellus Shale with Data from Drilling Operations." MS Thesis, Petroleum & Natural Gas Engineering, West Virginia University, August 2017.

M. El Sgher, K. Aminian, S. Ameri: "The impact of the hydraulic fracture properties on gas recovery from Marcellus Shale," SPE 185628, SPE Western Regional Conf., Bakersfield, California, April 2017.

Elsaig, M., Aminian, K., Ameri, S. and M. Zamirian: "Accurate Evaluation of Marcellus Shale Petrophysical Properties," SPE-Error! Reference source not found.84042, SPE Eastern Regional Conf., Canton, OH, September 2016.

Filchock, J.J., Aminian, K. and S. Ameri: "Impact of Completion Parameters on Marcellus Shale Production," SPE-184073, SPE Eastern Regional Conf., Canton, OH, September 2016.

Tawfik Elshehabi and H. Ilkin Bilgesu: "Well Integrity and Pressure Control in Unconventional Reservoirs: A Comparative Study of Marcellus and Utica Shales," SPE 184056, SPE Eastern Regional Conf., Canton, OH, September 2016

Meso- and Macro-Scale Facies and Chemostratigraphic Analysis of Middle Devonian Marcellus Shale in Northern West Virginia, USA for Eastern Section American Association of Petroleum Geologists Annual Meeting September 26-27. Authors: Thomas Paronish, Timothy Carr, West Virginia University; Dustin Crandall and Jonathan Moore, National Energy Technology Laboratory, U.S. Department of Energy

The presentation was made at the annual SEG convention in Dallas (see <http://library.seg.org/doi/pdf/10.1190/segam2016-13866107.1>) and the paper was submitted to the Journal Interpretation. The journal submission is titled Marcellus Shale model stimulation tests and microseismic response yield insights into mechanical properties and the reservoir DFN

McCawley M, Dzomba A, Knuckles T, and Nye M. 2017. Use of trace elements for estimating community exposure to Marcellus shale development operations. Poster presented at: Van Liere Poster Competition. WVU Health Sciences Center; 2017; Morgantown, WV
Khajouei Golnoosh, Hoil Park, Jenna Henry, Harry Finklea, Lian-Shin Lin. <i>Produced water treatment using electrochemical softening system</i> . Institute of Water Security and Science (IWSS) symposium, February 28, Morgantown, West Virginia.
Wilson T, and Sharma S. 2017. Inferring biogeochemical interactions in deep shale reservoirs at the Marcellus Shale Energy and Environment Laboratory (MSEEL). Joint 52nd northeastern annual section/ 51st north-central annual section meeting March 19-21, Pittsburgh, PA.
Agarwal V, Sharma S, and Warrier A. 2016. Understanding kerogen composition and structure in pristine shale cores collected from Marcellus Shale Energy and Environment Laboratory. Eastern Section American Association of Petroleum Geologists' Meeting, Lexington, Kentucky, September 2016
Akondi R, Trexler RV, Pfiffner SM, Mouser PJ, Sharma S. 2016. Comparing Different Extraction Methods for Analyses of Ester-linked Diglyceride Fatty Acids in Marcellus Shale. Eastern Section American Association of Petroleum Geologists' Meeting, Lexington, Kentucky, September 2016
Booker AE, Borton MA, Daly R, Welch S, Nicora CD, Sharma S, et. al., 2016. Sulfide Generation by Dominant Colonizing Halanaerobium Microorganisms in Hydraulically Fractured Shales. Eastern Section American Association of Petroleum Geologists' Meeting, Lexington, Kentucky, September 2016
Crandall D, Moore J, Paronish T, Hakala A, Sharma S, and Lopano C 2016. Preliminary analyses of core from the Marcellus Shale Energy and Environment Laboratory. Eastern Section American Association of Petroleum Geologists' Meeting, Lexington, Kentucky, September 2016.
Daly RA, Borton MA, Wilson T, Welch S., Cole D. R., Sharma S., et. al., 2016. Microbes in the Marcellus Shale: Distinguishing Between Injected and Indigenous Microorganisms, Eastern Section American Association of Petroleum Geologists' Meeting, Lexington, Kentucky, September 2016
Evert M, Panescu J, Daly R, Welch S, Hespen J, Sharma S, Cole D, Darrah TH, Wilkins M, Wrighton K, Mouser PJ 2016. Temporal Changes in Fluid Biogeochemistry and Microbial Cell Abundance after Hydraulic Fracturing in Marcellus Shale. Eastern Section American Association of Petroleum Geologists' Meeting, Lexington, Kentucky, September 2016
Hanson AJ, Trexler RV, Mouser PJ (2016). Analysis of Microbial Lipid Biomarkers as Evidence of Deep Shale Microbial Life. Eastern Section American Association of Petroleum Geology (AAPG), Lexington, KY, Sept 25-27, 2016.
Lopano, C.L., Stuckman, M.Y., and J.A. Hakala (2016) Geochemical characteristics of drill cuttings from Marcellus Shale energy development. Annual Geological Society of America Meeting, Denver, CO, September 2016.
Panescu J, Evert M, Hespen J, Daly RA, Wrighton KC, Mouser PJ (2016). Arcobacter isolated from the produced fluids of a Marcellus shale well may play a currently unappreciated role in sulfur cycling. Eastern Section American Association of Petroleum Geology (AAPG), Lexington, KY, Sept 25-27, 2016.

Sharma S, Carr T, Vagnetti R, Carney BJ, Hewitt J. 2016. Role of Marcellus Shale Energy and Environment Laboratory in Environmentally Prudent Development of Shale Gas. Annual Geological Society of America Meeting, Denver, CO, September 2016.
Sharma S, Agrawal V, Akondi R, and Warriar A. 2016. Understanding biogeochemical controls on spatiotemporal variations in total organic carbon in cores from Marcellus Shale Energy and Environment Laboratory. Eastern Section American Association of Petroleum Geologists' Meeting, Lexington, Kentucky, September 2016
Trexler RV, Akondi R, Pfiffner S, Daly RA, Wilkins MJ, Sharma S, Wrighton KC, and Mouser, PJ (2016). Phospholipid Fatty Acid Evidence of Recent Microbial Life in Pristine Marcellus Shale Cores. Eastern Section American Association of Petroleum Geology (AAPG), Lexington, KY, Sept 25-27, 2016.
Wilson T and Sharma S 2016. Assessing biogeochemical interactions in the reservoir at Marcellus Shale Energy and Environment Laboratory Annual Geological Society of America Meeting, Denver, CO, September 2016.
Marcellus Shale Energy and Environment Laboratory (MSEEL): Subsurface Reservoir Characterization and Engineered Completion; Presenter: Tim Carr; West Virginia University (2670437)
Depositional environment and impact on pore structure and gas storage potential of middle Devonian organic rich shale, Northeastern West Virginia, Appalachian Basin; Presenter: Liaosha Song, Department of Geology and Geography, West Virginia University, Morgantown, WV, (2667397)
Seismic monitoring of hydraulic fracturing activity at the Marcellus Shale Energy and Environment Laboratory (MSEEL) site, West Virginia; Presenter: Abhash Kumar, DOE, National Energy Technology Laboratory (2670481)
Geomechanics of the microseismic response in Devonian organic shales at the Marcellus Shale Energy and Environment Laboratory (MSEEL) site, West Virginia; Presenter: Erich Zorn, DOE, National Energy Technology Laboratory (2669946)
Application of Fiber-optic Temperature Data Analysis in Hydraulic Fracturing Evaluation- a Case Study in the Marcellus Shale; Presenter: Shohreh Amini, West Virginia University (2686732)
The Marcellus Shale Energy and Environmental Laboratory (MSEEL): water and solid waste findings-year one; Presenter: Paul Ziemkiewicz WRI, West Virginia University (2669914)
Role of organic acids in controlling mineral scale formation during hydraulic fracturing at the Marcellus Shale Energy and Environmental Laboratory (MSEEL) site; Presenter: Alexandra Hakala, National Energy Technology Laboratory, DOE (2670833)
MSEEL Water and Waste Findings - RPSEA Onshore Workshop
MSEEL Water and Waste Findings - Eastern Sec. AAPG annual meeting
Sharma S., 2016. Unconventional Energy Resources: A view from the Appalachian Basin. US Embassy Berlin, Germany 25 May 2016.
Sharma S., 2016. Biogeochemistry of Marcellus Shale. German National Research Centre for Earth Sciences GFZ, Postdam, Germany. May 22, 2016
Sharma S. 2016.,. Biogeochemistry of Marcellus Shale. SouthWestern Energy, Houston, Texas. May 5, 2016.
Sharma S. 2016. Marcellus Shale Energy and Environment Laboratory (MSEEL), West Virginia University Extension Conference, Clarksburg, WV. May 18, 2016.

Sharma S. 2016. Role of Geochemistry in Unconventional Resources Development. Appalachian Geological Society Meeting, Morgantown, April 5, 2016.
Sharma S. 2016. Marcellus Shale Energy and Environment Laboratory (MSEEL), Exxon WVU visit, Morgantown, June 23, 2016.
On July 20, 2016, Paul Ziemkiewicz, Task 5a lead investigator gave a presentation titled: WVU – Northeast Natural Energy Marcellus Hydraulic Fracture Field Laboratory Environmental Research Update at the WVU/PTTC/NETL/RPSEA Onshore Technology Workshop Appalachian Basin Technology in Canonsburg, PA.
Abstract entitled “Addressing Health Issues Associated with Air Emissions around UNGD Sites” by Michael McCawley, Travis Knuckles, Maya Nye and Alexandria Dzomba accepted for the 2016 Eastern Section – American Association of Petroleum Geologists’ meeting in Lexington, Kentucky on September 27, 2016.
Sharma S. 2016, Environmentally Prudent Development of Unconventional Shale Gas: Role of Integrated Field Laboratories. Invited talk at International Shale Gas and Oil Workshop , India, 28-29 January, 2016
Sharma S. 2016, Role of Geochemistry in Unconventional Resource Development. Invited talk at Appalachian Geological Society Meeting, Morgantown, April 5 2016. Hakala, J.A., Stuckman, M., Gardiner, J.G., Phan, T.T., Kutcho, B., Lopano, C. 2016
Application of voltammetric techniques towards iron and sulfur redox speciation in geologic fluids from coal and shale formations, American Chemical Society Fall Meeting 2016 Philadelphia, PA.
Phan, T.T., Hakala, J.A. 2016. Contribution of colloids to major and trace element contents and isotopic compositions (Li and Sr) of water co-produced with natural gas from Marcellus Shale. American Chemical Society Fall Meeting 2016 Philadelphia, PA.
Environmentally Friendly Drilling Conference on 11/15/2015 by Sunil Moon and Michael McCawley, Diesel Traffic Volume Correlates with Ultrafine Particle Concentrations but not PM2.5.
Agrawal V, Sharma S , Chen R, Warriar A, Soeder D, Akondi R. 2015. Use of biomarker and pyrolysis proxies to assess organic matter sources, thermal maturity, and paleoredox conditions during deposition of Marcellus Shale. Annual Geological Society of America Meeting, Baltimore, MD, November 1-4.
Akondi R, Sharma S, Pfiffner SM, Mouser PJ, Trexler R, Warriar A. 2015. Comparison of phospholipid and diglyceride fatty acid biomarker profiles in Marcellus Shale cores of different maturities. Annual Geological Society of America Meeting, Baltimore, MD, November 1-4.
Mouser, PJ, Daly, RA, Wolfe, R. and Wrighton, KC (2015). Microbes living in unconventional shale during energy extraction have diverse hydrocarbon degradation pathways. Oral presentation presented at 2015 Geological Society of America Annual Conf. Baltimore, MD, Nov 1-4.
Sharma S and Wilson T. 2015. Isotopic evidence of microbe-water-rock interaction in Shale gas produced waters. Annual Geological Society of America Meeting, Baltimore, MD, November 1-4.
Sharma S, Chen R, Agrawal V. 2015 Biogeochemical evidences of oscillating redox conditions during deposition of organic-rich intervals in the middle Devonian Marcellus Shale. Annual Geological Society of America Meeting, Baltimore, MD, November 1-4.

Trexler RV, Pfiffner SM, Akondi R, Sharma S, Mouser PJ.(2015) Optimizing Methods for Extracting Lipids from Organic-Rich Subsurface Shale to Estimate Microbial Biomass and Diversity. Poster session presented at: 2015 Geological Society of America Annual Meeting. 2015 Nov 1-4; Baltimore, MD.

Wrighton, KC; Daly, R; Hoyt, D; Trexler, R; MacRae, J; Wilkins, M; Mouser, PJ (2015), Oral presentation at the American Geophysical Union Annual Meeting. Something new from something old? Fracking stimulated microbial processes. Presentation# B13K-08. San Francisco, CA, Dec 14-18, 2015.

Mouser, P, The Impact of Fracking on the Microbiology of Deep Hydrocarbon Shale, American Society for Microbiology (ASM) Annual Conference, New Orleans, LA, May 30-June 2, 2015.

Wrighton et al, Drivers of microbial methanogenesis in deep shales after hydraulic fracturing. American Society of Microbiology. New Orleans, LA. May 30-June 2, 2015.

Daly et al, Viral Predation and Host Immunity Structure Microbial Communities in a Terrestrial Deep Subsurface, Hydraulically Fractured Shale System. American Society of Microbiology. New Orleans, LA.

APPENDIX C – Special MSEEL Sessions

Paper prepared for presentation at the Unconventional Resources Technology Conference (URTeC) held in Denver, Colorado, USA, 22-24 July 2019, 10 pages, DOI 10.15530/urtec-2019- 415.
Odegarden, Natalie and Timothy Carr, Vein Evolution due to Thermal Maturation of Kerogen in the Marcellus Shale, Appalachian Basin, Paper presented at the Annual Meeting of the Geological Society of America 22-25 September 2019 Phoenix, AZ.
URTeC (URTeC: 2902641) for presentation in Houston (July) by Payam Kavousi Ghahfarokhi, Timothy Carr, Shuvajit Bhattacharya, Justin Elliott, Alireza Shahkarami and Keithan Martin entitled A Fiber-optic Assisted Multilayer Perceptron Reservoir Production Modeling: A Machine Learning Approach in Prediction of Gas Production from the Marcellus Shale. 2019
8/15/2017 - Coordinate and hold MSEEL session at URTEC 2017 (Scheduled 8/30/2017; Completed 8/30/2017)
4/30/2017 - Conduct preliminary analysis of production log data and present to DOE. (Completed and being worked into a new reservoir simulation – Review meeting held at WVU
26 Jul 2017: URTeC, Austin, TX, Manuscript attached
27 Sep 2017: Marcellus Shale Coalition, Shale Insight,
SPE-184073, SPE Eastern Regional Conf., Canton, OH, September 2016.
2016 SEG meeting in Dallas
2014 American Geophysical Union (AGU) Fall Meeting in December 2014 to discuss next steps in the project. At AGU, we hosted a special session on Biogeochemistry of Deep Shale,

National Energy Technology Laboratory

626 Cochrans Mill Road
P.O. Box 10940
Pittsburgh, PA 15236-0940

3610 Collins Ferry Road
P.O. Box 880
Morgantown, WV 26507-0880

13131 Dairy Ashford Road, Suite 225
Sugar Land, TX 77478

1450 Queen Avenue SW
Albany, OR 97321-2198

Arctic Energy Office
420 L Street, Suite 305
Anchorage, AK 99501

Visit the NETL website at:
www.netl.doe.gov

Customer Service Line:
1-800-553-7681



U.S. DEPARTMENT OF
ENERGY

**NATIONAL ENERGY
TECHNOLOGY LABORATORY**